

國立臺灣大學電機資訊學院電信工程學研究所



博士論文

Graduate Institute of Communication Engineering
College of Electrical Engineering and Computer Science
National Taiwan University
Doctoral Dissertation

下一代異質性網路智能技術之研究

On the Efficiency of Intelligent Technologies for Next Generation
Heterogeneous Networks

陳贊羽

Zanyu Chen

指導教授：林宗男 博士

Advisor: Tsung-Nan Lin, Ph.D.

中華民國 104 年 7 月

July, 2015

國立臺灣大學博士學位論文
口試委員會審定書

下一代異質性網路智能技術之研究
On the Efficiency of Intelligent Technologies for Next
Generation Heterogeneous Networks

本論文係陳贊羽君(D98942025)在國立臺灣大學電信工程學研究所完成之博士學位論文，於民國 104 年 7 月 20 日承下列考試委員審查通過及口試及格，特此證明

口試委員：

林宗男 (簽名)
(指導教授)

<u>王柔翔</u>	<u>蔣志宏</u>
<u>廖婉君</u>	<u>陳俊良</u>
<u>蔡子傑</u>	

所長 吳宗霖 (簽名)

誌謝



無論順利與否，終於畢業了，感謝的是林宗男老師推了我一大把，朝著博士學位努力，過程中的鼓勵也在最低落的時候起了很大的作用，最終才能夠將本論文順利產出。

感謝在博士班的這段日子當中，實驗室學弟們在各方面的陪伴，R97 的書銘、育宏、琮訓，R98 的訓甫、賢祥、舜橋、政偉，R99 的重良、彥志、明甫、中超，R00 的致程、崇瑋、俊凌、潘叡，R01 的康林、大豪、智彥、韋翰，R02 的洋銘、瑋時、柏宇、冠翔，R03 的三豐和昇毅，相信大家離開 507 之後都擁有相當美好的未來。

感謝的還有平常在一起鬼混打牌、羽球、出遊、爬山、下海的歐肥、keter、昊呆和佳雯，在博士班的生涯當中，多了許多的變化，最後自然還有總是能夠尊重我決定的父母，在這段時間的支持，雖然總是問何時要畢業，還好終於畢業了！

摘要



在今日的異質性網路中包含了許多的大、小型基站，然而目前這些基站的配置無法滿足未來的使用者需求，實際上在對來的預測當中，至少在 2020 年的時候需要比今日還要增加 100 倍的網路容量，才有辦法應付各方面的需求，因此網路的供應商和營運商們，仔細思考著他們手邊所能夠使用的方法，來提升網路的容量。在這場即將到來的戰役之中，有三個面向是值得來思考的：增加網路的密度、使用更多的頻譜和增加頻譜使用效率的各種技術。在本論文當中，我們針對在增加網路密度所遭遇到的各種可能情況來研究，增加網路的密度會採用大量的小型基站，像是家用基站、微型基站和轉傳節點。本論文主要分為兩個部份來探討：首先是關於在合作式通訊當中，轉傳節點選擇的問題，第二個主題是在異質性網路當中干擾管理的問題，關於第一個主題，我們提出了一個完全分散式的演算法稱為「分散式學習為基礎的轉傳選擇」，解決在合作式通訊中的轉傳選擇問題，另一方面在第二個主題當中，我們提出一個稱為「多調子訊框」方案，來減輕在異質性網路當中的干擾問題。

關鍵詞 ——異質性網路、合作式通訊、轉傳選擇、干擾管理、近乎空白子訊框、原對偶內點法。



Abstract

Today's heterogeneous networks comprised of mostly macrocells and small cells will not be able to meet the upcoming traffic demands. Indeed, it is forecasted that at least a $100\times$ network capacity increase will be required to meet the traffic demands in 2020. As a result, vendors and operators are now looking at using every tool at hand to improve network capacity. In this epic campaign, three paradigms are noteworthy, i.e., network densification, the use of higher frequency bands, and spectral efficiency enhancement technique. In this dissertation, we focus on the issue on network densification, which contains many small cells in the network such as femtocells, picocells and relay nodes. The dissertation can be divided into two parts: the first one is about relay node selection in cooperative communication, and the other is about interference management in heterogeneous networks. We proposed an fully decentralized algorithm call "Decentralized Learning based Relay Assignment" algorithm to solve the relay assignment problem in cooperative communication. On the other hand, in the topic about interference management, we propose an approach called "Multi-Tone Subframes" to mitigate the interference in heterogeneous networks.

Keywords: Heterogeneous Network, Cooperative Communication,

Relay Selection, Interference Management, Almost Blank Subframe,

Primal-Dual Interior Point Method

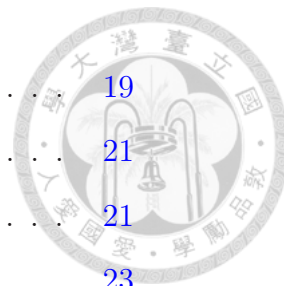




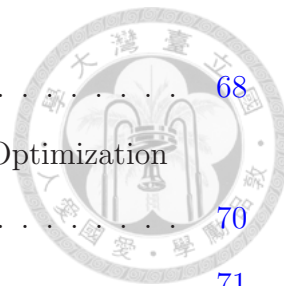
Contents

List of Figures	v
List of Tables	ix
1 Introduction	1
1.1 Technology Trends and Motivations of the Dissertation	1
1.2 Topic to Be Addressed	4
1.2.1 Cooperative Communication	4
1.2.2 Interference Management	5
1.3 Dissertation Organization	5
2 Related Work	7
2.1 Cooperative Communication	7
2.2 enhanced Inter-Cell Interference Management (eICIC)	9
2.2.1 Range Expansion and Inter-cell Interference Coordination	9
2.2.2 Literature Review	11
3 Decentralized Learning-Based Relay Assignment for Cooperative Communications	15
3.1 Background Information	15
3.2 System Model	18
3.2.1 Cooperative Communication Modes	18

CONTENTS



3.2.2	Network Model	19
3.3	Decentralized Learning based Relay Assignment algorithm	21
3.3.1	SLA: Stochastic Learning Automata	21
3.3.2	Proposed Algorithm	23
3.3.3	Complexity	25
3.4	Mathematical Analysis	27
3.4.1	Convergency	27
3.4.2	Asymptotic Theorems	29
3.4.3	Performance	35
3.5	performance evaluation	40
3.5.1	Cooperative Ad Hoc Network	40
3.5.1.1	Simulation Settings	40
3.5.1.2	Comparisons	41
3.5.2	LTE-Advanced Network	43
3.5.2.1	Simulation Settings	43
3.5.2.2	Convergency	45
3.5.2.3	Capacity and Fairness	49
3.6	Concluding Remarks	55
4	Multi-Tone Subframes for Enhanced Inter-Cell Interference Co-ordination in LTE HetNets	57
4.1	Background Information	57
4.2	System Model and Problem Formulation	63
4.2.1	System Model	63
4.2.2	Problem Formulation	64
4.3	Interior Point MTS Optimization Algorithm	67



4.3.1	Basic Idea of the Interior Point Methods	68
4.3.2	Detailed Description of Interior Point MTS Optimization Algorithm	70
4.3.2.1	The Relaxed Problem	71
4.3.2.2	Algorithm for The Relaxed MTS Assignment Prob- lem	73
4.3.2.3	Integer Rounding for Relaxed MTS Assignment	77
4.3.2.4	Proof of Optimality	80
4.3.2.5	Complexity Analysis	80
4.3.2.6	Summary	82
4.4	Numeric Example	82
4.4.1	Correlation Among The Approaches	83
4.4.2	Example	84
4.4.3	Summary	91
4.5	Simulation Results	91
4.5.1	Simulation Settings	91
4.5.2	Compare with Optimal Solution	92
4.5.3	User Clustering	94
4.5.4	System Capacity	99
4.5.5	Power Consumption	102
4.5.6	VoLTE Latency	104
4.5.7	Summary	105
4.6	Concluding Remarks	105
5	Conclusion	109

CONTENTS

Bibliography



111

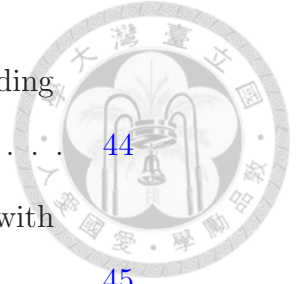


List of Figures

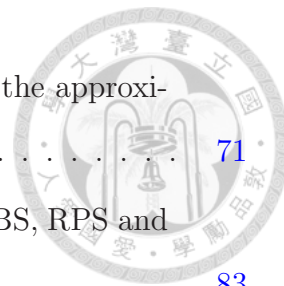
1.1 Existing paradigms to improve network capacity: Spectrum (more spectrum), Technology (more spectral efficiency) and Topology (more spatial efficiency).	2
2.1 The concept of Cell Range Expansion (CRE).	10
2.2 The transmission power on each subframe of approaches: ABS, RPS and DRPS.	12
3.1 A Stochastic learning automata.	21
3.2 State transition diagram of DLRA.	35
3.3 Markov chain model of DLRA.	37
3.4 The number of transitions DLRA would take vs. the probability $\xi(b)$	39
3.5 The CDF of the capacity of all source nodes for the two algorithms in the environment while $N_s < N_r$	41
3.6 The CDF of the capacity of all source nodes for the two algorithms in the environment while $N_s > N_r$	42
3.7 The 5%-outage, median and mean capacity of DLRA and ORA in both cases.	43

LIST OF FIGURES

3.8	The network topology of the simulation and the corresponding relay selection result for each source node.	44
3.9	The variation of aggregate performance of average results with different values of Δ	45
3.10	The average convergent time with different values of Δ	46
3.11	The state evolution of source node 5.	47
3.12	The performance evolution for source node 5.	48
3.13	The probability vector evolution for source node 5 without small scale fading.	49
3.14	The probability vector evolution for source node 5 with Rayleigh fading.	50
3.15	Different initialization of P_0 : (a) Uniform distribution, (b) Non-uniform distribution and the probability of the best state is not equal to 0, and (c) the probability of the best state is equal to 0.	52
3.16	The CDF of capacity for all algorithms.	53
3.17	The aggregate capacity for all algorithms.	53
3.18	The average improvement for all algorithms.	54
3.19	The fairness index for all algorithms.	54
4.1	Illustration of coverage area in different transmission.	59
4.2	The comparison of the capacity: the original case means the maximum transmission power on one subframe and the after case means use 1/3 maximum transmission power on each subframes.	62
4.3	Example of coverage area of MBS for 7 power levels.	69

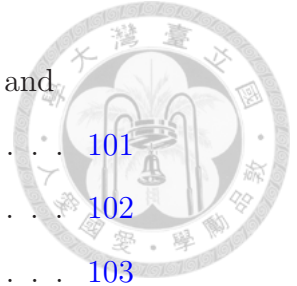


4.4	Effect of t on approximation accuracy. As t increase, the approximation becomes more accurate.	71
4.5	The sketch map of the performance relation among ABS, RPS and MTS with different levels.	83
4.6	The topology used in the simple numeric analysis.	85
4.7	The distance between the MBS and the PBS is 800 meters, and different ABS proportions are evaluated.	87
4.8	The distance between the MBS and the PBS is 500 meters, and different ABS proportions are evaluated.	88
4.9	The distance between the MBS and the PBS is 500 meters, and different ABS proportions are evaluated.	89
4.10	The performance loss rate with different power levels compared to the optimal solution obtained from the interior point relaxed MTS optimization algorithm.	93
4.11	The user association in the center cell.	94
4.12	The group of UEs served by the power level P_2	96
4.13	The group of UEs served by the power level P_3	96
4.14	The group of UEs served by the power level P_4	97
4.15	The group of UEs served by the power level P_5	97
4.16	The group of UEs served by the power level P_6	98
4.17	The group of UEs served by the power level P_7	98
4.18	Comparison of the capacity of the MBS and the PBS in the original ABS scheme and the proposed MTS approach.	99
4.19	The average throughput of cells in different approaches.	100



LIST OF FIGURES

4.20 The CDF of UEs' capacity in three approaches: RPS, DRPS and MTS.	101
4.21 The distribution of transmission power levels in the system.	102
4.22 The power consumption of all approaches.	103
4.23 The over-the-air delay of the ABS scheme and the proposed approaches.	104





List of Tables

4.1	Definitions of Notations	65
4.2	Simulation Settings	92
4.3	Transmission Power Level	93
4.4	Number of UEs in the Groups	95

LIST OF TABLES





Chapter 1

Introduction

1.1 Technology Trends and Motivations of the Dissertation

The phenomenal growth in mobile broadband has created a massive challenge for the industry to satisfy the thirsty for data. The rapid and continuing growth of mobile data has the industry gearing up to meet a new challenge. In view of such significant future traffic demands, the mobile industry has set its targets high, and has decided to improve the capacity of today's networks by a factor of $100\times$ or more over the next 20 years - $1000\times$ the most ambitious [1].

In order to achieve this goal, vendors and operators are currently looking at using every tool they have at hand, where the existing tools can be classified within the following three paradigms as illustrated in Fig. 1.1:

- Enhance spatial reuse through network densification, i.e., Heterogeneous Networks (HetNets) and small cells [2–5].
- Use of larger bandwidths, exploiting higher carrier frequencies, both in licensed and unlicensed spectrum [6–8].

1. INTRODUCTION

- Enhance spectral efficiency through multi-antenna transmissions [9], cooperative communications [10], dynamic TDD techniques [11, 12], etc.

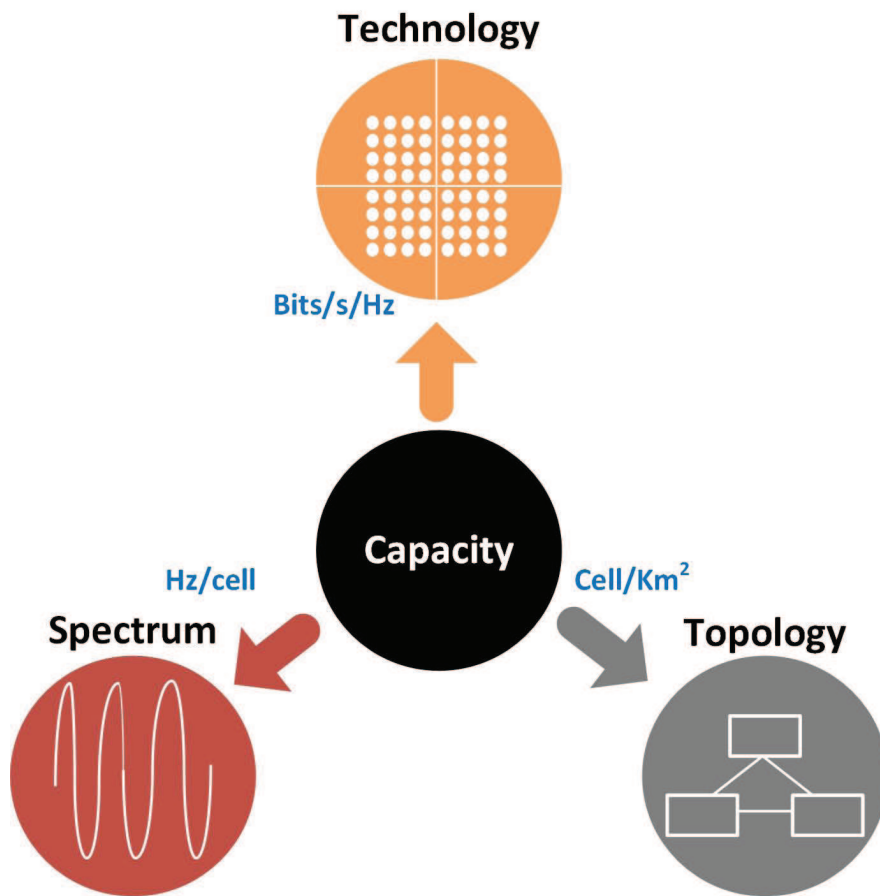


Figure 1.1: Existing paradigms to improve network capacity: Spectrum (more spectrum), Technology (more spectral efficiency) and Topology (more spatial efficiency).

Given the different approaches to enhance network capacity, it may be worth understanding how network capacity has been improved in the past and which have been the lessons learnt to make sure the best choices are taken. To this end, according to [13], the different methods used to enhance network capacity from 1950 to 2000, and the wireless capacity has increased around a 1 million fold in

50 years. The breaking down of these gains is as follows: $15\times$ improvement was achieved from a wider spectrum, $5\times$ improvement from better Medium Access Control (MAC) and modulation schemes, $5\times$ improvement by designing better coding techniques, and an astounding $2700\times$ gain through network densification and reduced cell sizes. According to this data, it seems obvious that if we are looking for a $1000\times$ improvement in network performance, network densification through ultra-dense small cell deployments is the most appealing approach, and today's networks have already started going down this path.

In order to meet the exponentially increasing traffic demands [14], mobile operators are already evolving their network form traditional macrocellular-only networks to HetNets [15, 16], in which small cells reuse the spectrum locally and provide most of the capacity while macrocells provide a blanket coverage for mobile UEs. Currently, small cells are deployed in large numbers. Indeed, according to recent surveys, in 2012, the number of small BSs was already larger than that of macro BSs [17]. These small cell deployments are mainly in the form of home small cells, known as femtocells [3, 4, 18], but many operators have also already started to deploy outdoor small cell solutions to complement their macrocellular coverage [19].

Since there many technology to improve the network capacity, we focus on the topics in the HetNets, which are considered as the main technology to meet the increasing data traffic demands. HetNets include traditional macrocells and low-power smallcells. Smallcells, such as femtocells, picocells and relay nodes, are sharing the same spectrum resource as macrocells. Therefore, the interference is the main factor affecting the performance of smallcells. Besides, relay nodes are also used to increase the cell edge capacity in HetNets. We would address this



two topic in this thesis.

1.2 Topic to Be Addressed

In this dissertation, we consider two different types of small cells: relay nodes and pico base stations. In the first, we take relay nodes into consideration. Relay assignment problem in cooperative communication will be addressed. Second, we consider a heterogeneous network which consists of macro BS and pico BSs. We study a topic about interference management among these cells.

1.2.1 Cooperative Communication

Spatial diversity, in the form of employing multiple transceiver antennas, is shown to be very effective in coping fading in wireless channel. However, equipping a wireless node with multiple antennas may not be practical, as the footprint of multiple antennas may not fit on a wireless node. To achieve spatial diversity without requiring multiple transceiver antennas on the same node, the so-called cooperative communications has been introduced. Under cooperative communications, each node is equipped with only a single transceiver, and spatial diversity is achieved by exploiting the antenna on another node the network.

In this dissertation, we study the relay node assignment problem in cooperative communication system, which includes ad hoc network and LTE relay networks. We propose an algorithm which is fully decentralized called "Decentralized Learning based Relay Assignment" (DLRA). We evaluate DLRA from many aspects: mathematical analysis, performance manipulation and computer simulation.



1.2.2 Interference Management

HetNet is a two-tier network scenario, and co-channel cross-tier interference is a major factor affecting network performance. To handle this problem, a framework called Enhanced Inter-Cell Interference Coordination (eICIC) is proposed by 3GPP. Almost blank subframes (ABSs) are the major part of eICIC, and the concept is to blank some subframes of the interferer tier, where only pilot and system signals are transmitted [20]. Because FBSs and PBSs are deployed overlaid on coverage range of MBSs, the interference from MBSs is severe. Therefore, adopting ABSs can lead these small BSs to have better performance during ABSs.

In this work, we address some weak points of ABS scenarios and propose our approach to improve them. First, the latency of real-time traffic, such as voice, would get longer if the proportion of ABSs is getting higher. Because user information can not be delivered by MBSs in ABS periods, some real-time information can not be transmitted in time while MBSs under heavy load. The more proportion of ABSs is adopted, the longer latency is got in MBSs. Second, ABS scenarios sacrifice some subframes to protect PBSs, and the behavior decrease the spectrum utilization. It leads to capacity loss in MBSs, and the performance of users served by MBSs is degraded.

1.3 Dissertation Organization

The rest of this dissertation is organized as follows. In Chapter 2, we review some related literature about this work. The topic about relay assignment is in Chapter 3 and the proposed "Decentralized Learning based Relay Assignment" (DLRA) algorithm is shown in the same chapter. We show the proposed interference

1. INTRODUCTION

management technique in Chapter 4, and the proposed "Multi-Tone Subframes" (MTS) is evaluated in the same chapter. In the last, we conclude this work in Chapter 5





Chapter 2

Related Work

In this chapter, some works related to the thesis are introduced, and some literature is also reviewed.

2.1 Cooperative Communication

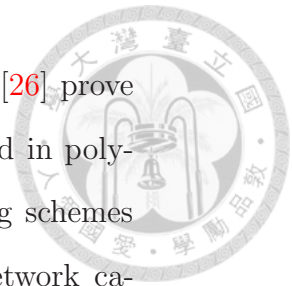
The concept of cooperative communication was pioneered by a paper by van der Meulen [21] and Cover and EL Gamal [22]. This section focuses on related works on the relay node selection problem. Zhao et al. [23] show that it is sufficient to choose the best relay node for transmission rather than having multiple relay nodes participate. This work thus considers a scheme in which each source node chooses at most one relay node for transmission.

The problem is studied in many works, and from several different aspects. The basic structure of a cooperative communication system is also discussed in this section. For example, Yang et al. [24] introduce TDD/FDD system frame structures in LTE-advanced and WiMax systems. To implement cooperative communication systems in the real world, the degree of complexity must be limited. Jing et al. [25] therefore propose a relay selection scheme with polynomial

2. RELATED WORK

time complexity to achieve an optimal SNR. In addition, Yang et al. [26] prove that an optimal relay node selection problem solution can be obtained in polynomial time. Furthermore, many works have adopted network coding schemes in cooperative communication systems [27–29]. In these schemes, network capacity can be significantly increased, but it is fairly challenging to implement network coding schemes in real-world systems [30,31]. Instead of using a centralized mechanism, Cai et al. [32] propose a semi-distributed algorithm with a greedy algorithm methodology. There is therefore no performance guarantee in this algorithm [33]. Other works consider relay selection with a power allocation problem in the system [34–39]. These approaches achieve the goal of energy-saving in relay networks. [40] and [41] combine relay selection problems and rate adaptation to achieve higher system performance. Abouelseoud et al. [42] combine many different protocols in relay networks in order to enhance system performance.

The last part of this section introduces the works to be compared with DLRA in this dissertation. The first is that proposed by Sharma et al., called "Optimal Relay Assignment" (ORA); the goal is to maximize the minimal performance in the system. [43]. A linear marking algorithm is proposed in ORA; the idea is to mark the node with the worst performance. ORA tries to increase its performance without decreasing the worst performance in the system. A relay node can only be shared by one source node in ORA. The second is proposed by Yang et al., called "OPTimal Relay Assignment" (OPRA), and the goal is to maximize the total system performance [44]. OPRA discusses the possibility of allowing a relay node to be shared by multiple source nodes to achieve its objective, and formulates the problem as a maximum weighted bipartite matching problem; it then solves it with the corresponding algorithm. The third work is proposed by Cai et al., and



is a semi-distributed approach [32]. Cai's algorithm is to consecutively have each source node randomly select a relay node, a process based on a greedy approach.



2.2 enhanced Inter-Cell Interference Management (eICIC)

2.2.1 Range Expansion and Inter-cell Interference Coordination

Cell association is usually performed according to the RSRP [45]. Due to the large difference of transmission power between an MBS and a PBS, a pseudo bias is added to RSRP from PBS. The so called CRE is proposed by 3GPP to allow load balancing among macrocells and picocells. 3GPP has studied the concept of CRE throughput handover biasing and resource partitioning among nodes with different levels of transmission powers [46,47]. The larger value of the bias is, the more UEs can be associated to picocells. CRE approach is simply to add an offset on RSRP of picocells to increase the coverage range, however, the downlink signal quality of those users, which we call CRE users in this work, in the expanded range is significant reduced. Fig. 2.1 illustrate the users are offloaded from macrocells to picocells. CRE users do not associate to the cells which provide the best downlink signal quality, and they may suffer severe interference while CRE is adopted.

In 3GPP LTE Release 8-9, ICIC schemes have not consider HetNet environment yet. To handle the cross-tier interference, 3GPP proposes ABS to enhance ICIC, which is referred to eICIC, in order to mitigate the cross-tier interference. According to [48], the ICIC techniques in 3GPP Release 10-12 can be

2. RELATED WORK

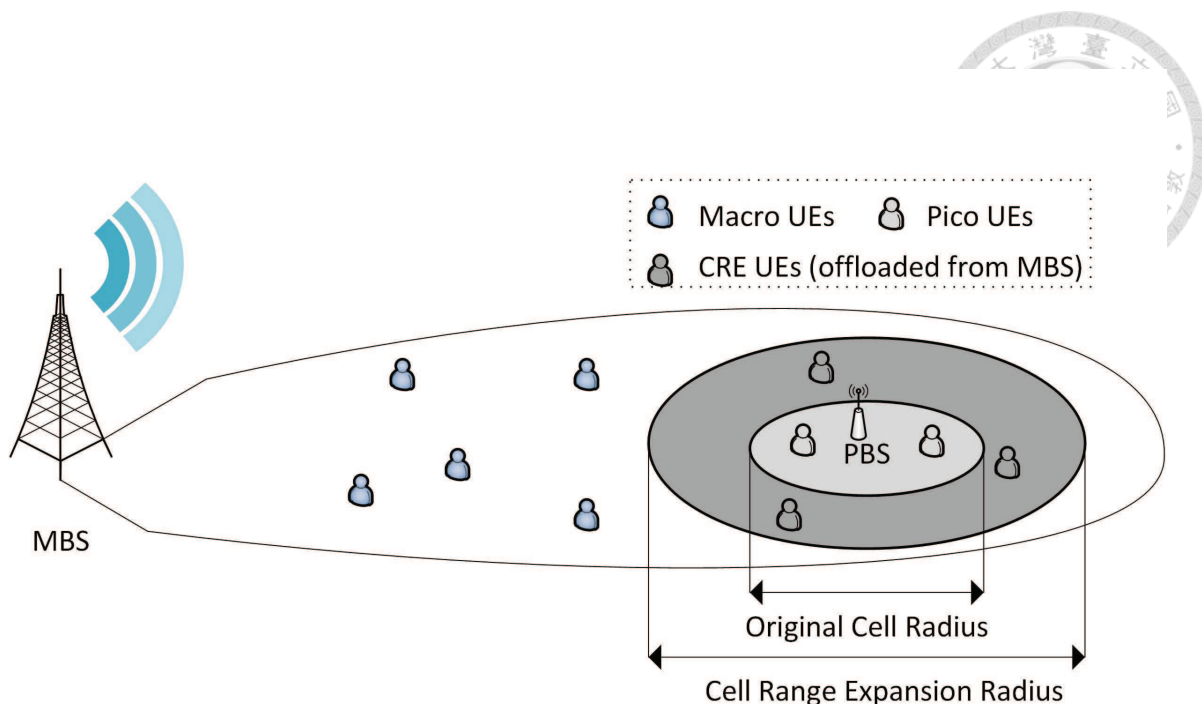


Figure 2.1: The concept of Cell Range Expansion (CRE).

grouped into four categories: time-domain, frequency-domain, power based and antenna/spatial-based techniques [46, 49]. ABS belongs to the time-domain ICIC techniques. The idea of ABS is to mute some subframes of MBS in order to protect PUEs. In these muted subframes, no data is transmitted to MUEs, therefore, CRE users do not suffer the severe interference from MBSs anymore. The illustration of ABS scheme is shown in Fig. 2.2(a).

The drawback of ABS can be seen significantly: it wastes much spectrum resource of MBSs. Although the performance of picocells is increased, the performance of MBSs is sacrificed. According to [46], instead of muting the MBS completely during ABS, transmitting at reduced power to serve only its nearby UEs would considerably improve the HetNet performance in terms of the trade-off between cell-edge and average throughputs. Latter on, reduced power subframe (RPS) transmission has also been standardized under LTE Release 11 of

3GPP, and commonly referred therein as further-enhanced ICIC (FeICIC) [50]. In another study [51], simulation results show that FeICIC is less sensitive to the duty-cycle of ABS than the eICIC. The illustration of RPS is shown in Fig. 2.2(b).

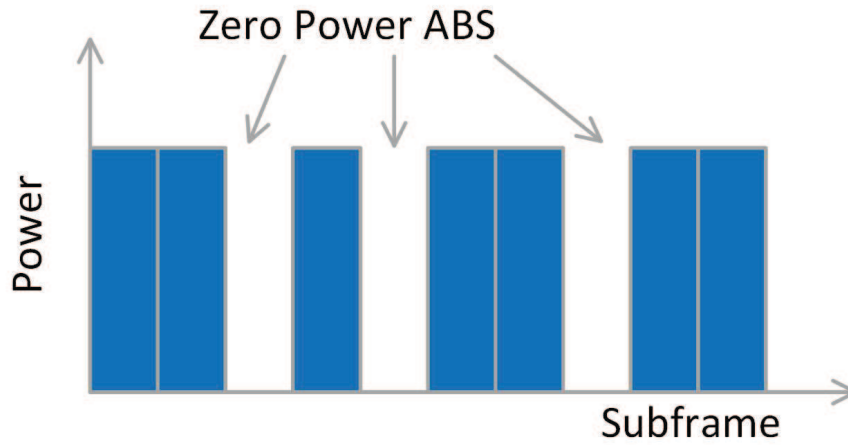
RPS is to transmit reduced power during the original ABS, however, the purpose to blanking these frames is to protect CRE users. The reduced power transmission would interfere CRE users, although the interference is lighten compared to full power transmission. The performance of CRE users are sacrificed compared to ABS scenario. So, an approach called dynamic RPS (DRPS) is proposed, and the illustration of DRPS is shown in Fig. 2.2(c). Compared to RPS, DRPS gives more flexible transmission power on the original ABS.

2.2.2 Literature Review

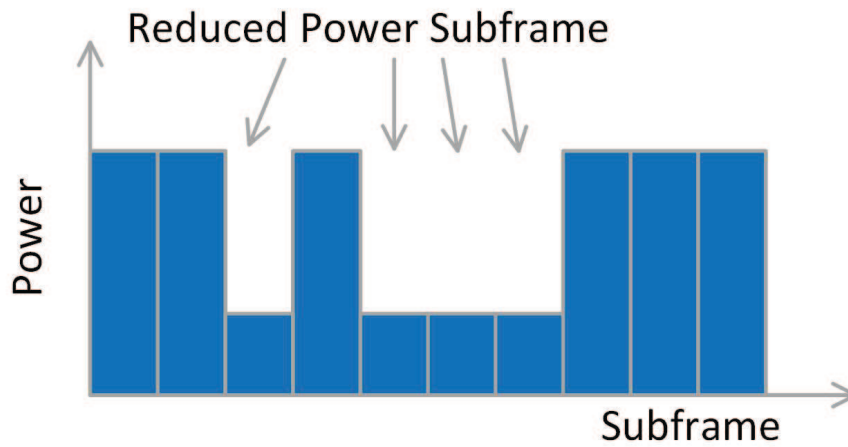
there is a sizeable body of literature on the use of CRE for traffic load balancing in HetNets; see e.g. [19, 52–60]. Lopez-Perez et al. [19] calculate CRE bias values for different range expressions strategies, e.g., equal downlink RSS boundary and equal path-loss boundary, and closed-form expression are derived. Guvenc et al. [52] propose cell selection procedure based on subframes blanking to improve downlink capacity and UE's fairness. Shirakabe et al. [57] provide the performance of different CRE values and different ration of protected subframes, which is based on system level simulations. Using tools from stochastic geometry, analytical models accounting for BS and UE locations have been studied to analyze spectral efficiencies in range expanded picocell networks in [56], which has later been extended to ICIC scenarios in [58, 59].

For the purpose of interference management, frequency domain interference

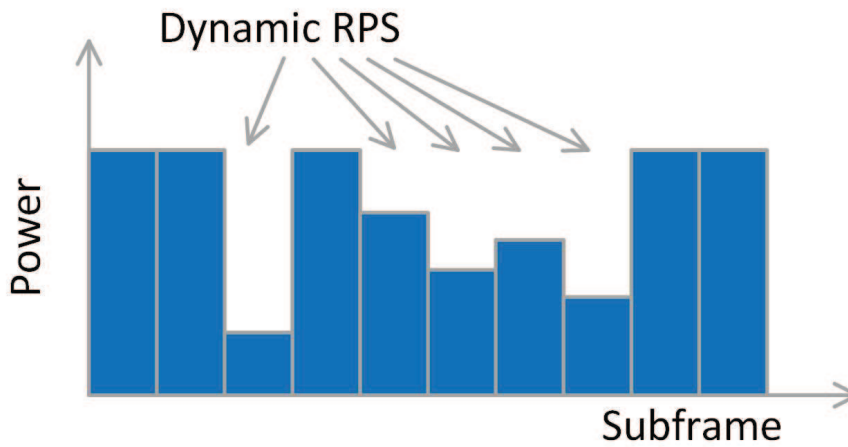
2. RELATED WORK



(a) ABS



(b) RPS



(c) DRPS

Figure 2.2: The transmission power on each subframe of approaches: ABS, RPS and DRPS.

2.2 enhanced Inter-Cell Interference Management (eICIC)

coordination techniques have also been studied in literature. The simplest strategy is called universal reuse or reuse of factor 1. It allows each cell access the whole bandwidth without any restriction. Simonsson [61] shows the fact that the universal reuse performs best for wideband services. Decentralized inter-cell interference coordination is proposed by Ellenbeck et al. [62]. Many carrier aggregation based ICIC techniques have also been proposed in literature; see e.g. [63–66].

For the aspect of time-domain ICIC, Wang et al. [67] consider time and power domain interference management in HetNets. However, the authors apply ABSs and power reduction on small BSs, it may reduce the performance of small BSs. The purpose of eICIC is to protect the transmissions of small BSs. Cherny et al. [68] study the work that the number of necessary ABSs is needed in HetNets. The problem is addressed by the authors by tools from stochastic geometry, and they show moderate performance gain for victim users in HetNets. Deb et al. [69] formulate the same problem as an optimization problem, and find it is NP-hard. So, the authors propose a distributed approach to obtain the suboptimal solution of the problem. The problem of ABS duty cycles is addressed in [70, 71]. Ding et al. [12] evaluate dynamic time-duplex TDD transmission by CRE and ABS in co-channel HetNets.

To enhance ABS, many researches are provided to increase the performance of ABS. Soret et al. [72] propose a scheme named low-power ABS. Through this scheme, MBSs reduced their transmission power in particular subframes instead of blanking them. Merwaday et al. [59, 60] provide the performance of HetNets with reduced power subframes. The authors show the impact of interference coordination in HetNets by using stochastic geometry techniques. Soret et al. [73]

2. RELATED WORK

propose ABS fast muting adaptation algorithms to handle bursty traffic.





Chapter 3

Decentralized Learning-Based Relay Assignment for Cooperative Communications

3.1 Background Information

Cooperative communication [74] is considered a promising approach to achieving spatial diversity and addressing the increasing demand for data throughput in wireless networks. Network systems achieve spatial diversity by exploiting the broadcast nature and antennas of other nodes, i.e. relay nodes. Such systems therefore do not require multiple antennas on individual nodes. In addition, the deployment of relay nodes is also able to address increasing mobile user demands. Only an appropriate relay node can lead to better performance; an inappropriate relay assignment may negatively affect network performance [75].

To date, many approaches to solving the relay selection problem have been proposed. The two leading approaches are: maximizing the aggregate performance [44], and maximizing the minimal performance [43]. Many studies have developed centralized algorithms to handle the problem [23, 76–82], for example,

3. DECENTRALIZED LEARNING-BASED RELAY ASSIGNMENT FOR COOPERATIVE COMMUNICATIONS

formulating relay selection problems as optimization problems. The centralized approaches always require link metrics, such as signal-to-noise-ratio (SNR), distance between nodes or channel state information, to make the relay assignment decisions. When the numbers of source nodes and relay nodes increase, optimization problems become increasingly complicated. In order to address this problem, some distributed algorithms have been proposed [32, 83, 84]. Some of these distributed approaches are based on opportunistic cooperation, which still causes system overhead.

This study proposes a fully distributed algorithm called "Decentralized Learning-based Relay Assignment" (DLRA), which is based on stochastic learning automata (SLA), to solve the relay selection problem in cooperative communications. SLA are used in many areas, such as, pattern recognition [85] and robot systems [86]. The idea of SLA is attempting to solve a problem without having any information regarding the solutions. An action is selected according to a probability vector, the feedback is observed from the environment, the probability vector is updated according the feedbacks, and the procedure is repeated. Finally, the most suitable solution will be found in the end.

DLRA is a self-organizing algorithm; it can give each source node self-optimizing and self-learning abilities. Each source node is therefore able to select an appropriate relay node for itself without exchanging information with all of the other source nodes. Thus, it is unnecessary for DLRA to maintain a central control unit to handle the whole system. In addition, the complexity of DLRA does not increase with the number of source nodes.

DLRA performance is evaluated by mathematical analysis and computer experiments. The convergency and optimality of DLRA is demonstrated in the



mathematical analysis. In the computer experiments, two different cooperative network systems are constructed: one is a cooperative ad hoc network, and the other is an LTE-advanced relay network. This study demonstrates the effectiveness of DLRA in the first network system, where all simulation topologies and parameters follow [43]. DLRA performance is then compared with that of other algorithms in the second network system to show its superiority.

The main contributions of this study are summarized as follows:

- A fully distributed and self-optimizing algorithm based on SLA is proposed. The need for information exchange among all source nodes is eliminated since each source node is able to individually and autonomously find the most appropriate relay node for transmission.
- The selection mechanism is based on existing environmental feedback, which enables source nodes to adjust the preferred transmission method, and no additional overhead is produced in the system; it balances the load of the relay nodes in turn.
- Through mathematical analysis, the proposed algorithm converges into one state; it is shown that the convergent state exhibits the best performance. The optimality of the proposed algorithm is also shown in the mathematical analysis.
- The experiments are not performed in a specified network system. Different network systems are used to apply the proposed algorithm, and the experimental results show that the proposed algorithm exhibits good performance in different network systems. The proposed algorithm can therefore be applied to various cooperative communication systems.



3.2 System Model

3.2.1 Cooperative Communication Modes

Two modes of cooperation communication are considered in this section: amplify-and-forward (AF) and decode-and-forward (DF) [75]. The expressions for capacity in cooperation communications are also given in this section.

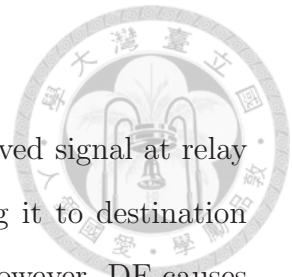
Amplify-and-Forward (AF)

In AF mode, relay nodes simply amplify the received signal from the source nodes and transmit it to the destination nodes. It is a simple method, and makes for low-cost implementation. However, it also amplifies noise at relay nodes with the desired signal component, thus decreasing the received SNR and reducing the enhanced gain. According to [75], the capacity of AF can be expressed as:

$$\begin{aligned} C_{AF}(s, r, d) &= \frac{W}{2} \log_2 \left(1 + SNR_{sd} + \frac{SNR_{sr} SNR_{rd}}{1 + SNR_{sr} + SNR_{rd}} \right) \\ &= WI_{AF}(SNR_{sd}, SNR_{sr}, SNR_{rd}) \end{aligned} \tag{3.1}$$

,where W is the transmitted bandwidth, s , r and d denote the source node, relay node and destination node respectively. SNR_{sd} is the signal-to-noise-ratio at destination nodes while the signal is from source nodes, and SNR_{sr} and SNR_{rd} are similar.

Decoded-and-Forward (DF)



In DF mode, relay nodes demodulate and decode the received signal at relay nodes, and modulate and encode it again before transmitting it to destination nodes. DF offers better performance gain compared to AF. However, DF causes a delay associated with the modulation/demodulation and encoding/decoding processes. The capacity of DF can be expressed as:

$$\begin{aligned}
 C_{DF}(s, r, d) &= \frac{W}{2} \log_2(\min\{1 + SNR_{sr}, 1 + SNR_{sd} + SNR_{rd}\}) \\
 &= WI_{DF}(SNR_{sd}, SNR_{sr}, SNR_{rd})
 \end{aligned}
 \tag{3.2}$$

Direct Transmissions

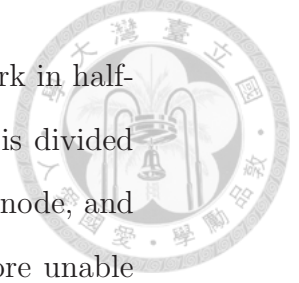
When a source node communicates with a destination node without using relay nodes, it is a direct transmission. The capacity of direct transmission is expressed as:

$$C_D(s, d) = W \log_2(1 + SNR_{sd}) \tag{3.3}$$

3.2.2 Network Model

This work assumes that a network system has N nodes, with each node being either a source node, a destination node, or a relay node. Denote $\mathcal{X} = \{x_1, \dots, x_{N_x}\}$ as the set of source nodes, $\mathcal{Y} = \{y_1, \dots, y_{N_y}\}$ as the set of destination nodes, and $\mathcal{R} = \{r_1, \dots, r_{N_r}\}$ as the set of relays. The destination node of source node i , namely x_i is denoted by $Y(x_i)$, and the relay node used by x_i is $R(x_i)$. Note that if x_i doesn't get a relay node, then $R(x_i) = \phi$. This may be caused by the fact that direct transmission is better than transmission via relay nodes.

3. DECENTRALIZED LEARNING-BASED RELAY ASSIGNMENT FOR COOPERATIVE COMMUNICATIONS



Suppose that all nodes are equipped with a single antenna, and work in half-duplex mode. So, the structure of on transmission is that one frame is divided into two time slots, where one is used for the source node to the relay node, and the other is the relay node to the destination node. They are therefore unable to simultaneously transmit and receive. For both AF and DF, the capacity of S_i while $R(S_i) \neq \phi$ can be written as:

$$WI_R(SNR_{x_i, Y(x_i)}, SNR_{x_i, R(x_i)}, SNR_{R(x_i), Y(x_i)}) \quad (3.4)$$

where $I_R(\cdot) = I_{AF}(\cdot)$ for AF and $I_R(\cdot) = I_{DF}(\cdot)$ for DF.

If x_i does not use a relay, the capacity is calculated as the direct transmission, namely

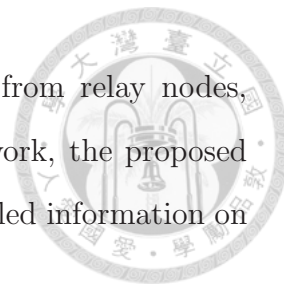
$$W \log_2(1 + SNR_{x_i, Y(x_i)}) \quad (3.5)$$

Denote $A(r_i)$ as the number of source nodes which use the relay node r_i . When multiple source nodes choose the same relay node, it is assumed that the source nodes share radio resources equally. In this work, the proposed algorithm is a decentralized approach. There is no information exchanged among source nodes. The number of source nodes served by a relay node is only known by that relay node. From the viewpoint of relay nodes, the capacity of x_i while using relay node $R(x_i)$ is denoted as $C(x_i, R(x_i))$, and can be shown as follows:

$$C(x_i, R(x_i), Y(x_i)) = \begin{cases} \frac{W}{A(R(x_i))} I_R(SNR_{x_i, Y(x_i)}, SNR_{x_i, R(x_i)}, SNR_{R(x_i), Y(x_i)}), \\ \quad \text{if } R(x_i) \neq \phi \\ W \log_2(1 + SNR_{x_i, Y(x_i)}), \\ \quad \text{if } R(x_i) = \phi \end{cases} \quad (3.6)$$

3.3 Decentralized Learning based Relay Assignment algorithm

Source nodes only send and receive information to and from relay nodes, allowing them to obtain the capacity among them. In this work, the proposed algorithm is evaluated in two different network systems. Detailed information on both systems is shown in Section 3.5.



3.3 Decentralized Learning based Relay Assignment algorithm

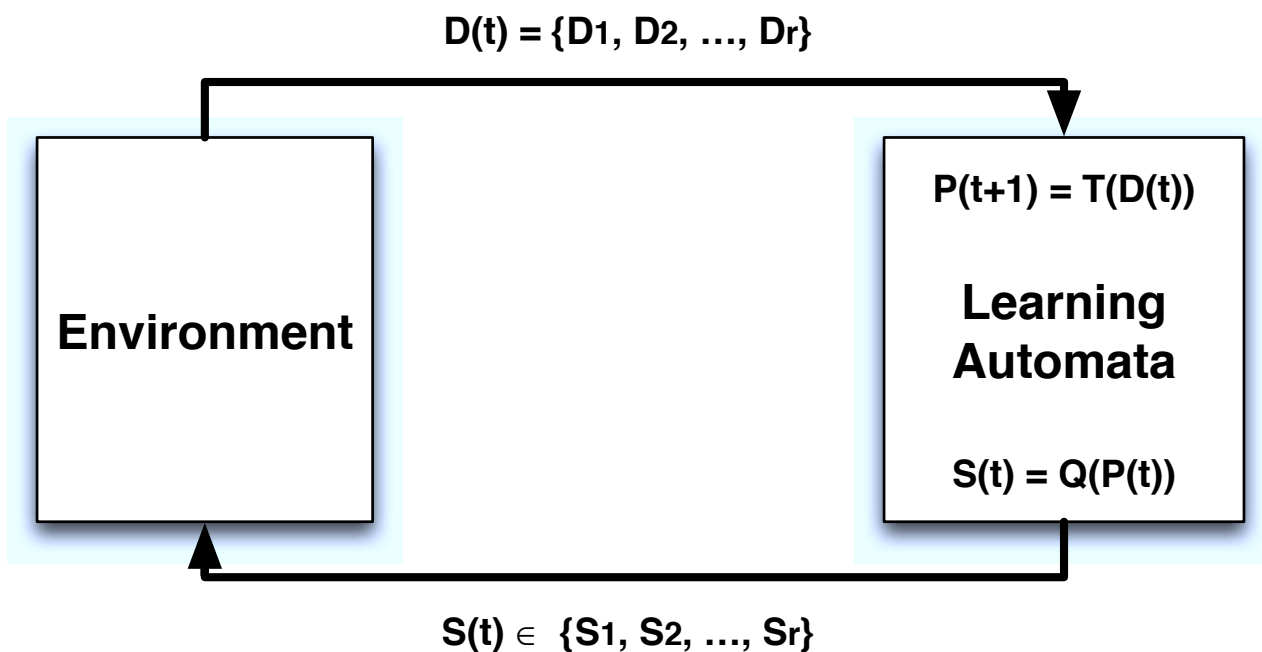


Figure 3.1: A Stochastic learning automata.

3.3.1 SLA: Stochastic Learning Automata

Stochastic learning automatas are self-optimizing, reinforcement learning techniques in machine learning [87]. An SLA is a finite state machine which interacts

3. DECENTRALIZED LEARNING-BASED RELAY ASSIGNMENT FOR COOPERATIVE COMMUNICATIONS

with an unknown environment and attempts to learn the best action offered by that environment via a learning process [88]. SLAs learn by means of the feedback from their environments, which can tell an SLA whether or not its selection is good. The learning process is iteratively performed until the SLA reaches a stable condition. There is no predetermined relationship between actions and responses, and SLAs are therefore suitable for use in unknown network environments, for example, cooperative networks where UEs do not know which relays are the best for them. So, SLAs are an attractive mechanism in such environments, and many studies have been conducted to apply them to network systems. In [89], a rate adaptation mechanism of 802.11 networks is proposed based on SLA. In [90], an algorithm to perform opportunistic spectrum access is based on SLA. In [66], SLA is used to conduct an energy-saving algorithm in LTE-advanced networks.

An illustration of SLA is given in Figure 3.1, and SLA is defined by the 5-tuples.

- $\mathcal{S} = \{S_1, \dots, S_n\}$ is the set of n states in the system. The selected state at time t is symbolized as : $S(t) = S_i \in \mathcal{S}$
- $\mathcal{D} = \{D_1, \dots, D_n\}$ is the set of environmental responses corresponding to each state.
- \mathcal{P} is the probability distribution over the set of states, and $P(t) = \{P_1(t), \dots, P_n(t)\}$ where $P_i(t)$ is the probability of state $S_i \in \mathcal{S}$ at time t .
- T is the learning algorithm that modifies the probability vector $P(t+1)$ at the next iteration according to $D(t)$.
- \mathcal{Q} is the output function from $P(t)$ to $S(t)$.

3.3 Decentralized Learning based Relay Assignment algorithm

In SLA, each agent has many available states, denoted by set S , and must choose a state, $S(t)$, according to the probability vector $P(t)$ of the states and output function Q . After an agent selects a state, the selected state triggers the environment by responding with a performance estimation $D(t)$. After time period T , an agent updates the probability vector $P(t+1)$ in the next time instant based on $D(t)$.

3.3.2 Proposed Algorithm

In this section, the proposed algorithm is described: DLRA (Decentralized Learning-based Relay Assignment), which is based on SLA and is an online and totally distributed algorithm. The goal of DLRA is to choose an appropriate relay for transmission, so that each relay selection stands for different states. Then, a probability distribution is covers these states, and DLRA chooses a relay node according to this probability. Once a state, namely a relay node, is chosen, the system will give feedback information, which is a performance measure in DLRA, about of this relay node. DLRA updates the probability distribution according to the performance over every period T . So, the five tuples defined in the previous section are described as follows:

- $\mathcal{S} = \{1, \dots, N_r + 1\}$ is the set of relay nodes, and each relay nodes represents a state. The state $N_r + 1$ means the direct transmission, and state i ($i \neq N_r + 1$) is using relay node i for the transmission.
- $\mathbf{D}_t^i = \{d_t^i(1), \dots, d_t^i(N_r+1)\}$ is the performance vector of source node i at time t . When a relay node is chosen, a environmental response is obtained; it represents the performance measure of the chosen relay node. The capacity

3. DECENTRALIZED LEARNING-BASED RELAY ASSIGNMENT FOR COOPERATIVE COMMUNICATIONS



of source nodes is used as the performance measure. So, $d_t^i(r)$ means the capacity of source node i at time t when choosing relay node r .

- $\mathbf{P}_t^i = \{p_t^i(1), \dots, p_t^i(N_r + 1)\}$ is a probability vector. DLRA chooses a relay node according to this vector. For example, $P_t^i(r)$ is the probability of source node i choosing relay node r at time t .
- T is the period after which DLRA updates the probability vector.
- Q_t^i is the output function from P_t^i to S . $Q_t^i(P_t^i) = r$ means that source node i picks up state r at time t according to P_t^i .

In DLRA, source node i picks out a state from set \mathcal{S} according to its probability vector P_t^i at time t . After selecting a state, e.g., state r is chosen, DLRA will obtain feedback from the system and denote it by $d_t^i(r)$, which is the capacity of source node i when choosing state r at time t in cooperative communication. DLRA then has a performance vector for source node i , namely $D_t^i = \{d_t^i(1), \dots, d_t^i(N_r + 1)\}$. DLRA updates the probability of the source node i according to the performance vector D_t^i .

Before updating the probability vector, DLRA needs to find the best state for the source node. The best state for source node i is the state with the highest capacity among all states, and is denoted by b_t^i at time t , so:

$$b_t^i = \arg \min_j d_t^i(j) \quad (3.7)$$

After the best state is obtained, the next step is to update the probability vector. DLRA applies the discrete pursuit reward inaction (DPRI) algorithm for updating probability vectors [91], which is able to obtain the best reward. The

3.3 Decentralized Learning based Relay Assignment algorithm

DPRI algorithm has been shown to exhibit good convergent properties, where the probability of the best state is increased and the probabilities of the other states are decreased. Thus, the minimum probability for all states is zero. The probabilities are updated according to the following equation:

$$P_{t+1}^i(j) = \begin{cases} \max\{p_t^i(j) - \Delta, 0\} & , \text{if } j \neq b_t^i \\ 1 - \sum_{j \neq b_t^i} p_{t+1}^i(j) & , \text{if } j = b_t^i \end{cases} \quad (3.8)$$

where $\Delta = \frac{1}{n(N_r+1)}$ is the smallest step size, and $n \in [1, \infty)$ is a resolution parameter used to determine the size of Δ . The pseudo code of DLRA is shown in Table 1 where T is the training period, and *end* means DLRA converges to one state.

3.3.3 Complexity

There are five loops in the pseudo-code, where the first loop contains a variable j from 1 to $N_r + 1$. The complexity the first loop is $O(N_r)$. The second loop contains the first loop and a variable from from 1 to T . The complexity of the second loop is $O(TN_r)$. The third loop contains a variable l from 1 to $N_r + 1$, so the complexity of the third loop is $O(N_r)$. The fourth loop contains a variable j from 1 to $N_r + 1$,so the complexity of the fourth loop is $O(N_r)$.

The fifth loop contains the second, third, fourth loop and a variable t from 1 to *end*. We use E to represent *end* which signifies the iterations that a source node needs for DLRA to converge. The complexity of the fifth loop is $O(E(TN_r + N_r + N_r)) = O(ETN_r)$. T and E are two constants for a node, so the complexity of DLRA is $O(N_r)$. It is the first degree polynomial in N_r . In contrast, the complexity of ORA and OPRA includes $O(N_s N_r^2)$ and $O(N_s^2 N_r)$, respectively.

3. DECENTRALIZED LEARNING-BASED RELAY ASSIGNMENT FOR COOPERATIVE COMMUNICATIONS

Algorithm 1 DLRA: Decentralized Learning based Relay Assignment algorithm

Initialization:

$$p_0(k) = \frac{1}{S}, \text{trial}(k) = 0, D(k) = 0, \forall k \in \{1, \dots, N_r + 1\}$$

$$i = 1, j = 1, l = 1, t = 0, \text{state} = 0, \text{Best} = 1$$

repeat

repeat

$$temp = rand()$$

repeat

if $temp < p_t(j)$ **then**

$$state \leftarrow j$$

$$trial(j) \leftarrow trial(j) + 1$$

break

else

$$temp \leftarrow temp - p_t(j)$$

continue

end if

$$j \leftarrow j + 1$$

until $j = N_r + 1$

 Calculate the capacity of the state according to (3.4).

$$D(\text{state}) \leftarrow D(\text{state}) + \text{capacity}$$

$$j \leftarrow 1$$

$$i \leftarrow i + 1$$

until $i = T$

$$i \leftarrow 1$$

repeat

$$D(l) = D(l)/\text{trial}(l)$$

if $D(\text{Best}) > D(l)$ **then**

$$Best \leftarrow l$$

end if

until $l = N_r + 1$

$$trail(k) = 0 \quad \forall k$$

$$D(k) = 0 \quad \forall k$$

$$p_{t+1}(\text{Best}) \leftarrow 1$$

repeat

if $j \neq \text{Best}$ **then**

if $p_t(j) > \Delta$ **then**

$$p_{t+1}(j) \leftarrow p_t(j) - \Delta$$

else

$$p_{t+1}(j) \leftarrow 0$$

end if

end if

$$p_{t+1}(\text{Best}) \leftarrow p_{t+1}(\text{Best}) - p_t(j)$$

$$j \leftarrow j + 1$$

until $j = N_r + 1$

$$t \leftarrow t + 1$$

until $t = \text{end}$





Although all three algorithms have polynomial complexity, it is obvious that the complexity of DLRA is much lower than the others.

3.4 Mathematical Analysis

3.4.1 Convergency

In this study, DLRA converges if a probability of one state achieves its maximum value, namely 1. DLRA then converges to this state. This section shows the convergency of DLRA. Suppose that the update policy as in (3.8) will increase the probability of the actual best state, $p_t(b)$ (the superscript i is dropped for brevity), with probability $\xi_t(b)$ and will decrease with probability $1 - \xi_t(b)$ at time t . Thus:

$$p_{t+1}(b) = \begin{cases} 1 - \sum_{j \neq b} \max\{p_t(j) - \Delta, 0\}, & \text{w.p. } \xi_t(b) \\ \max\{p_t(b) - \Delta, 0\}, & \text{w.p. } 1 - \xi_t(b) \end{cases} \quad (3.9)$$

where w.p. stands for "with probability." The algorithm is converged when $p_t(b) = 1 - N_r \Psi$. Suppose that the algorithm has not converged to state b yet; there then exists a state j with probability $p_t(j)$ ($j \neq b$) which satisfies the following:

$$p_t(j) > \max\{p_t(j) - \Delta, 0\} \quad (3.10)$$

According to the second axiom of probability:

$$p_t(b) = 1 - \sum_{j \neq b} p_t(j) \quad (3.11)$$

3. DECENTRALIZED LEARNING-BASED RELAY ASSIGNMENT FOR COOPERATIVE COMMUNICATIONS



and, thus

$$1 - \sum_{j \neq b} \max\{p_t(j) - \Delta, 0\} > p_t(b) \quad (3.12)$$

As long as there is at least one $p_t(j)$ which is larger than 0, $p_t(b)$ can be increased by decreasing $p_t(j)$, and the increasing amount is at least $\min\{p_t(j), \Delta\}$.

Therefore, (3.9) is re-written as:

$$p_{t+1}(b) = \begin{cases} p_t(b) + a_t \Delta, & \text{w.p. } \xi_t(b) \\ p_t(b) - \Delta, & \text{w.p. } 1 - \xi_t(b) \end{cases} \quad (3.13)$$

where $a_t \in (0, N_r]$.

For a given source node, the current system state which includes the algorithm state of the other source nodes is denoted as θ_t , and the probability vector of the source node is P_t . So, the expected value of $p_t(b)$ conditioned on θ_t and P_t can be calculated, and can be written as

$$E[p_t(b)|\theta_t, P_t] = \xi_t(b)\{p_t(b) + a_t \Delta\} + (1 - \xi_t(b))\{p_t(b) - \Delta\} \quad (3.14)$$

In (3.14), $p_t(b)$ does not achieve its maximum value 1. In the next step, the condition for $p_t(b)$ is derived to be a submartingale which means that the condition $p_t(b)$ is increased by achieving its maximum value 1. The definition of submartingale is shown as follows:

Definition 1. Submartingale: A discrete-time submartingale is a sequence $X_1, X_2, \dots, X_n, \dots$ of integrable random variables satisfying $E[X_{n+1}|X_1, \dots, X_n] \geq X_n$



Since the maximum value of $p_t(b)$ is 1, then:

$$\sup_{t \geq 0} E[p_t(b)|\theta_t, P_t] < \infty \quad (3.15)$$

and (3.14) can be rewritten as

$$E[p_t(b) - p_{t-1}(b)|\theta_t, P_t] = [\xi_t(b)(a_t + 1) - 1]\Delta \quad (3.16)$$

The right-hand-side of (3.16) ≥ 0 if and only if

$$\begin{aligned} \xi_t(b)(a_t + 1) - 1 &\geq 0 \\ \Rightarrow \quad \xi_t(b) &\geq 1/(a_t + 1) \end{aligned} \quad (3.17)$$

It is therefore a submartingale when (3.17) holds. Suppose that the algorithm satisfies the condition at time t_0 , and the condition holds for all $t > t_0$. So, according to the submartingale convergent theorem [92], the sequence $\{p_t(b)\}_{t > t_0}$ converge, such that

$$E[p_{t+1}(b) - p_t(b)|\theta_t, P_t] \rightarrow 0 \text{ w.p. } 1 \quad (3.18)$$

and the maximum value of $p_t(b)$, namely 1, is achieved as $t \rightarrow \infty$.

3.4.2 Asymptotic Theorems

Asymptotic theory is often used in mathematical sciences to provide limiting approximations of the probability distribution of sample statics. In this section, three asymptotic theorems of DLRA based on the technique presented by Oommen et al. [93] are established. In Theorem 1, it is shown that DLRA can reach the required number of trials in a finite time. Theorem 2 shows that if each state

3. DECENTRALIZED LEARNING-BASED RELAY ASSIGNMENT FOR COOPERATIVE COMMUNICATIONS



is chosen more than the required times, the best rate chosen actually has the best performance. Theorem 3 shows the optimality of DLRA.

Theorem 1. *For each state s_i , suppose $p_0(i) \neq 0$. Then, for any constant $\delta > 0$ and $M < \infty$, there exists $t_0 < \infty$ and $n_0 < \infty$ such that under DLRA algorithm, $\forall t > t_0, \forall n > n_0$:*

$$\Pr \{ \text{each state chosen more than } M \text{ times at time } t \} \geq 1 - \delta$$

Proof. Denote a random variable Z_i^t as the number of times that state s_i was chosen up to time t . Next, for any iteration of DLRA algorithm

$$\Pr\{s_i \text{ is chosen}\} \leq 1 \tag{3.19}$$

Likewise, the magnitude by which the probability of any state can decrease in any single iteration is bounded by Δ . Therefore, during any of the first t iterations of DLRA:

$$\Pr\{s_i \text{ is not chosen}\} \leq 1 - \max\{p_0(i) - t\Delta, 0\} \tag{3.20}$$

According to (3.19) and (3.20), the probability that state s_i is chosen at most M times among t choices satisfies the following:

$$\begin{aligned} \Pr\{Z_i^t \leq M\} &\leq \sum_{j=0}^M \binom{t}{j} (1)^j (1 - \max\{p_0(i) - t\Delta, 0\})^{t-j} \\ &= \sum_{j=0}^M \binom{t}{j} (1)^j \varphi^{t-j} \end{aligned} \tag{3.21}$$

It must now be shown that (3.21) is less than or equivalent to δ . To show the m th term in (3.21) is less than or equivalent to $\delta/(M + 1)$, and is sufficient to make a sum of $(M + 1)$ terms in (3.21) less than δ . Therefore, it must be proved that:

$$\begin{aligned} \binom{t}{m} (1)^m \varphi^{t-m} &\leq \delta/(M + 1) \\ \Rightarrow (M + 1) \binom{t}{m} \varphi^{t-m} &\leq \delta \end{aligned} \tag{3.22}$$

It is observed $\binom{t}{m} \leq t^m$, thus:

$$(M+1)t^m \varphi^{t-m} \leq \delta \quad (3.23)$$

In order to make the L.H.S. of (3.23) less than δ as t increases, φ must be strictly less than unity. Therefore, the value of $\Delta = 1/n(N_r + 1)$ is bounded to achieve this goal with respect to t by $\varphi < 1$. Thus:

$$\begin{aligned} 1 - [p_0(i) - t/n(N_r + 1)] &< 1 \\ \Rightarrow n &> \frac{t}{p_0(t)(N_r + 1)} \end{aligned} \quad (3.24)$$

So, the value of n is set to $\frac{2t}{p_0(t)(N_r + 1)}$ to achieve the requirement. Then, according to (3.21), (3.22) and (3.23):

$$\Pr\{Z_i^t \leq M\} \leq (M+1)t^m \varphi^{t-m} \quad (3.25)$$

The R.H.S. of (3.25) is considered when t approaches infinity:

$$\lim_{t \rightarrow \infty} (M+1)t^m \varphi^{t-m} = (M+1) \lim_{t \rightarrow \infty} t^m \frac{1}{(1/\varphi)^{t-m}} \quad (3.26)$$

By using L'Hopital's rule m times, the following is obtained:

$$(M+1) \lim_{t \rightarrow \infty} \frac{m!}{(\ln(\frac{1}{\varphi}))^m (\frac{1}{\varphi})^{t-m}} = 0 \quad (3.27)$$

Thus, since the limit exists, for every state s_i , there is a $t(i)$ such that $\Pr\{Z_i^t \leq M\} \leq \delta$ for all $t > t(i)$. In addition, for any $t > t(i)$, since $Z_i^{t(i)} \geq M$ implies $Z_i^t \geq M$. So, by the law of probability:

$$\Pr\{Z_i^t \leq M\} > \Pr\{Z_i^{t(i)} \leq M\} \quad (3.28)$$

Therefore, for any state s_i , $\Pr\{Z_i^t \leq M\} \leq \delta$ whenever $t > t(i)$. Define

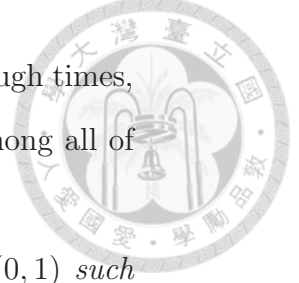
$$t_0 = \max_{1 \leq i \leq N_r + 1} \{t(i)\} \quad (3.29)$$

In this way, it is true, for all $t > t_0$, $\Pr\{Z_i^t \leq M\} \leq \delta$ for all i , and it implies

$$\Pr\{Z_i^t \geq M\} \geq 1 - \delta \quad (3.30)$$

□

3. DECENTRALIZED LEARNING-BASED RELAY ASSIGNMENT FOR COOPERATIVE COMMUNICATIONS



Next, the second theorem shows that if all the states are chosen enough times, the best state chosen by DLRA actually has the best performance among all of the states.

Theorem 2. *There exists an integer, denoted by M , for every $\delta \in (0, 1)$ such that if every state s_i is selected at least M times by time t :*

Pr {the best state chosen by DLRA actually has the best performance among all states} $> 1 - \delta \Rightarrow \Pr\{\hat{b}_t = \arg \max_j d(j)\} > 1 - \delta$

Proof. Denote h as the difference between the two largest performances in the network system. By this assumption, the best performance for the best state, $d(b)$, is unique, therefore, $h > 0$ and $d(b) - h \geq d(i) \forall i \neq b$. Let Z_i^t be the number of times s_i is chosen up to time instant t . Suppose $\hat{d}_t(i)$ is the estimator of the performance of state s_i at time t , Then, according to the weak law of large numbers, for a given $\delta > 0$, there exists an $M_i < \infty$, such that, if s_i is chosen at least M_i times:

$$\Pr\{|\hat{d}_t(i) - d(i)| < h/2\} > 1 - \delta \quad (3.31)$$

Let $M = \max_{1 \leq i \leq N_r+1} \{M_i\}$, and if $\min_{1 \leq i \leq N_r+1} \{Z_i^t\} > M$, then:

$$\Pr\{|\hat{d}_t(b) - d(j)| < h/2\} < 1 - \delta, \forall j \neq b \forall t \quad (3.32)$$

From Theorem 1, a t_0 can be found such that

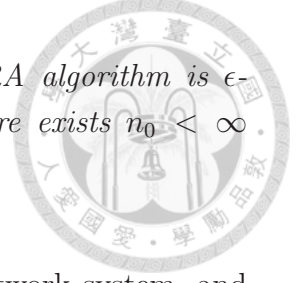
$$\Pr\{\min_{1 \leq i \leq N_r+1} \{Z_i^t\} > M\} > 1 - \delta, \forall t > t_0 \quad (3.33)$$

Therefore, it is known that each $\hat{d}_t(i)$ will be in an $h/2$ neighborhood of $d(i)$ if all states are chosen at least M times. So:

$$\begin{aligned} \hat{d}_t(b) &\geq d(b) - h/2 > d(i) - h/2 \\ \Rightarrow \hat{d}_t(b) &\geq \hat{d}_t(i) \end{aligned} \quad (3.34)$$

□

Based on the two previous theorems, the last theorem can be obtained. The last theorem shows the optimality of DLRA which means that the probability of the best state achieves its maximal value.



Theorem 3. *In every stationary network system, the DLRA algorithm is ϵ -optimal. More explicitly, given any $\epsilon > 0$ and $\delta > 0$, there exists $n_0 < \infty$ and $t < \infty$ such that:*

$$\Pr\{|p_b(t) - 1| < \epsilon\} > 1 - \delta$$

Proof. According to Theorem 2, M is a constant for each network system, and by Theorem 1, there exists $t_0 < \infty$ and $n_0 < \infty$, such that, under DLRA:

$$\Pr\{Z_i^t > M\} > 1 - \delta \quad (3.35)$$

Then, define U and V as the two events shown as follows:

$$\begin{cases} U \equiv |p_b(t) - 1| < \epsilon \\ V \equiv \max_{1 \leq i \leq N_r+1} \{\hat{d}_t(i) - d(i)\} < h/2 \end{cases} \quad (3.36)$$

So

$$\Pr\{U|V\} = \Pr\{|p_b(t) - 1| < \epsilon \mid \max_{1 \leq i \leq N_r+1} \{\hat{d}_t(i) - d(i)\} < h/2\} \quad (3.37)$$

According to the previous discussion:

$$\lim_{t \rightarrow \infty} \Pr\{U|V\} \rightarrow 1 \quad (3.38)$$

By Theorem 2 and (3.35):

$$\lim_{t \rightarrow \infty} \Pr\{V\} \rightarrow 1 - \delta \quad (3.39)$$

By the law of total probability and probability is a continuous function, then:

$$\lim_{t \rightarrow \infty} \Pr\{U\} \geq \lim_{t \rightarrow \infty} \Pr\{U|V\} \lim_{t \rightarrow \infty} \Pr\{V\} \quad (3.40)$$

From (3.38), (3.39), and (3.40):

$$\lim_{t \rightarrow \infty} \Pr\{|p_b(t) - [1 - N_r \Psi]| < \epsilon\} \geq 1 - \delta \quad (3.41)$$

□

Proposition 1. *DLRA converges under any initialization of P_0 .*

Proof. Assume that $P_0 = \{P_0(1), P_0(2), \dots, P_0(N_r + 1)\}$, and we discuss in three cases:

3. DECENTRALIZED LEARNING-BASED RELAY ASSIGNMENT FOR COOPERATIVE COMMUNICATIONS



(1) If $P_0(i) > 0 \forall i$:

The discussion was mentioned before in this section. When (3.17) holds, the sequence $p_b(t)$ is a submartingale, therefore, DLRA converges to the best state. According to theorem 2, there always exists an integer M ; thus, (3.17) always holds true. DLRA converges to the best state under this case.

(2) If $P_0(i) = 0$ and $i \neq b$

When DLRA converges to the best state, the value of $P_0(i) \forall i$ is zero. Therefore, we can say that the sequence $p_t(i)$ converged in this initial condition. Therefore, DLRA would converge to the best state, namely $P_b(t) = 1$, eventually.

(3) If $P_0(b) = 0$

Since the probability of the best state is zero in the initial condition, DLRA cannot converge to the best state b . Suppose \hat{b} , the best state, excludes the original best state b among all states. Therefore, denote $\xi(\hat{b})$ as the probability that the update policy would actually increase the value of $p_t(\hat{b})$. We can consider this condition as signifying that the best state b no longer exists in the system. It is the case (1) where the best state becomes \hat{b} . So, DLRA will converge to the state \hat{b} , namely $p_{\hat{b}}(t) = 1$.

According to the discussion on the three cases, we conclude that DLRA converges under any initialization of P_0 . \square

Proposition 2. *DLRA converges under any channel fading model.*

Proof. The impact of channel fading model is included in the variable θ_t . According to Theorem 2, there always exists an M for variable $\xi_t(b)$ to meet (3.17). The different channel fading models have different value of M . Since M always exists, DLRA converges in any channel model. \square

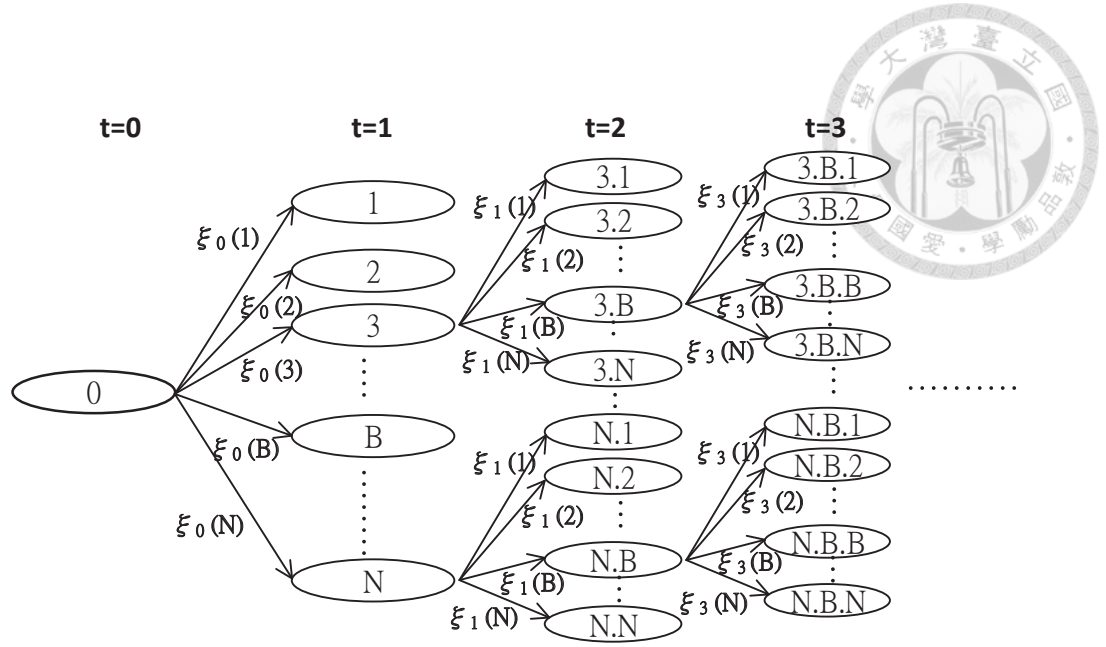


Figure 3.2: State transition diagram of DLRA.

3.4.3 Performance

In this section, we provide a comprehensive performance analysis based on mathematical manipulation. Assume that each source node assigns equal probability of each choice in the beginning, namely each choice has probability $1/N$ of being chosen. Fig. 3.2 shows the state transition diagram of one node in DLRA; the different states stand for the different evolutions of probability vector. In Fig. 3.2, N is the number of choice, $\xi_i(j)$ is the probability that the probability of choosing choice j is increased at time i , and S_i stands for the state i . In this section, different choices refer to different relay selections, and each state stands for a probability vector of relay selections. Suppose the performance of choice i is denoted by C_i . Therefore, the expected performance of initial state, namely

3. DECENTRALIZED LEARNING-BASED RELAY ASSIGNMENT FOR COOPERATIVE COMMUNICATIONS



state 0 in Fig. 3.2, is:

$$E[S_0] = \sum_{i=1}^N P_i \times C_i = \sum_{i=1}^N \frac{1}{N} \times C_i = \frac{\sum_{i=1}^N C_i}{N} \quad (3.42)$$

In Fig. 3.2, state i ($i \in \{1, \dots, N\}$) stands for the probability of choosing choice i is increased, and decreased for the others; assume the step size is Δ .

Therefore, the expected performance of state i is:

$$\begin{aligned} E[S_i] &= \sum_{j=1, j \neq i}^N \left(\frac{1}{N}\right) C_j + \left[\frac{1}{N} + (N-1)\Delta\right] C_i \\ &= \left(\frac{1}{N} - \Delta\right) \sum_{j=1, j \neq i}^N C_j + \frac{C_j}{N} + \Delta(N-1)C_j \\ &= \frac{\sum_{i=1}^N C_i}{N} + \Delta \sum_{j=1}^N (C_i - C_j) \end{aligned} \quad (3.43)$$

In this state diagram, there are 1 and N states when $t = 0$ and $t = 1$, respectively. The number of states is N^2 when $t = 2$, and the value is increased to N^T when $t = T$. It is an unaccepted number of states and too complicated to solve, via this diagram, when t is getting larger.

We combine the states which are not the best choice into one state, and assume that these states have the same performance which is denoted by C_a , and less than the best one denoted by C_b . Besides, we assume that $\xi_b(t)$ is the same for all t . According to the asymptotic theorem, this hypothesis is reasonable, and $p = \xi_b(t)$ is assumed for simplicity. Therefore, the new diagram is modeled as a Markov chain and is shown as Fig. 3.3.

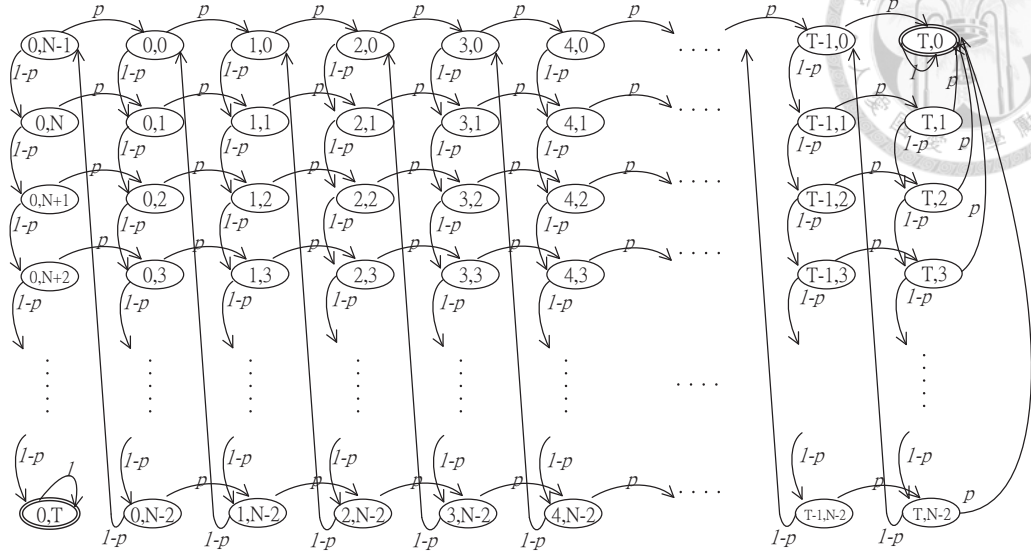


Figure 3.3: Markov chain model of DLRA.

In Fig. 3.3, the initial state is $(0, 0)$, and the two absorbing states are $(T, 0)$ and $(0, T)$. The absorbing states mean that the probability of choosing the best choice is equal to either 1 or 0, and $T = \text{ceil}(1/\Delta N)$. State (i, j) transits to state $(i + 1, j)$ with probability p ; it means that the probability of choosing the best choice is increased by $(N - 1)\Delta$ with probability p . Similarly, state (i, j) transits to state $(i, j + 1)$ with probability $1 - p$; it means the probability of choosing the best choice is decreased by Δ . On the other hands, the probability of the best choice is equal to 1 and 0 in the states $(T, 0)$ and $(0, T)$, respectively. According to the asymptotic theorem, the probability to absorb in state $(0, T)$ approaches to zero.

State (i, j) can be considered as that the probability of choosing the best choice is increased by i times and decreased by j times from the initial state.

3. DECENTRALIZED LEARNING-BASED RELAY ASSIGNMENT FOR COOPERATIVE COMMUNICATIONS



Therefore, the probability can be calculated as follows:

$$p_b^{ij} = \frac{1}{N} + [(N-1)i - j]\Delta \quad (3.44)$$

Then, we have the expected performance of state (i, j) :

$$E[S_{ij}] = (1 - p_b^{ij})C_a + p_b^{ij}C_b \quad (3.45)$$

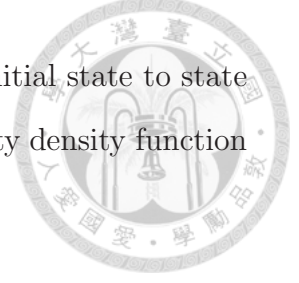
Now, we show the expected performance after t transitions from the initial state. If there are i transitions to increase the probability of choosing the best choice, and j transitions to decrease this value, the state after this $(i+1)$ transitions will be: $(\min\{i - \text{floor}(\frac{j}{N-1}), T\}, j\%(N-1))$. Therefore, suppose that there are i transitions to increase the probability of choosing the best choice among all t transitions. The state will be $(f(i), g(i))$ with probability $p^i(1-p)^j$, where $f(i)$ and $g(i)$ are shown as follows:

$$\begin{cases} f(i) &= \min\{i - \text{floor}(\frac{t-i}{N-i}, T)\} \\ g(i) &= (t-i)\%(N-1) \end{cases} \quad (3.46)$$

So, the expected performance after t transitions is:

$$E[\text{performace at } t] = \sum_{i=0}^t \binom{t}{i} p^i (1-p)^{t-i} E[S_{f(i),g(i)}] \quad (3.47)$$

Next, we calculate how many transitions DLRA will take from the initial state to the absorbing state $(T, 0)$. Assume Y is the number of transitions DLRA will take from the initial state to state $(T, 0)$. The least value of Y is T and $\Pr\{Y = T\} = p^T$. It occurs while the probability of choosing the best choice is always increased from the initial state. If the decrement happens only once before transiting to the state $(T, 0)$, the value of Y is $T+2$ and $\Pr\{Y = T+2\} =$



$\binom{T+2}{1}P^{T+1}(1-p)$. Generally, it takes $T + N$ steps from the initial state to state $(T, 0)$ with probability $\binom{T+N}{N-1}p^{T+1}(1-p)^{N-1}$. So, the probability density function of Y is shown as follows:

$$\Pr\{Y = T + j + ij\} = \begin{cases} p^T & , i = j = 0 \\ \binom{T+j+ij}{T+j} p^T [p(1-p)]^j & , i \in \mathcal{N}, j = 1, \dots, N-1 \\ 0 & , i = 0, j \neq 0 \end{cases} \quad (3.48)$$

Thus, we have the expected number of transitions of DLRA would take; it can be shown as follows:

$$E[Y] = p^T T + \sum_{j=1}^{\infty} \sum_{i=1}^{N-1} \binom{T+j+ij}{T+j} p^T [p(1-p)]^j (T+i+ij) \quad (3.49)$$

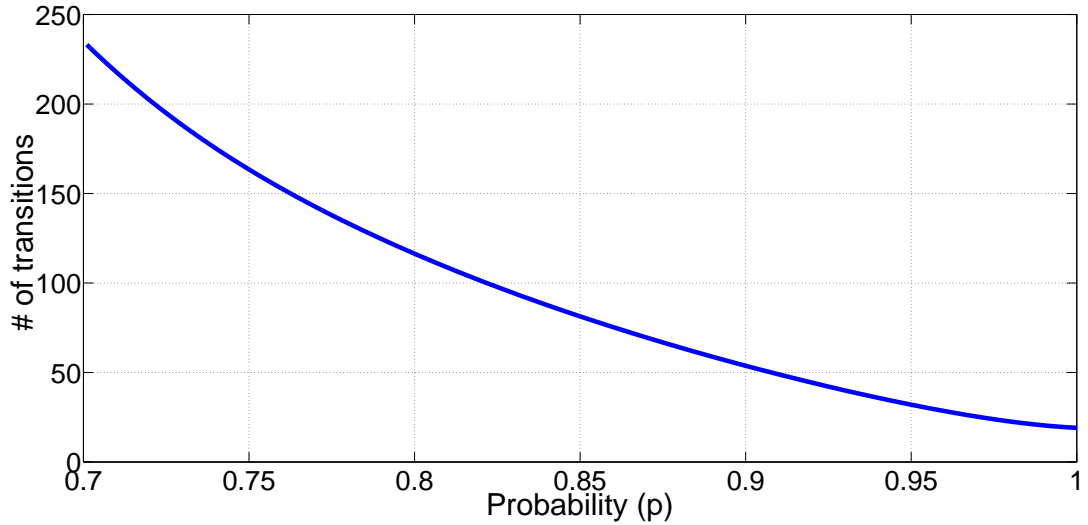


Figure 3.4: The number of transitions DLRA would take vs. the probability $\xi(b)$

According to (3.49), we have Fig. 3.4 where we suppose $N = 11$ and $\Delta = 0.005$. It is obvious that the number of transitions increased with the decreased value of p . It takes about 250 transitions to converge when the probability is equal to 0.7.



3.5 performance evaluation

In this section, experimental results are presented for the evaluation of the performance of the DLRA algorithm. The experiments are performed in two different network systems: one is a cooperative ad hoc network, and the other is a cooperative communication system in an LTE-advanced network.

3.5.1 Cooperative Ad Hoc Network

In this section, the goal is to show that DLRA, which is a decentralized approach, is efficient as centralized approaches. The centralized approach compared is ORA, proposed by Sharma et al. [43], because it is possible to obtain the whole detailed network topology according to the work. A cooperative ad hoc network topology is constructed, in which each source node is associated with a specific destination node. The number of source nodes and destination nodes is therefore the same. It is assumed that the capacity of each source node is obtained from the feedback information of the relay nodes. The simulation topologies and parameters are the same as in [43]. These simulation settings are first used to evaluate the performance of ORA. The performance of DLRA is then compared with that of ORA with these settings to show DLRA's effectiveness in cooperative communications.

3.5.1.1 Simulation Settings

Two cases are considered in this experiment: one is that the number of source nodes is larger than the number of relay nodes, and the other is that there are

fewer source nodes than relay nodes. In the first case, there are 30 source-destination pairs, and 40 relay nodes, namely: $N_x = N_y = 30$ and $N_r = 40$; in the second case, there are 40 source-destination pairs, and 20 relay nodes, namely: $N_x = N_y = 40$ and $N_r = 20$. The location of each node is given in [43].

Assume $W = 10$ MHz bandwidth for each channel, and the transmission power of each node is set to 1 watt. The AF mode is employed on each relay node, and the channel gain only considers the path-loss component between two nodes with path-loss index 4. The AWGN channel is assumed to have a variance of noise of 10^{-10} watts at all nodes.

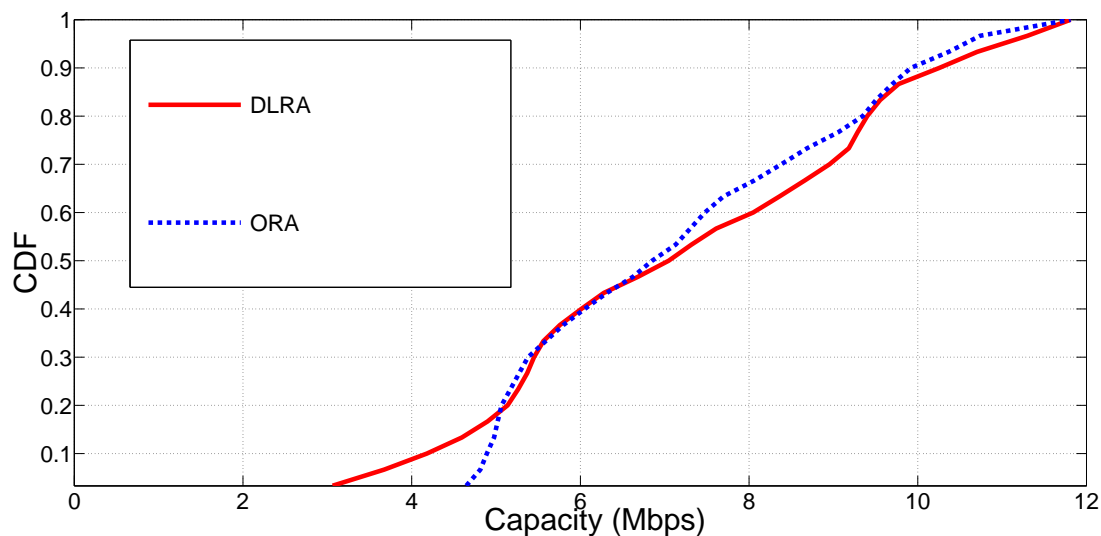


Figure 3.5: The CDF of the capacity of all source nodes for the two algorithms in the environment while $N_s < N_r$.

3.5.1.2 Comparisons

3. DECENTRALIZED LEARNING-BASED RELAY ASSIGNMENT FOR COOPERATIVE COMMUNICATIONS

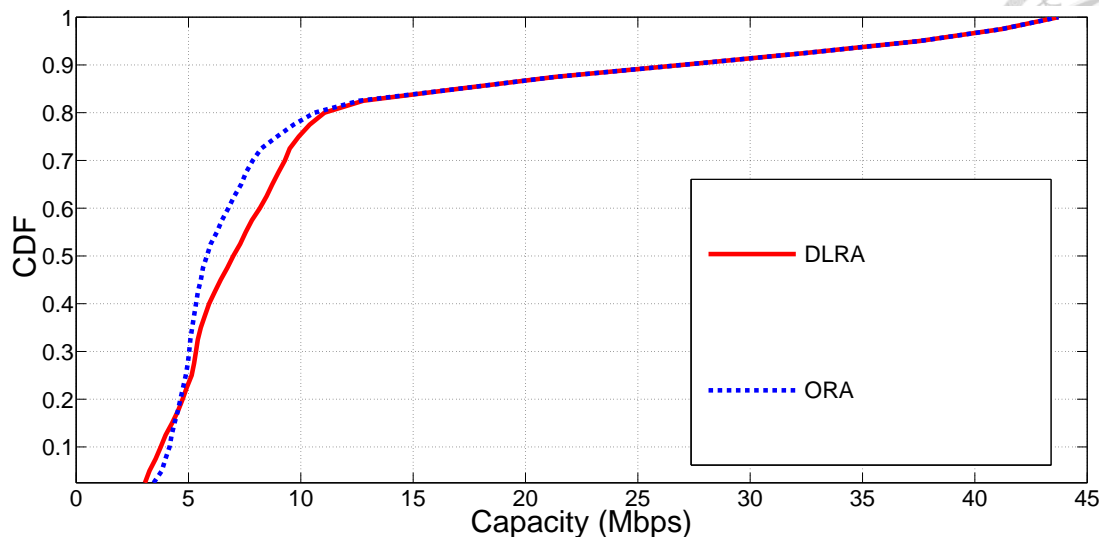


Figure 3.6: The CDF of the capacity of all source nodes for the two algorithms in the environment while $N_s > N_r$.

Figs. 3.5 and 3.6 represent the cumulative distribution function (CDF) of ORA and DLRA in two different cases respectively, and the simulation topologies are shown in [43]. The goal of the experiments is to show the effectiveness of DLRA in a cooperative communication system; the performance of DLRA is compared with that of ORA to achieve this.

Because ORA maximizes the minimal capacity, the performance of the 95th percentile user in ORA is better in DLRA. On the other hand, DLRA exhibits better performance than ORA in both mean and median, as shown in Fig. 3.7. In Fig. 3.6, the number of source nodes is larger than the number of relay nodes, so many source nodes exhibit the best performance with direct transmission. Therefore, the CDF of ORA and DLRA overlap on about the top 20% of users.

The experimental environments are designed to first evaluate the performance of ORA. In this experiment, for the edge users, ORA is better than DLRA; for average performance and median users, DLRA is better than ORA. So, it is

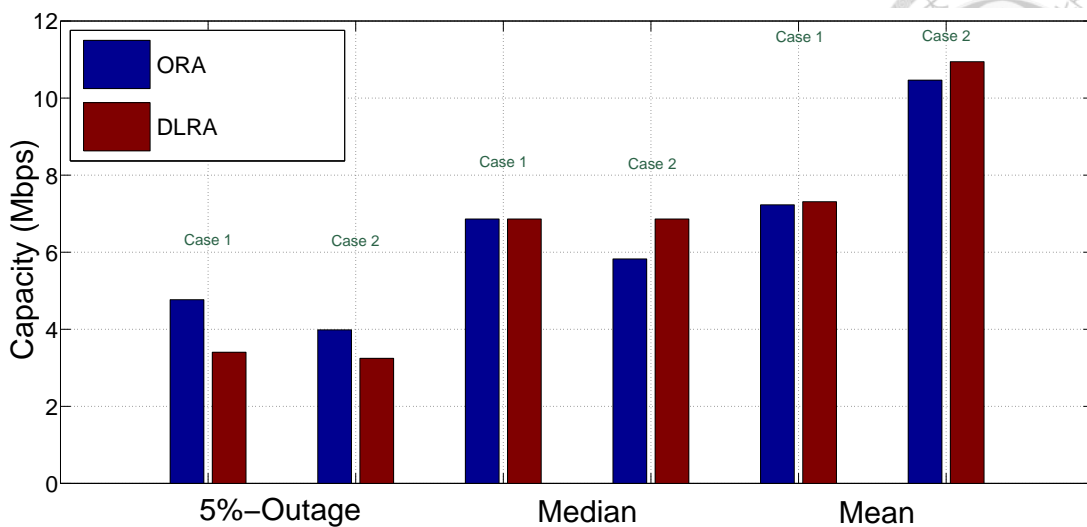


Figure 3.7: The 5%-outage, median and mean capacity of DLRA and ORA in both cases.

hard to say which one is better. According to the results, DLRA, which is a decentralized approach, and ORA, which is a centralized approach, are both effective in cooperative ad hoc networks.

3.5.2 LTE-Advanced Network

The second network system is a relay network in an LTE-Advanced environment. In this experiment, many user devices transmit to the macro base station (BS) with the help of relay nodes.

3.5.2.1 Simulation Settings

3. DECENTRALIZED LEARNING-BASED RELAY ASSIGNMENT FOR COOPERATIVE COMMUNICATIONS

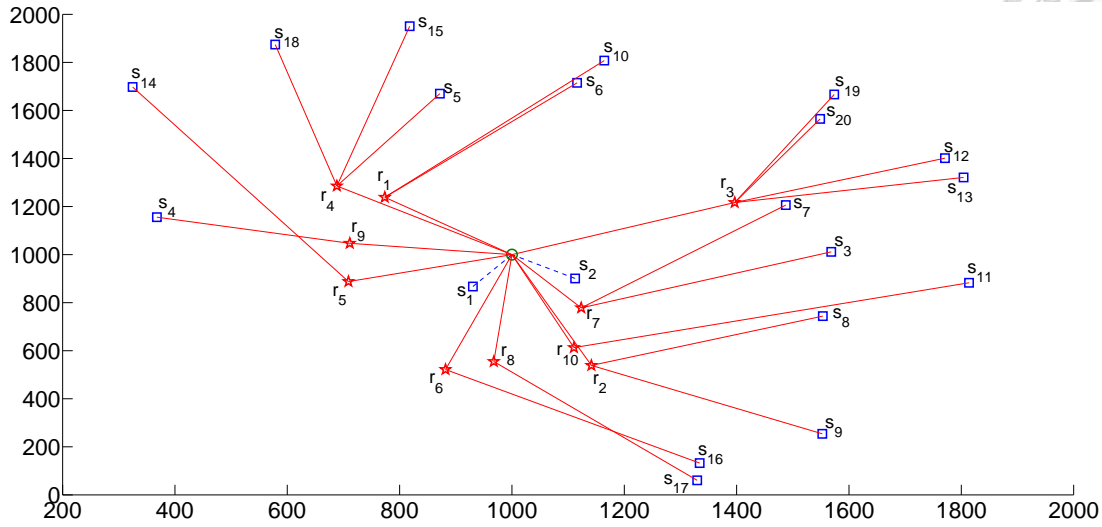


Figure 3.8: The network topology of the simulation and the corresponding relay selection result for each source node.

A relay network topology, as shown in Fig. 4.6, is assumed, in which all source nodes have the same destination. In this topology, there are 20 source nodes, 10 relay nodes and 1 destination node at position (1000,1000). Since relay nodes are used to expand the coverage range of the macro BS in LTE-advanced networks, all source nodes, namely UEs, transmit data to the destination, namely the macro BS. So, $N_x = 20$, $N_r = 10$, and $N_y = 1$ which means that $Y(x_1) = \dots = Y_{x_{N_x}}$, and the experimental parameters follow the simulation methodologies of 3GPP specifications [94]. Both large and small scale fading is adopted in the simulations: the shadowing model is two-way ground fading and the fading model is a Rayleigh fading model. The maximum transmission power of UEs and relay nodes are set to 23 dBm and 30 dBm, respectively. The total bandwidth of the system is 100 MHz and the noise power density of the system is -174 dBm/Hz.

When a source node chooses a relay node for transmission, it receives a physical downlink control channel (PDCCH) which contains information detailing the

radio resources available to the source node. The source node reports the channel information to the relay node by channel quality index (CQI), and the source node knows the modulation and coding scheme (MCS) that it uses. Therefore, the source nodes understand the capacity according to the information received.

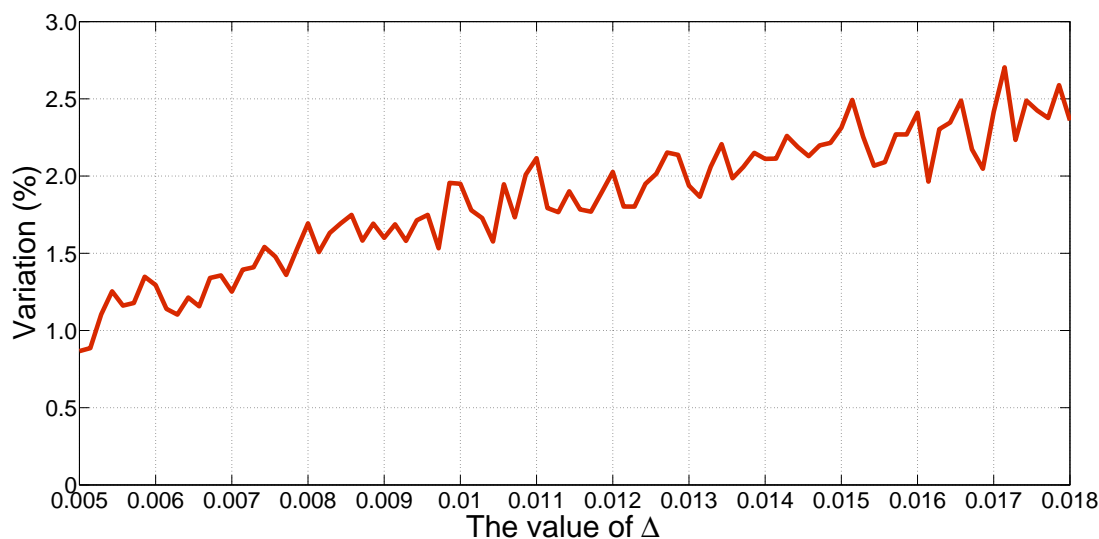


Figure 3.9: The variation of aggregate performance of average results with different values of Δ .

3.5.2.2 Convergency

This section shows the performance of DLRA with different parameters and the convergent process. The Δ parameter influences the learning rate and final results; the convergency of DLRA over Δ is examined first. Fig. 3.9 shows the variation of aggregate performance over Δ , where experiments are run 1000 times to obtain each point in the fixed topology, as shown in Fig. 4.6. A smaller Δ implies that a stable state is more precisely found, but takes more time to

3. DECENTRALIZED LEARNING-BASED RELAY ASSIGNMENT FOR COOPERATIVE COMMUNICATIONS

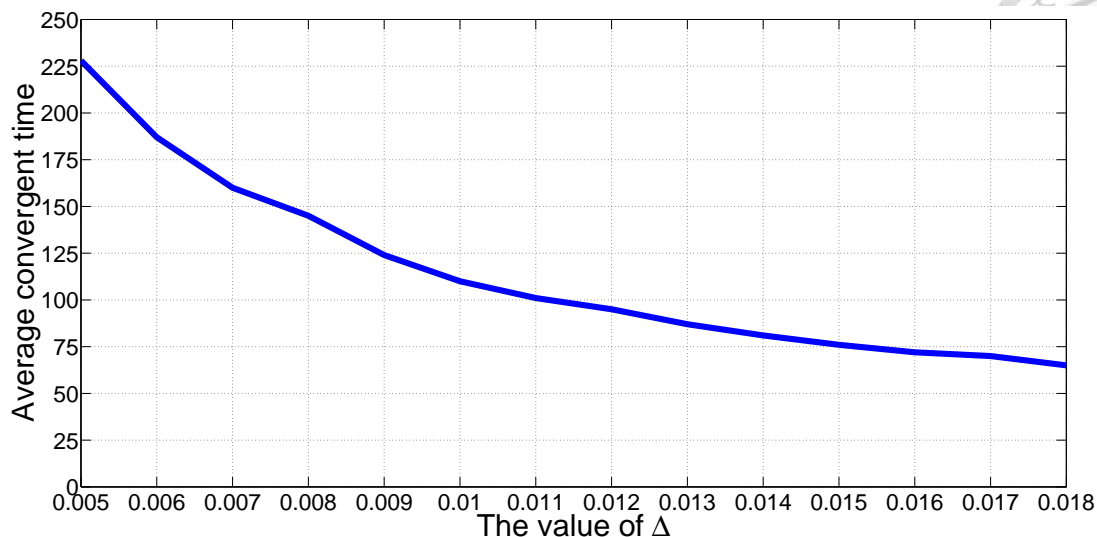


Figure 3.10: The average convergent time with different values of Δ .

converge. DLRA with $\Delta = 0.005$ effects about a 1% variation of aggregate performance for average results. Because of the distributed nature of DLRA, the convergent time of each UE is not the same. The average convergent time of DLRA over Δ is shown in Fig. 3.10. DLRA converges in 75 iterations with $\Delta = 0.0018$ and in about 225 iterations with $\Delta = 0.005$ —the larger Δ makes the convergent time shorter.

Fig. 4.6 also shows the DLRA relay node selection result, which is represented by the solid red lines. It is observed that most UEs are served by relay nodes, besides s_1 and s_2 . Both know that transmitting using shared relay nodes is pointless from the environmental feedbacks since they are close to the macro BS. On the other hand, DLRA also performs load balancing for relay nodes within the network; for example, s_7 chooses a lighter loaded r_7 rather than the nearest, but heavily loaded r_3 . In this scenario, r_3 is actually more necessary for other users like s_{12} and s_{19} , and r_3 therefore responds to s_7 with feedback that is less

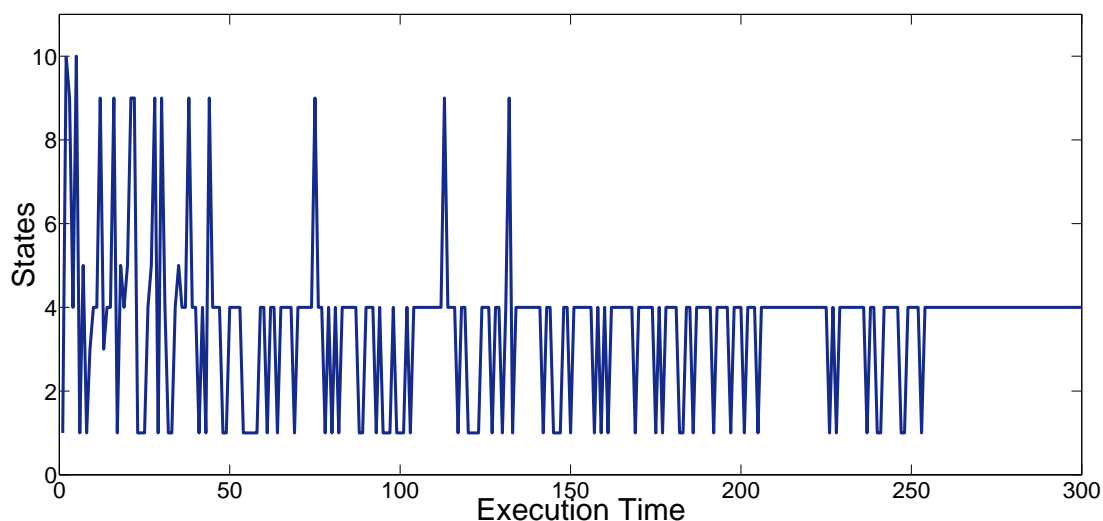


Figure 3.11: The state evolution of source node 5.

unsatisfied than the feedback r_7 .

Next, s_5 is chosen to show the convergency of DLRA. Figs. 3.11 and 3.12 show the state and performance evolution for s_5 , respectively. In the beginning of the experiment, they oscillate dramatically because the probability of each state is the same. As time passes, it is observed that the selected states of s_5 oscillate between r_1 , r_4 and r_9 in Fig. 3.11. The selected probabilities of other inappropriate states (the farther relay nodes) are decreased to zero. Finally, s_5 converges to r_4 and its performance converges to about 7 Mbps.

The evolution of the probability distribution over time for s_5 is plotted in Fig. 3.13. The probability of each state is the same in the beginning, and then the probabilities of r_1 , r_4 and r_9 increase while those of others decrease. Finally, s_5 converges to r_4 in about 275 iterations. In these results, the small scale fading is not adopted in the simulation. Next, we show the impact of different fading models on DLRA. Figs. 3.13 and 3.14 show the evolution of the probability

3. DECENTRALIZED LEARNING-BASED RELAY ASSIGNMENT FOR COOPERATIVE COMMUNICATIONS

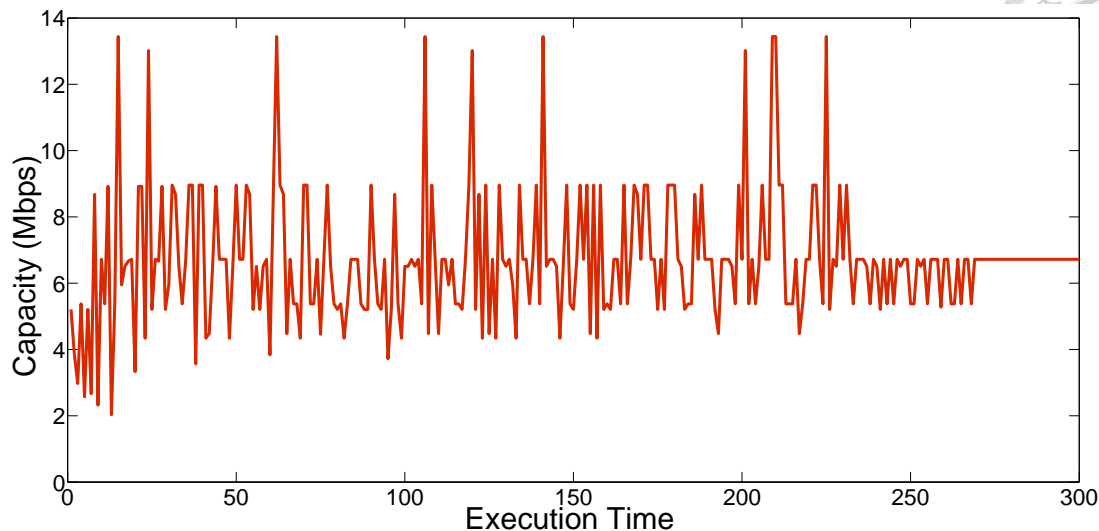


Figure 3.12: The performance evolution for source node 5.

distribution over time for s_5 without and with Rayleigh fading, respectively. The results follow our intuition that DLRA takes more time to converge under a dramatically varying channel. Fig. 3.14 shows that DLRA takes about 550 iterations to converge with Rayleigh fading.

Lastly, we show the convergency under different initialization of P_0 . We pick s_3 for this simulation, and r_7 is the best choice for s_3 according to Fig. 4.6. The simulation is run in three cases of P_0 :(1) uniform distribution, (2) non-uniform distribution where the probability of the best state is not equal to 0, and (3) the probability of the best state is equal to 0. In the second case, we set the probability of the best state much lower than r_{10} , which is the second best state. According to Proportion 2, DLRA converges under initialization of P_0 . Figs. 3.15(a) and 3.15(b) shows that DLRA eventually converges to the best state; even the probability of the best state is much lower than the others. Fig. 3.15(c) shows DLRA converges to r_{10} , and the convergent speed is fast because that r_7

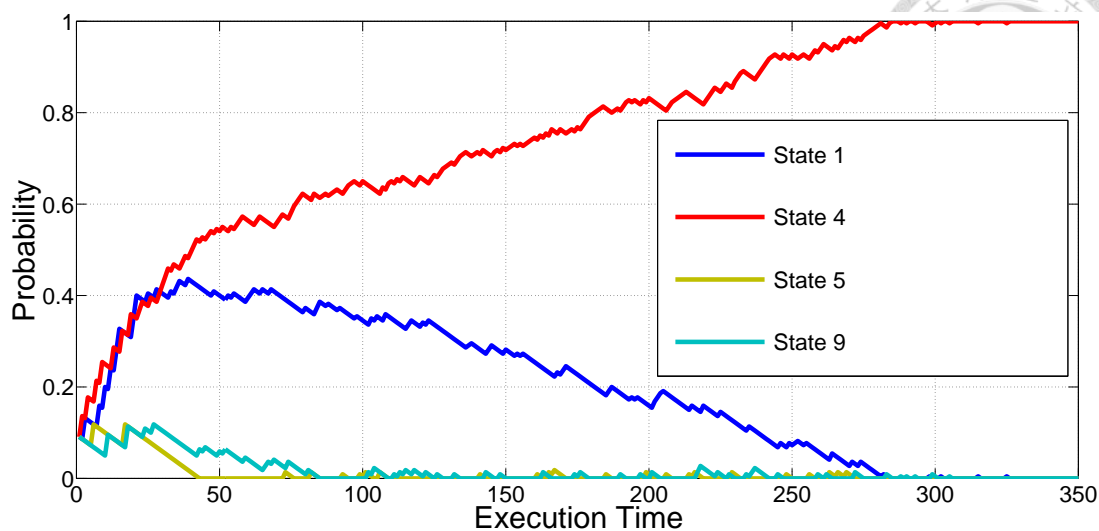


Figure 3.13: The probability vector evolution for source node 5 without small scale fading.

and r_{10} compete in the first and the second case, but the competition disappears when the probability of r_7 is equal to 0. Therefore, DLRA converges to r_{10} fast.

3.5.2.3 Capacity and Fairness

In this section, the performance of DLRA is compared with those of other algorithms, namely OPRA, ORA, Greedy and direct transmission, from the viewpoints of capacity and fairness. Fig. 3.16 shows the CDF capacity of all algorithms. Because the objective of OPRA is to maximize the aggregate capacity, it assigns relay nodes to UEs with good channel conditions in order to achieve this goal. This objective results in a gap between cell-edge UEs and superior UEs. Assigning relay nodes to UEs with good channel conditions infringes on the essential goal of relay nodes. By contrast, ORA aims to maximize the minimum capacity among all UEs, and therefore attempts to assign relay nodes to cell-edge

3. DECENTRALIZED LEARNING-BASED RELAY ASSIGNMENT FOR COOPERATIVE COMMUNICATIONS

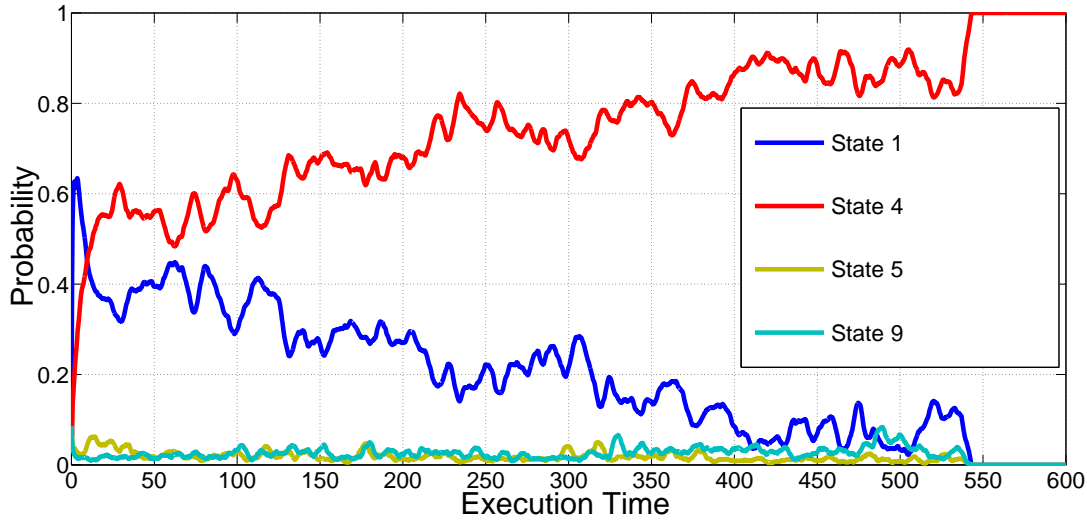


Figure 3.14: The probability vector evolution for source node 5 with Rayleigh fading.

UEs. ORA assumes that each relay node only serves one UE. Therefore, when the number of relay nodes is less than the number of UEs, the benefits of ORA are limited. DLRA performs better than ORA since it helps more inferior UEs that determine their own preferred states according to environmental feedback.

Fig. 3.17 shows the aggregate capacity of all algorithms. As expected, OPRA performs best in this objective regardless of the original intention of relay nodes. DLRA is the second among them, and it shows that by having each UE choose its preferred method for transmission, good performance can be achieved. Although DLRA is not optimal in terms of aggregate capacity, its performance is close to that of OPRA. To quantify the effect of enhancement after relay nodes help, the *improvement factor* is defined as:

$$\text{Improvement Factor} = \frac{C_{Final} - C_{Direct}}{C_{Direct}} \quad (3.50)$$

where C_{Final} is the final performance of each UE after relay assignment, and

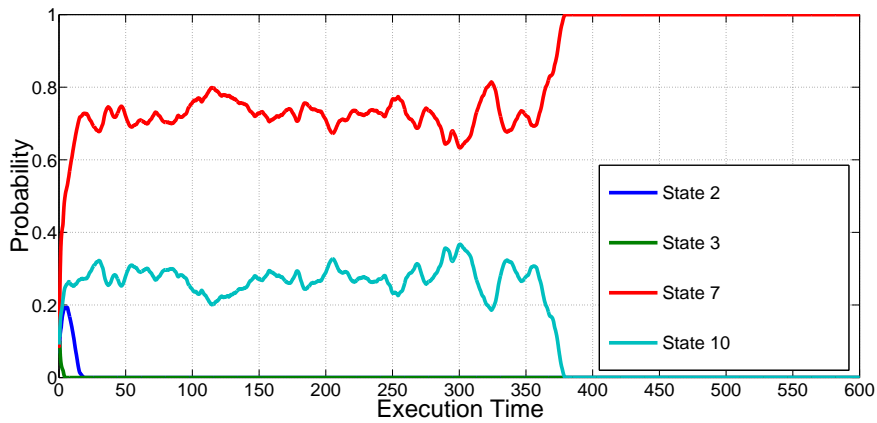
C_{Direct} is the performance with direct transmission. Fig. 3.18 shows the average improvement for all algorithms. The average improvement of OPRA is less than that of ORA because the ratio of enhancement to direct transmission is relatively small for superior UEs. DLRA decreases the enhancement of performance for originally benefited UEs, particular superior UEs, in order to improve the capacity of other UEs. So, the number of UEs which get help and the average improvement are both increased. DLRA, being a fully-distributed algorithm, is thus better than centralized algorithms in terms of this aspect.

Finally, the fairness among all algorithms is compared. Jain's fairness index (JFI) [95] is used as the criterion of comparison among all algorithms, and JFI is:

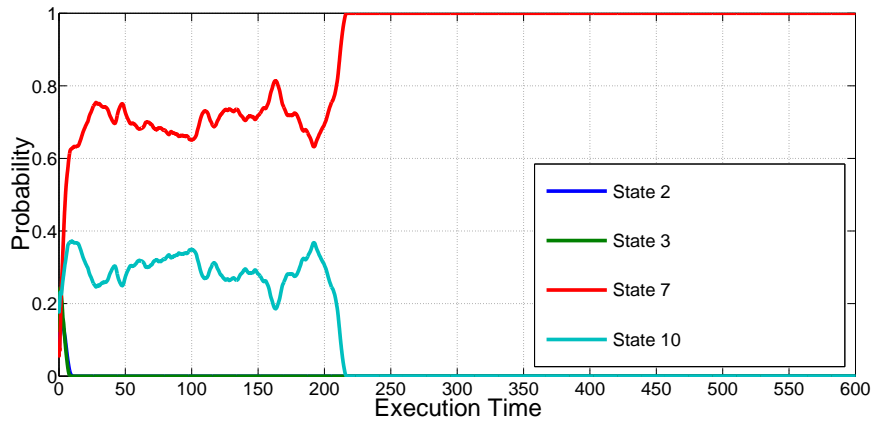
$$JFI = \frac{(\sum_{i=1}^n C_i)^2}{n \sum_{i=1}^n C_i^2} \quad (3.51)$$

Compared with other algorithms, UEs collect environmental information and determine the best relay nodes for themselves in DLRA. Therefore, the difference of the final capacity among UEs is not large. The JFI of DLRA is the best among these algorithms. ORA has the second highest JFI since it assigns relay nodes to cell-edge UEs, but ORA is limited; in that each relay node can serve only one UE. Therefore, the JFI of ORA slightly less than that of DLRA.

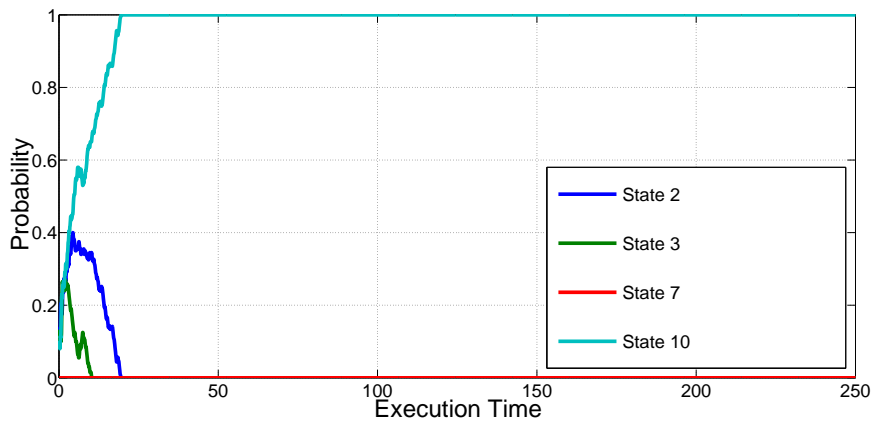
3. DECENTRALIZED LEARNING-BASED RELAY ASSIGNMENT FOR COOPERATIVE COMMUNICATIONS



(a)



(b)



(c)

Figure 3.15: Different initialization of P_0 : (a) Uniform distribution, (b) Non-uniform distribution and the probability of the best state is not equal to 0, and (c) the probability of the best state is equal to 0.

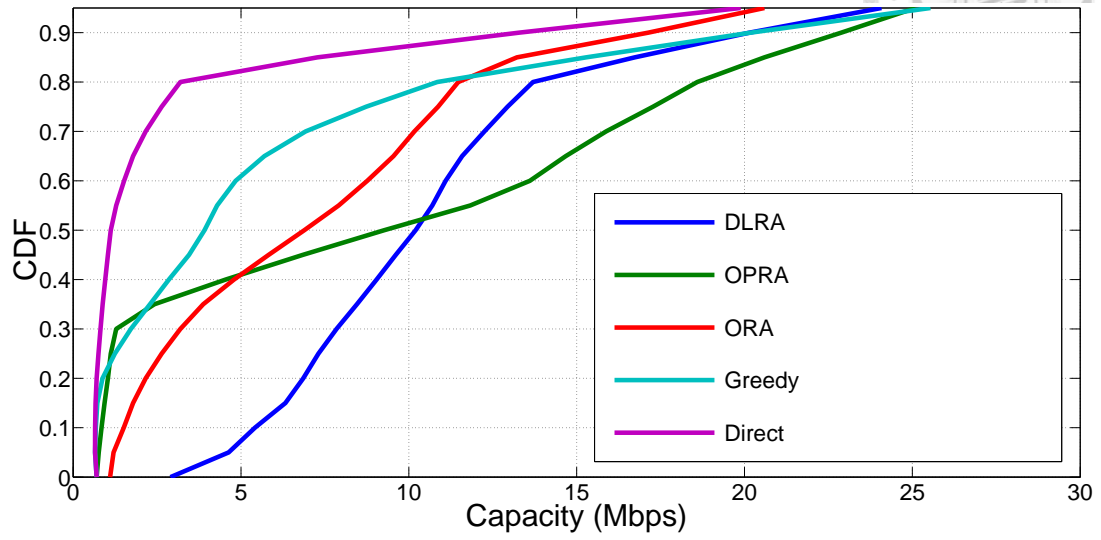
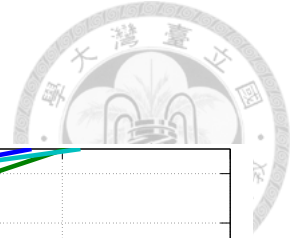


Figure 3.16: The CDF of capacity for all algorithms.

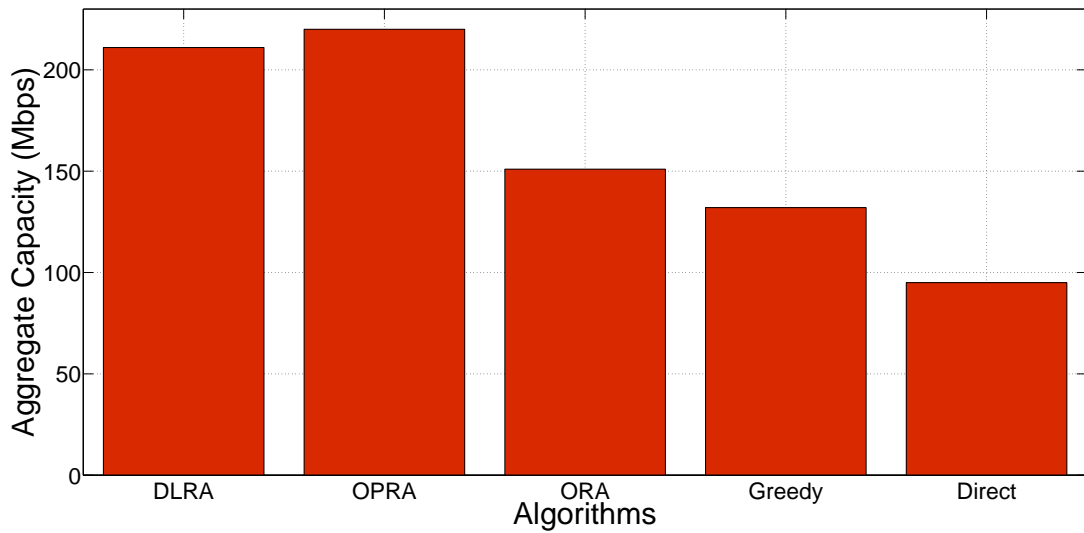


Figure 3.17: The aggregate capacity for all algorithms.

3. DECENTRALIZED LEARNING-BASED RELAY ASSIGNMENT FOR COOPERATIVE COMMUNICATIONS

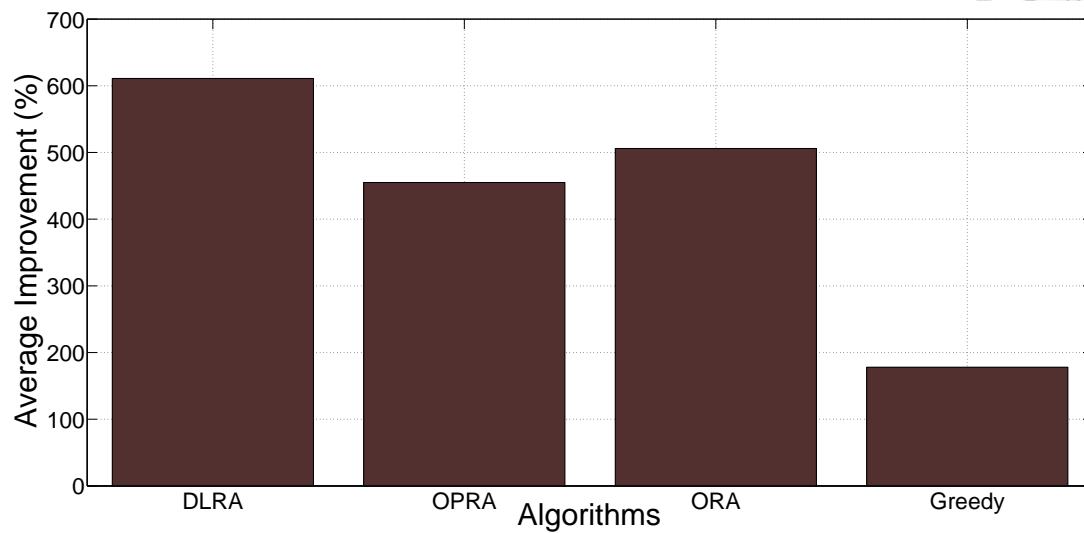
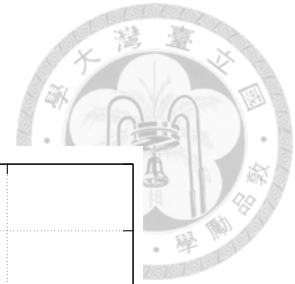


Figure 3.18: The average improvement for all algorithms.

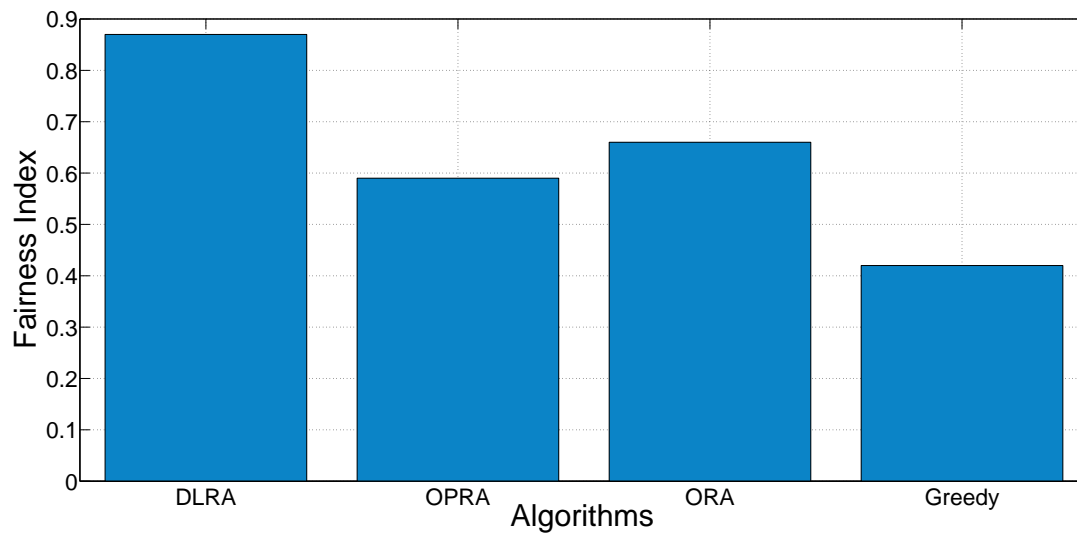


Figure 3.19: The fairness index for all algorithms.

3.6 Concluding Remarks

Cooperative communication increases the data rate in wireless networks by exploiting spatial diversity via relay node antennas. Therefore, the relay node selection problem significantly affects system performance. It is a difficult to assign relay nodes to source nodes when the number of source nodes increases. The complexity involved in adopting a centralized approach to handle this task is very high. This paper enables source nodes to select relay nodes for themselves. A fully-distributed approach based on reinforcement-learning technique called "Decentralized Learning-based Relay Assignment" algorithm is proposed in this work. It is assumed that one relay node is able to serve multiple source-destination pairs, whereas many other works assume that one relay node is only able to serve one pair. This study also gives source nodes self-optimizing and self-learning abilities.

Both mathematical analysis and experimental results are given to show the performance of DLRA. The convergency and the optimality of DLRA are shown in the mathematical analysis. Two different cooperative communication systems, a cooperative ad hoc network and a relay network in an LTE-Advanced system, are considered in the experiments. The effectiveness of DLRA in cooperative ad hoc networks, defined by previous work, is demonstrated. The experimental results obtained in both systems show that DLRA is effective, and exhibits good performance compared with other existing algorithms.



3. DECENTRALIZED LEARNING-BASED RELAY ASSIGNMENT FOR COOPERATIVE COMMUNICATIONS





Chapter 4

Multi-Tone Subframes for Enhanced Inter-Cell Interference Coordination in LTE HetNets

4.1 Background Information

In recent years, wireless data traffic has seen significant growth due to data-oriented devices such as mobile phones. According to [96], the global mobile traffic is estimated to increase thirteen-fold; therefore, cellular operators will inevitably experience a boom in mobile traffic growth. To address this rapid growth, we must to exploit the available radio spectrum as efficiently as possible. Small cells have been identified as the most promising solution for coping with these increasing demands. Heterogeneous networks (HetNets) are mixed with traditional cellular networks, which are known as macrocells, and small cells. In Long-Term-Evolution (LTE) HetNets, small cells are usually called femtocells and picocells. Femtocells are typically for indoor use with a coverage radius of few tens of meters and its use is restricted to a handful of users in closed subscriber group. Picocells have a coverage of a couple of hundreds of meters and are open subscriber

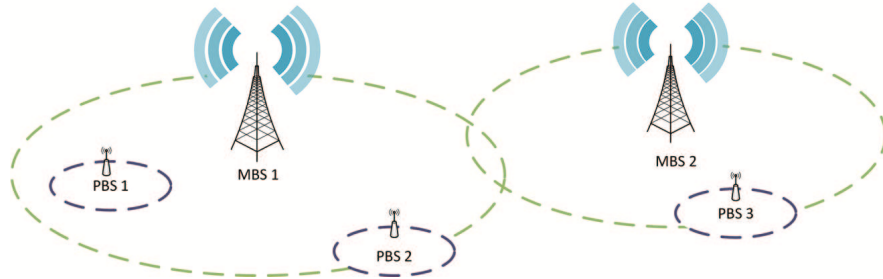
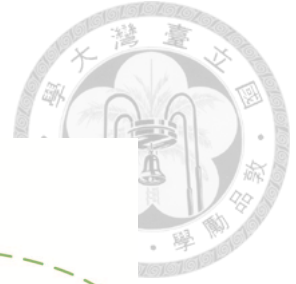
4. MULTI-TONE SUBFRAMES FOR ENHANCED INTER-CELL INTERFERENCE COORDINATION IN LTE HETNETS

group cells with access permission to all subscribers of the operator. Picos are typically deployed near malls, offices, business localities with dense mobile usage, etc. Picos are mostly deployed outdoors, but there could be indoor deployments in large establishments.

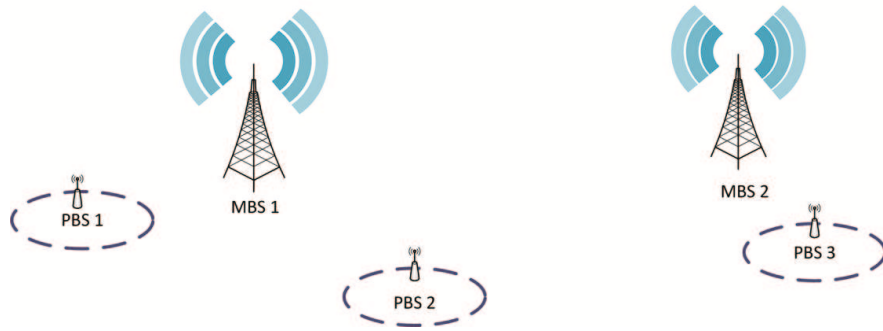


A HetNet is a two-tier network architecture; for example, picocells are overlaid on the coverage range of macrocells. Compared to a macro base station (MBS) in a macrocell, a pico base station (PBS) in a picocell has much lower transmission power. There are two factors that could handicap the net capacity of a pico access node in the downlink. First, the downlink pico transmissions to its associated user equipments (UEs) could be severely interfered by high-power macro transmission [97]. For example, in Fig. 4.1(a), downlink transmissions to UEs associated with PBS 1 could easily be interfered by downlink transmissions of MBS 1. Second, UEs, who are close to PBS and could benefit from associating with the macro access node due to higher received signal strength from the high-power MBS. For example, UEs not too close to PBS 3 but still within the coverage area of PBS 3 could end up associating with MBS 2. Indeed, this could leave the pico underutilized, thus defeating the purpose of deploying that PBS.

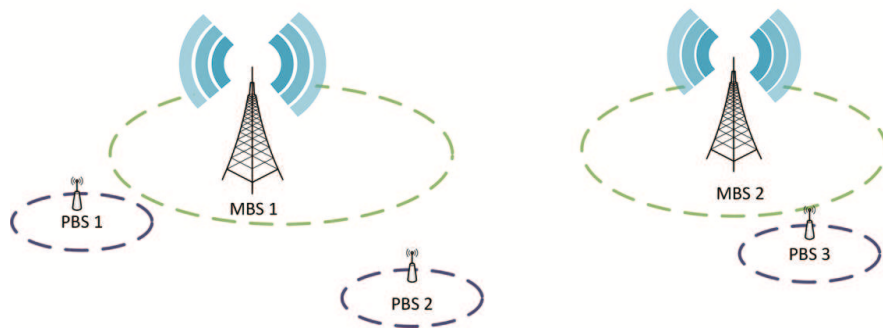
Due to the large difference in downlink transmit powers between PBSs (≈ 30 dBm) and MBSs (≈ 46 dBm) [16], the coverage range of picocells becomes very small. According to [?], coverage range of picocells is only 4.43 meters when distance between a PBS and an MBS is 50 meters, and the range increases to 42.08 meters, which is still a short range, when the distance increases to 450 meters. UEs which are more close to PBSs may end up associating with MBSs. Cell range expansion (CRE) [15] is proposed to cope with this situation. The idea is to add a bias on reference signal receiving power (RSRP) to PBSs, there-



(a) Maximum Transmission Power (non-ABS subframes)



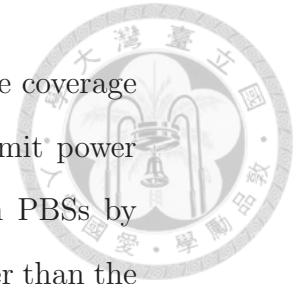
(b) Zero Transmission Power (ABS subframes)



(c) Reduced Transmission Power (RPS subframes)

Figure 4.1: Illustration of coverage area in different transmission.

4. MULTI-TONE SUBFRAMES FOR ENHANCED INTER-CELL INTERFERENCE COORDINATION IN LTE HETNETS



fore, the coverage range of PBSs is expanded. Although we expand the coverage range of picocells with CRE, essentially, the large difference of transmit power between MBSs and PBSs is still existing. UEs which associate with PBSs by CRE would receive interference from MBSs, of which the power is larger than the received signal power. Thus, the performance of these UES is worse due to large interference. To handle this problem, a framework called "Enhanced Inter-Cell Interference Coordination" (eICIC) is proposed by 3rd Generation Partnership Project (3GPP). Almost Blank Subframe (ABS) is the major part of eICIC, and the concept is to blank some subframes of MBSs, where only pilot and system signals are transmitted [20].

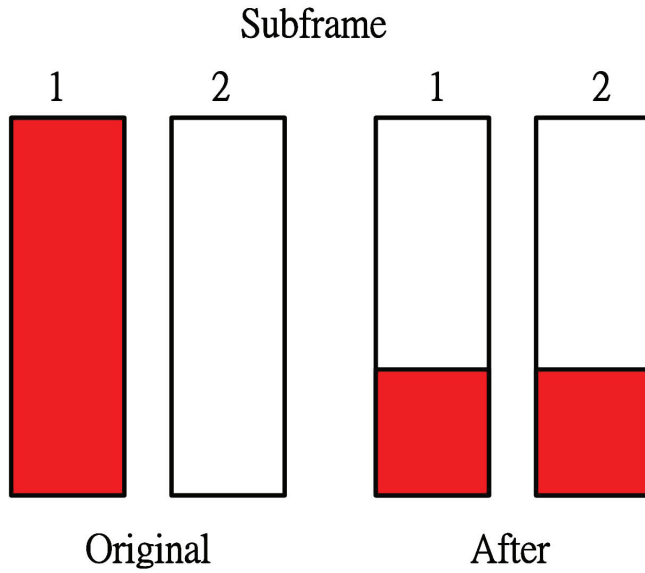
With the help of ABSs, the UEs can transmit their data in these muted subframes, therefore, they experience no interference from MBSs and get better performance during these subframes. However, the mechanism of the ABS forces MBSs to stop using some subframes, and it degrades the performance of macro-UEs. As shown in Fig. 4.1(b), MBSs can not do anything during ABS. The spectrum utilization decreases at the same time, and the goal to exploit the available radio spectrum as efficiently as possible is disobeyed. In addition, Fig. 4.2 shows that there are two subframes and that the "Original" case in (a) displays the same behaviour as ABS: full power on subframe 1 and muted on subframe 2. In the other case, we use only 1/3 of the maximum power on two subframes, and (b) shows the Shannon capacity of the two cases, where the x-axis is the signal-to-interference-plus-noise-ratio (SINR) under maximum power. The "After" case is clearly better than the "Original" case and also involves less power consumption. Lower power consumption leads to a higher capacity because the spectrum is used more efficiently. This phenomenon inspires this study. Therefore, as shown

in Fig. 4.1(c), MBSs are degenerated to PBSs instead of being blanked. MBSs do not interfere PBSs under this circumstance, and the spectrum utilization is increased.

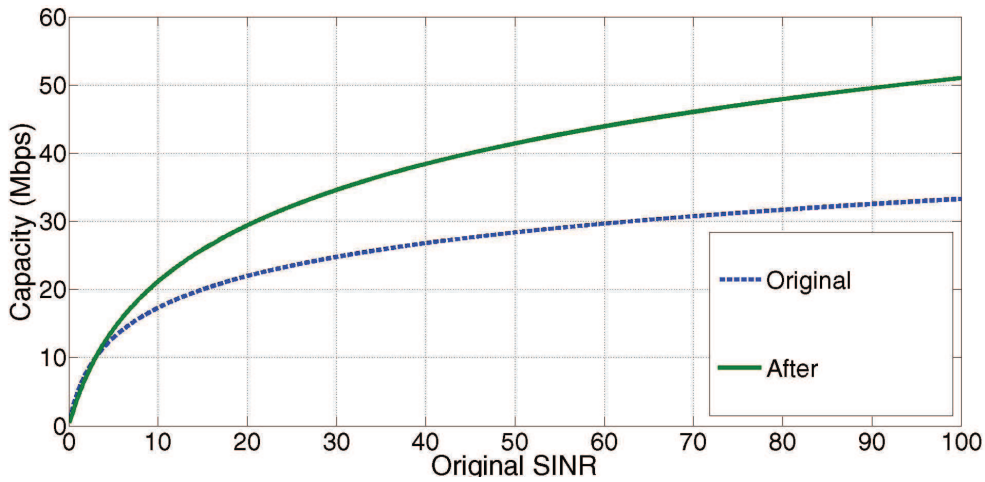
The MBSs transmit at reduced power instead of muting subframes only to serve the nearby UEs. The so-called reduced-power subframes (RPSs) have been standardized under 3GPP release 11 and are commonly referred to as further-enhanced ICIC (FeICIC) [59]. The use of RPSs increases the throughput of MUEs and the spectrum utilisation of MBSs. However, the performance of PBSs is reduced because the interference is greater than with the original muting subframes. The use of RPSs is considered to be a trade-off between the cell-edge and average throughput.

In this thesis, we address the weak points of RPSs and propose the multitone subframe (MTS) to make up for their insufficiencies. We also compare the performance of MTS with dynamic RPS (DRPS), which is introduced in the following section. As we know, RPS and ABS involve a trade-off between the average system capacity and the capacity of edge UEs. The use of the MTS can improve the performance of the whole system, including the system capacity and edge UEs. The proposed algorithm is based on the interior point method and consists of two steps. Detailed information on the proposed algorithm is introduced in Section ???. In addition, we provide various simulation results to evaluate the performance of the proposed algorithm; the results show the success of the proposed algorithm.

4. MULTI-TONE SUBFRAMES FOR ENHANCED INTER-CELL INTERFERENCE COORDINATION IN LTE HETNETS



(a) Illustration of the original case and the after case



(b) Capacity of the two cases

Figure 4.2: The comparison of the capacity: the original case means the maximum transmission power on one subframe and the after case means use 1/3 maximum transmission power on each subframes.

4.2 System Model and Problem Formulation



4.2.1 System Model

We define a HetNet that contains macrocells and picocells in an LTE-Advanced system. A macrocell, in an LTE-advanced HetNet, has a base station, referred to in this study as an MBS, with a transmission power of around 20 to 40 W. The coverage range is typically around 0.5 to 2 km. In contrast, a picocell has a base station, referred to in this study as a PBS, with lower transmission power (around 2 to 5 W). Picocells are underlaid on the coverage range of macrocells to make up for insufficiencies in their deployment, such as coverage holes and indoor environments.

Denote \mathcal{M} and \mathcal{P} as MBSs and PBSs, respectively. We also use m and p to represent a typical MBS and PBS, respectively. The set of UEs is denoted as \mathcal{U} , and a typical UE is denoted as u . Denoting by \mathcal{U}_p and \mathcal{U}_m UEs that are associated with PBS p and MBS m , respectively. Denote $\mathcal{J}(p)$ as the set of MBSs that interfere with the PBS p . MBSs used by MBSs have L different power levels, and \mathcal{L} and l are denoted as the set of power levels and a typical power level, respectively.

Denote N_m^l as the number of subframes with power level l used by MBS m . For ABS scenarios, denote N_m^A as the number of ABS subframes used by MBS m . Denote A_p^l as the number of subframes that PBS p can use and that have interference with power level l . A UE associated with a PBS suffers from two types of interference, one from other PBSs and the other from the interfered MBS. Denote these two types of interference as $P_{int}^{pico}(u)$ and $P_{int}^{macro}(u)$ for an UE u .

4. MULTI-TONE SUBFRAMES FOR ENHANCED INTER-CELL INTERFERENCE COORDINATION IN LTE HETNETS



The SINR of UE $u \in \mathcal{U}_p$ can be modeled as:

$$SINR(u) = \frac{P_R(u)}{P_{int}^{pico}(u) + P_{int}^{macro}(u) + N_0} \quad (4.1)$$

where $P_R(u)$ is the received signal power of UE u .

User Capacity: In our scenario, we have a set of UEs denoted by \mathcal{U} , and we assume that we know which MBS or PBS associated with each UE. Denote r_{ul}^{macro} as the data rate for UE u that associates with the MBS when the power level of the MBS is l . A UE can associate with either an MBS or a PBS; therefore, r_u^l for UE u that associates with an MBS stands for the data rate achieved when the MBS uses subframes with power level l . On the other hand, r_u^l for UE u that associates with a PBS stands for the data rate achieved when the MBS that interferes with the PBS uses subframes with power level l . For ABS scenarios, we denote r_u^A and r_u^{nA} as the capacity of UE u on ABS and non-ABS subframes, respectively. The SINR of each UE u can be obtained via above the discussion, so the average PHY data rate of each UE u can be obtained by: (1) mapping the SINR to the data rate by looking up the table in LTE or (2) simply using the modified Shannon capacity.

4.2.2 Problem Formulation

In this study, our goal is to improve the performance of the entire system by means of the proposed MTS approach. Before formulating the problem, we define a variable A_p^l . A_p^l is the number of subframes that PBS p can use and have interference with the power level l . The MBSs that interfere with the PBS p are in the set $I(p)$. For simplicity, in each subframe, we only consider the greatest transmission power level in $J(p)$ for each PBS p . Therefore, we obtain the

4.2 System Model and Problem Formulation



Table 4.1: Definitions of Notations

Notations	Definitions
\mathcal{U}, u, U ($u \in \mathcal{U}$)	Set of UEs, index for a typical UE, number of UEs, respectively
\mathcal{M}, m, M ($m \in \mathcal{M}$)	Set of macros, index for a typical macro, number of macros, respectively
\mathcal{P}, p, P ($p \in \mathcal{P}$)	Set of picos, index for a typical pico, number of picos, respectively
\mathcal{L}, l, L ($l \in \mathcal{L}$)	Set of power levels, index for a typical power level, number of power levels, respectively
m_u	The macro that is best for UE u
p_u	The pico that is best for UE u
r_u^{ml}	Data rate achieved by UE u from m_u with power level l
r_u^{pl}	Data rate achieved by UE u from p_u in a subframe with the interference power level l
\mathcal{J}_p^{macro}	Set of macro eNBs that interfere with pico p
\mathcal{U}_m	Set of UEs for which macro m is the best macro eNB
\mathcal{U}_p	Set of UEs for which pico p is the best pico eNB
N_m^l	Variable for subframes with power level l used by macro m
A_p^l	Variable for subframes interfered by power level l used by pico p
x_u^l	Variable denoting UE u 's air-time from macro over subframe with power level l
y_u^l	Variable denoting UE u 's air-time from pico when the most transmission power used by the macros is l .

4. MULTI-TONE SUBFRAMES FOR ENHANCED INTER-CELL INTERFERENCE COORDINATION IN LTE HETNETS



following equations:

$$\begin{aligned}
 A_p^{l_{max}} &= \max_m \{N_m^{l_{max}}\}, m \in \mathcal{J}(p) \\
 A_p^{l_{max}-1} &= \max_m \{N_m^{l_{max}} + N_m^{l_{max}-1}\} - A_p^{l_{max}}, m \in \mathcal{J}(p) \\
 &\vdots \\
 A_p^{l_{max}-i} &= \max_m \left\{ \sum_{j=0}^i N_m^{l_{max}-j} \right\} - \sum_{j=0}^{i-1} A_p^{l_{max}-j}, m \in \mathcal{J}(p)
 \end{aligned} \tag{4.2}$$

According to (4.2), we find that the value of A_p^l is determined by the variable N_m^l . The problem to be solved in this study is to find N_m^l , namely, the variable for subframes with power level l used by macro m ; x_u^l , namely, the variable denoting UE u 's air-time from macro over subframe with power level l ; and y_u^l , namely, the variable denoting UE u 's air-time from pico when the greatest transmission power used by the macros is l , to maximise the performance of the entire system. The problem formulation is shown in the following:

Problem 1 (MTS Assignment Problem). *Maximise the aggregate log-capacity of UEs in the system, i.e.,*

$$\max_{N,x,y} \sum_{u \in \mathcal{U}} \ln(R_u)$$

1. *Association Constraints:*

$$\left(\sum_{l=1}^{l_{max}} x_u^l \right) \left(\sum_{l=1}^{l_{max}} y_u^l \right) = 0, x_u^l \geq 0, y_u^l \geq 0, \forall u \in \mathcal{U}, l \in \mathcal{L}$$

2. *MTS Integer Constraints:*

$$N_m^l \in \mathbb{Z}^+, \forall m \in \mathcal{M}, \forall l \in \mathcal{L}$$



3. *Macro and Pico Subframes Constrains:*

$$\sum_{l \in L} N_m^L = N^D, \forall m \in \mathcal{M}$$

$$A_p^l = \max_m \left\{ \sum_{i=l}^{l_{max}} N_m^i \right\} - \sum_{j=l+1}^{l_{max}} A_p^j$$

4. *Macro Air-time Constraints:*

$$\sum_{u \in \mathcal{U}_m} x_u^l \leq N_m^l, \forall l \in \mathcal{L}, m \in \mathcal{M}$$

5. *Pico Air-time Constraints:*

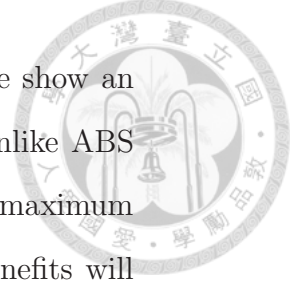
$$\sum_{u \in \mathcal{U}_p} y_u^l \leq A_p^l, \forall l \in \mathcal{L}, p \in \mathcal{P}$$

where the first constraint is that each UE can associate with either an MBS or a PBS at a particular moment. The second constraint is that the number of MTSs is a non-negative integer. The third constraint is that the total number of MTSs is equal to the length of a duty cycle. The fourth constraint is that the total air-time allocated to the UEs from an MBS is less than the total usable subframes. The last constraint is that the total air-time allocated to the UEs from a PBS is less than the total usable subframes.

4.3 Interior Point MTS Optimization Algorithm

In this section, we first present the system model which includes interference model and capacity calculation. The notations are also briefly introduced. Second, we formulate the MTS assignment problem, find that it is an mixed integer nonlinear programming problem, which is NP-hard in the literature. Therefore, in the next chapter, we will relaxed some constraints in the original to form a

4. MULTI-TONE SUBFRAMES FOR ENHANCED INTER-CELL INTERFERENCE COORDINATION IN LTE HETNETS



solvable problem which can be solve in a reasonable time. Fig 4.3, we show an illustration of coverage area of a MBS with different power levels. Unlike ABS and RPS, where ABS has only maximum and zero power and RPS has maximum and static reduced power, MTS has different power levels and the benefits will be introduced briefly in the following chapters.

4.3.1 Basic Idea of the Interior Point Methods

Consider an inequality constrained problem,

Problem 2.

$$\begin{aligned} & \text{minimize} && f(p) \\ & \text{subject to} && h_i(p) \leq 0, i = 1, \dots, m \end{aligned} \quad (4.3)$$

where p is the solution vector of dimension n , and m is the number of constraints.

This problem could be approximately formulated as an unconstrained problem. First, make the inequality constraints implicit in the objective. The inequality constraints are eliminated by placing in the indicator function,

Problem 3.

$$\text{minimize} \quad f(p) + \sum_{i=1}^m I_-(f_i(p)) \quad (4.4)$$

where $I_- : \mathbf{R} \rightarrow \mathbf{R}$ is the indicator function for the nonpositive reals,

$$I_-(u) = \begin{cases} 0, & u \leq 0 \\ \infty, & u > 0 \end{cases} \quad (4.5)$$

The Problem 3 has no inequality constraints, but its objective function is not differential, so Newton's method cannot be applied. Therefore, the logarithmic barrier is introduced to handle this situation. The basic idea of the barrier method is to approximate the indicator function I_- by the function

$$\hat{I}_-(u) = -(1/t)\log(-u), \quad \text{dom } \hat{I}_- = -\mathbf{R}_{++} \quad (4.6)$$

4.3 Interior Point MTS Optimization Algorithm

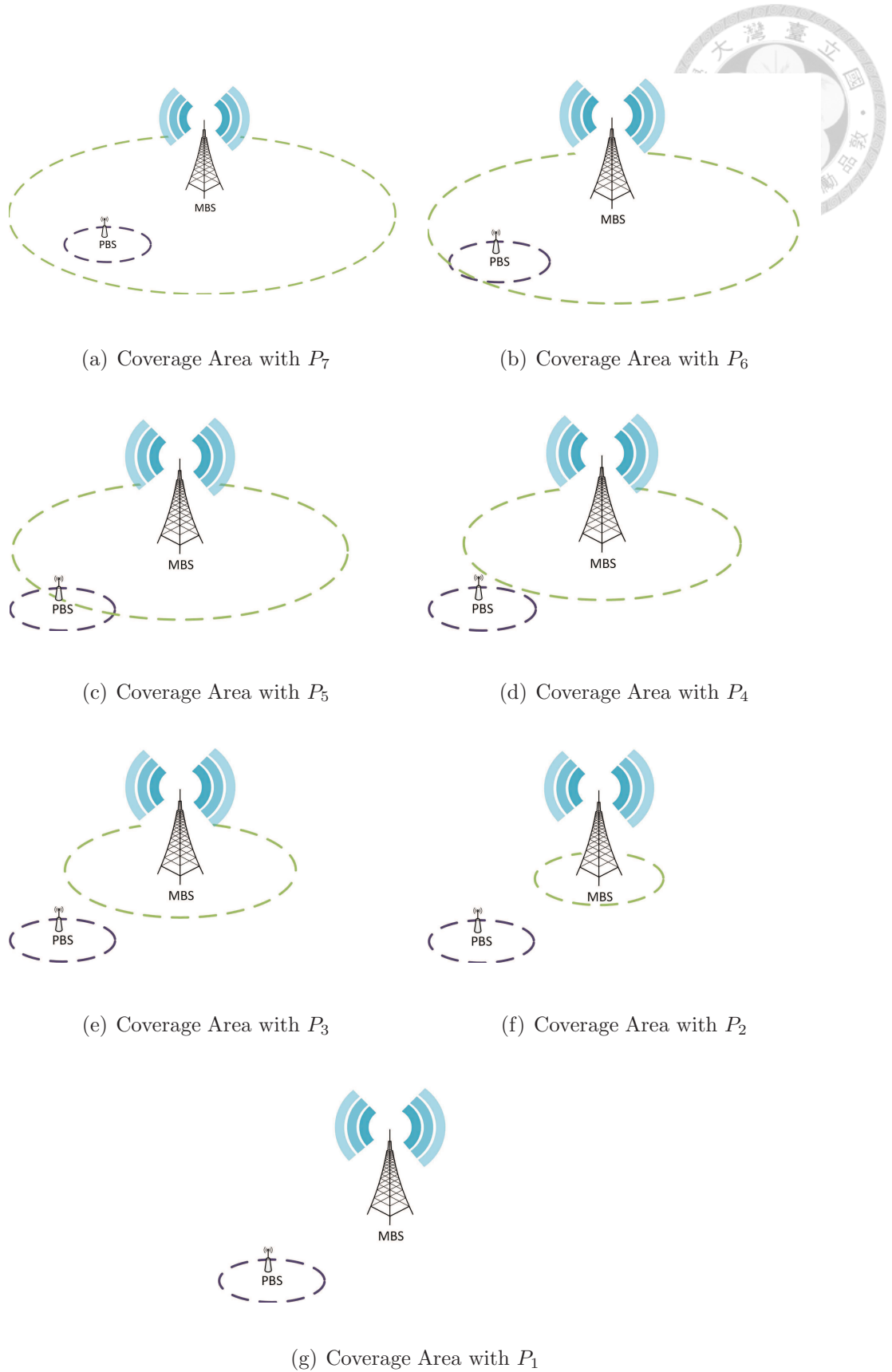


Figure 4.3: Example of coverage area of MBS for 7 power levels.

4. MULTI-TONE SUBFRAMES FOR ENHANCED INTER-CELL INTERFERENCE COORDINATION IN LTE HETNETS

where $t > 0$ is a parameter that sets the accuracy of the approximation. Like I_- , the function \hat{I}_- is convex and nondecreasing, and takes on the value ∞ for $u > 0$. Unlike \hat{I}_- , however, \hat{I}_- is differentiable and closed: the approximation \hat{I}_- , for several values of t . As t increases, the approximation becomes more accurate. Substituting \hat{I}_- for I_- in the Problem 3 gives the approximation,

Problem 4.

$$\text{minimize } f(p) + \sum_{i=1}^m -(1/t)\log(-f_i(p)) \quad (4.7)$$

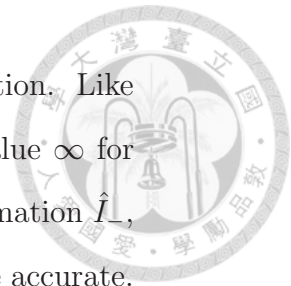
The objective here is convex, since $-(1/t)\log(-u)$ is convex and increasing in u , and differentiable. Assuming an appropriate closedness condition holds, Newton's method can be used to solve it.

One advantage of choosing the logarithmic penalty is that the approximation becomes more accurate as t increases. When $t \rightarrow \infty$, the optimal solution of Problem 4 converges to the optimal solution of the original Problem 2. Figure 4.4 shows the approximation accuracy as t increases. Solving Problem 2 is thus equal to solving a series of Problem 4 with increasing t .

Although the basic idea of the interior point methods is simple, it still requires careful considerations to design an suitable mechanism to solve the subproblems at hand. Design interior point methods is still an active research topic.

4.3.2 Detailed Description of Interior Point MTS Optimization Algorithm

Although the interior point methods were already proposed for several tens of years, the detailed design and implementation of the interior point methods are still active research areas. It is hard to provide reliable design guidelines that are suitable for all types of problems. Therefore, it is important to customize



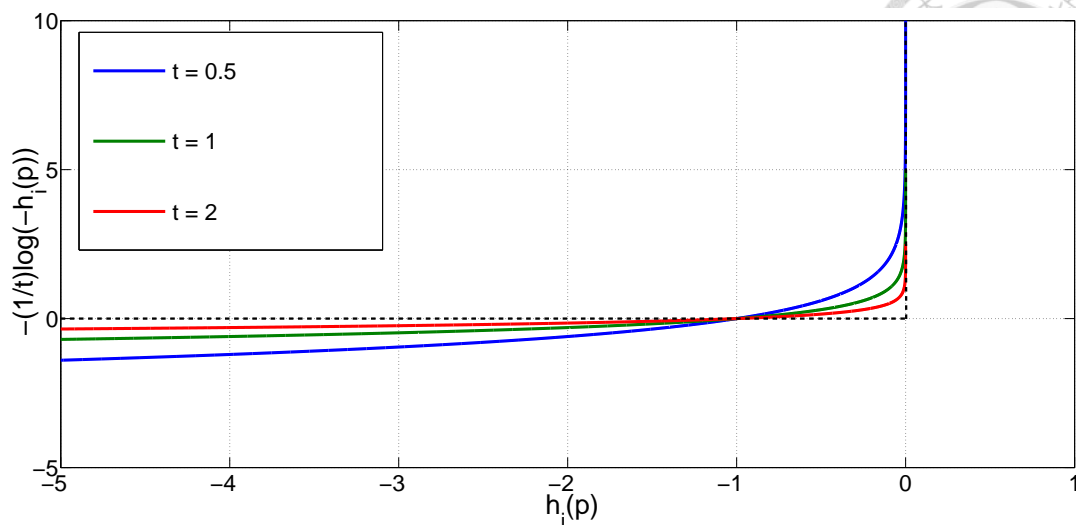


Figure 4.4: Effect of t on approximation accuracy. As t increase, the approximation becomes more accurate.

the solution to reflect the suitability for the problem at hand. In this section, we present the detailed description of the customized interior point algorithm to solve the MTS problem. First, we relax some constraints of the Problem ?? to get the relaxed problem, therefore, the interior point can be used on the MTS optimization. Second, the integer rounding algorithm is proposed to mapping the solution of the relaxed problem into the original problem.

4.3.2.1 The Relaxed Problem

Before solving Problem ??, the first step is to relax some constraints to make the problem solvable within a reasonable amount of time. The second step is to convert the solution obtained in the first step into a feasible solution for Problem ??.

Problem ?? is a mixed-integer nonlinear programming (NLP) problem and is considered to be an NP-hard problem in the literature. Therefore, we consider

4. MULTI-TONE SUBFRAMES FOR ENHANCED INTER-CELL INTERFERENCE COORDINATION IN LTE HETNETS



an NLP problem by ignoring the association constraints and relaxing the integer constraints in Problem 1. The new NLP problem is shown in the following:

Problem 5 (Relaxed MTS Assignment Problem). *Maximise the aggregate log-capacity of UEs in the system, i.e.,*

$$\max_{N,x,y} \sum_{u \in \mathcal{U}} \ln(R_u)$$

1. *MTS Constraints:*

$$N_m^l \geq 0, \forall m \in \mathcal{M}, \forall l \in \mathcal{L}$$

2. *Macro and Pico Subframes Constraints:*

$$\sum_{l \in \mathcal{L}} N_m^l = N^D, \forall m \in \mathcal{M}$$

$$A_p^l = \max_m \left\{ \sum_{i=l}^{l_{max}} N_m^i \right\} - \sum_{j=l+1}^{l_{max}} A_p^j$$

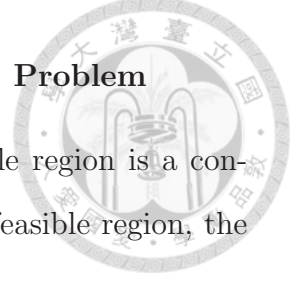
3. *Macro Air-time Constraints:*

$$\sum_{u \in \mathcal{U}_m} x_u^l \leq N_m^l, m \in \mathcal{M}, \forall l \in \mathcal{L}$$

4. *Pico Air-time Constraints:*

$$\sum_{u \in \mathcal{U}_p} y_u^l \leq A_p^l, p \in \mathcal{P}, \forall l \in \mathcal{L}$$

Because the association constraints are ignored, each UE can associate with both MBS and PBS at the same time. The second constraints in Problem 1 are no longer integer constraints, so we can take non-integer values into consideration. The relaxed problem is therefore an NLP problem.



4.3.2.2 Algorithm for The Relaxed MTS Assignment Problem

Since the constraints of Problem ?? are all linear, the feasible region is a convex set, With the concave objective function and the convex feasible region, the relaxed MTS problem could be a convex optimization problem.

We solve this problem by a primal-dual interior-point algorithm [98]. First, we show the Lagrangian of the relaxed MTS Assignment Problem in the following:

$$\begin{aligned}
 L(N, x, y, \lambda, \nu, \alpha, \beta) = & \sum_{u \in \mathcal{U}} \ln(R_u) - \sum_{\substack{m \in \mathcal{M} \\ l \in \mathcal{L}}} \lambda_{ml} N_m^l \\
 & - \sum_{m \in \mathcal{M}} \nu_m \left(\sum_{l \in \mathcal{L}} N_m^l - N_D \right) \\
 & - \sum_{\substack{m \in \mathcal{M} \\ l \in \mathcal{L}}} \alpha_{ml} \left(\sum_{u \in \mathcal{U}_m} x_u^l - N_m^l \right) \\
 & - \sum_{\substack{p \in \mathcal{P} \\ l \in \mathcal{L}}} \beta_{pl} \left(\sum_{u \in \mathcal{U}_p} y_u^l - A_p^l \right)
 \end{aligned} \tag{4.8}$$

where the variables λ , ν , α and β 's are dual variables and also called Lagrange multipliers. For notation simplicity, we use p to denotes the vector of all Lagrange multipliers, i.e., $p = (\lambda, \nu, \alpha, \beta)$. In the similar way, we use z to denotes the vector of all primal variables, i.e., $z = (N, x, y)$. Therefore, we can rewrite the problem in the following expression:

$$\begin{aligned}
 & \text{minimize} && f(z) \\
 & \text{subject to} && h_i(z) \leq 0, i = 1, \dots, c
 \end{aligned} \tag{4.9}$$

where c is the number of all constraints in Problem ??, and the function $f(z)$

4. MULTI-TONE SUBFRAMES FOR ENHANCED INTER-CELL INTERFERENCE COORDINATION IN LTE HETNETS



is equal to the objective function of Problem ?? multiply -1 . The Lagrangian is expressed as follows:

$$L(z, p) = f(z) + \sum_{i=1}^c p_i h_i(z). \quad (4.10)$$

where p_i is the i th element in vector p , $i = 1, \dots, c$, are the Lagrange multipliers.

There exist primal optimal z^* and dual optimal p^* which satisfy the Karush-Kuhn-Tucker (KKT) conditions.

$$\begin{aligned} h_i(z^*) &\leq 0, i = 1, \dots, c \\ p^* &\succeq 0 \\ \Delta f(z^*) + \sum_{i=1}^c p_i^* \Delta h_i(z^*) &= 0 \end{aligned} \quad (4.11)$$

We denote the value of the objective function with the optimal solution z^* as f^* . Combining (4.10) and (4.11), it is found that

$$\begin{aligned} L(z^*, p^*) &= f(z^*) + \sum_{i=1}^c p_i^* h_i(z^*) \\ &\leq f^* \end{aligned} \quad (4.12)$$

Define a function

$$\phi(z) = - \sum_{i=1}^m \ln(-h_i(z)) \quad (4.13)$$

which is the logarithmic penalty function for the problem (4.9). The gradient and Hessian of the logarithmic penalty function ϕ are given by

4.3 Interior Point MTS Optimization Algorithm



$$\begin{aligned}\Delta\phi(z) &= \sum_{i=1}^m \frac{-1}{h_i(z)} \Delta h_i(z) \\ \Delta^2\phi(z) &= \sum_{i=1}^m \frac{1}{h_i(z)^2} \Delta h_i(z) \Delta h_i(z)^T + \sum_{i=1}^2 h_i(z)\end{aligned}\tag{4.14}$$

We rewrite (4.7) as

$$\text{minimize } f(z) + (1/t)\phi(z)\tag{4.15}$$

which has the same minimizer as (4.7) does. We denote the solution of (4.15) as $z^*(t)$. The first order necessary condition for (4.15) is

$$\begin{aligned}0 &= \Delta f(z^*(t)) + (1/t)\Delta\phi(z^*(t)) \\ &= \Delta f(z^*(t)) + (1/t) \sum_{i=1}^m \frac{-1}{h_i(z^*(t))} \Delta h_i(z^*(t))\end{aligned}\tag{4.16}$$

where the second equality comes from (4.14). From (4.11) and (4.16), the dual feasible solution is defined as

$$p_i^*(t) = \frac{-1/t}{h_i(z^*(t))}, i = 1, \dots, c.\tag{4.17}$$

Since $t > 0$ and $h_i(z^*) < 0, i = 1, \dots, c$, it is guaranteed that $p_i^* \succ 0$, which meets the requirements shown in (4.11).

Applying (4.17) to (4.10),

4. MULTI-TONE SUBFRAMES FOR ENHANCED INTER-CELL INTERFERENCE COORDINATION IN LTE HETNETS



$$\begin{aligned}
 L(z^*(t), p^*(t)) &= f(z^*(t)) + \sum_{i=1}^c p_i^*(t) h_i(z^*(t)) \\
 &= f(z^*(t)) - c/t \\
 &\leq f^*
 \end{aligned} \tag{4.18}$$

where the last inequality comes from (4.12). Therefore,

$$f(z^*(t)) - f^* \leq c/t \tag{4.19}$$

(4.19) means that the primal feasible solution $z^*(t)$ is no more than c/t -suboptimal. The term c/t is called the duality gap. When $t \rightarrow \infty$, $z^*(t)$ converges to the optimal solution of the original problem (4.9).

With (4.17), the Karush-Kuhn-Tucker (KKT) conditions shown in (4.11) can be written as $r_t(z, p) = 0$, where the residual $r_t(z, p)$ is defined as

$$r_t(z, p) = \begin{bmatrix} \nabla f(z) + D_h(z)^T p \\ -\mathbf{diag}(p)h(z) - (1/t)\mathbf{1} \end{bmatrix} \tag{4.20}$$

for $t > 0$. Here $h(z)$ is the constrain matrix and its derivative matrix $D_h(z)$ are defined as

$$h(z) = \begin{bmatrix} h_1(z) \\ \vdots \\ h_c(z) \end{bmatrix}, \tag{4.21}$$

and

$$D_h(z) = \begin{bmatrix} \nabla h_1(z)^T \\ \vdots \\ \nabla h_c(z)^T \end{bmatrix}. \tag{4.22}$$

4.3 Interior Point MTS Optimization Algorithm

If (z, p) satisfies $r_t(z, p) = 0$, then $z = z^*(t)$ and $p = p^*(t)$ are the primal feasible and dual feasible solutions, respectively, and it lead to m/t -suboptimal solution. Next, we apply the Newton method in the following steps to solve the nonlinear equations $r_t(z, p) = 0$, for fixed t , at a point (z, p) which satisfies $h(z) \prec 0$, $p \succ 0$. The Newton step $\Delta x = (\Delta z, \Delta p)$ is $\Delta x = -Dr_t(x)^{-1}r_t(x)$. In terms of z and p , we have

$$\begin{aligned} & \begin{bmatrix} \nabla^2 f(z) + \sum_{i=1}^c p_i \nabla^2 h_i(z) & D_h(z)^T \\ -\mathbf{diag}(p)D_h(z) & -\mathbf{diag}(h(z)) \end{bmatrix} \begin{bmatrix} \Delta z \\ \Delta p \end{bmatrix} \\ = & -1 \times \begin{bmatrix} \nabla h(z) + D_h(x)^T p \\ -\mathbf{diag}(p)h(z) - (1/t)\mathbf{1} \end{bmatrix} \end{aligned} \quad (4.23)$$

Therefore, we have the primal-dual search direction $(\Delta z, \Delta p)$, and we find a suitable step length s by performing a backtracking line search method [99]. We update the next primal-dual point as $x = (z + s\Delta z, p + s\Delta p)$. When a pre-defined precision is met, the iteration stops. Boyd and Vandenberghe propose a surrogate duality gap [98], which is defined as

$$\hat{\eta}(z, p) = -h(z)^T \lambda \quad (4.24)$$

The surrogate duality gap is adopted to the algorithm to choose the approximation parameter t and to decide the termination condition. The overview of the first step algorithm is shown in Algorithm 2.

4.3.2.3 Integer Rounding for Relaxed MTS Assignment

In the second step of the proposed algorithm, the goal is to convert the solution obtained in the first step into a feasible solution for the MTS assignment problem. In the relaxed problem, each UE can associate with both an MBS and a PBS;

4. MULTI-TONE SUBFRAMES FOR ENHANCED INTER-CELL INTERFERENCE COORDINATION IN LTE HETNETS



Algorithm 2 Interior point relaxed MTS optimization algorithm.

Input: initial primal point z , $p \succ 0$, $\mu > 1$, α , β , $\epsilon_{feasible} > 0$, $\epsilon > 0$

Output: optimal solution \hat{z} for the relaxed problem

repeat

1. Determine t .

$$t = \mu c / \hat{\eta}$$

2. Compute the primal-dual search direction $\Delta x = (\Delta z, \Delta p)$.

$$\begin{aligned} & \begin{bmatrix} \nabla^2 f(z) + \sum_{i=1}^c p_i \nabla^2 h_i(z) & D_h(z)^T \\ -\text{diag}(p) D_h(z) & -\text{diag}(h(z)) \end{bmatrix} \\ & \times \begin{bmatrix} \Delta z \\ \Delta p \end{bmatrix} \\ & = -1 \times \begin{bmatrix} \nabla f(p) + D_h(p)^T p \\ -\text{diag}(p) h(p) - (1/t) \mathbf{1} \end{bmatrix}. \end{aligned}$$

3. Determine s by line search.

$$s^{max} = \min \{1, \min \{-\lambda_i / \Delta \lambda_i \mid \Delta \lambda_i < 0\}\}$$

$$s = 0.99 s^{max}$$

if $\|r_t(z^+, p^+)\|^2 \geq (1 - \alpha s) \|r_t(z, p)\|^2$ **then**

$$s = \beta \times s$$

end if

4. Update the primal-dual point.

$$z^+ = z + s \Delta z.$$

$$p^+ = p + s \Delta p.$$

$$z = z^+.$$

$$p = p^+.$$

until $\|\nabla f(z) + D_h(z)^T p\|^2 \leq \epsilon_{feasible}$, $\|-\text{diag}(p) h(p) - (1/t) \mathbf{1}\|^2 \leq \epsilon_{feasible}$,
and $\hat{\eta} \leq \epsilon$.

return $\hat{z} = z$

4.3 Interior Point MTS Optimization Algorithm

however, it can associate with only one of them in the original problem. We must therefore determine the association of each UE to either an MBS or a PBS.

We compute the throughput of each UE from MBS and PBS according to the solution obtained from the first step. The calculation is shown as follows:

$$\begin{aligned}
 R_u^{macro} &= \sum_{l=1}^{l_{max}} r_u^{ml} \hat{x}_u^l \\
 R_u^{pico} &= \sum_{l=1}^{l_{max}} r_u^{pl} \hat{y}_u^l
 \end{aligned} \tag{4.25}$$

If $R_u^{macro} \geq R_u^{pico}$, UE u would associate with MBS, otherwise, it associates with PBS. Denote \mathcal{U}_m^* and \mathcal{U}_p^* are the set of UEs which associate MBS m and PBS p after the procedure, respectively.

Next, we need to convert N_m^l solved in the first step into an integer. The goal of ABS is to protect PUEs, and we leave this property in the proposed algorithm. Therefore, we convert N_m^l into the greatest integer lower than N_m^l . The integer rounding procedure for N_m^l is shown as follows:

$$N_m^{*l} = \begin{cases} \lfloor \hat{N}_m^l \rfloor & , \forall m \in \mathcal{M}, \forall l \in \mathcal{L}, l \neq 1 \\ \hat{N}_m^l = \hat{N}^D - \sum_{l=2}^{l_{max}} \hat{N}_m^l & , \forall m \in \mathcal{M}, l = 1 \end{cases} \tag{4.26}$$

The value of A_p^{*l} is dependent on N_m^{*l} , and the calculation is according to (4.2).

The last step is to find the final value of x_u^{*l} and y_u^{*l} . For each MBS m , for all $u \in \mathcal{U}_m^*$, the x_u^{*l} is

$$x_u^{*l} = \frac{\hat{x}_u^l N_m^{*l}}{X_m^l} \tag{4.27}$$

4. MULTI-TONE SUBFRAMES FOR ENHANCED INTER-CELL INTERFERENCE COORDINATION IN LTE HETNETS



where $X_m^l = \sum_{m \in \mathcal{U}_m^*} \hat{x}_m^l$

Similarly, for each PBS p , for all $u \in \mathcal{U}_p^*$, the y_u^{*l} is

$$y_u^{*l} = \frac{\hat{y}_u^l A_p^{*l}}{Y_p^l} \quad (4.28)$$

where $Y_p^l = \sum_{m \in \mathcal{U}_p^*} \hat{y}_m^l$. The overview of the second step of the algorithm is shown in Algorithm 3.

4.3.2.4 Proof of Optimality

Theorem 4. *A limit point of the sequence $\{z^*(t)^{(k)}\}$ generated by the interior point relaxed MTS optimisation algorithm is a global minimum of the original optimisation problem (4.9).*

Proof. (By contradiction) Let \bar{z}^* be a limit point of the sequence $\{z^*(t)^{(k)}\}$. If \bar{z}^* is not a global minimum, a feasible \bar{z} exists such that $f(\bar{p}) < f(\bar{p}^*)$. By the definition of $z^*(t)^{(k)}$,

$$f(z^*(t)^{(k)}) - \frac{1}{t^{(k)}} \sum_{i=1}^c \ln(-h_i(z^*(t)^{(k)})) \leq f(\bar{z}) - \frac{1}{t^{(k)}} \sum_{i=1}^c \ln(-h_i(\bar{z})). \quad (4.29)$$

for all k . By taking the limit $k \rightarrow \infty$,

$$f(\bar{z}^*) - \lim_{k \rightarrow \infty} \frac{1}{t^{(k)}} \sum_{i=1}^c \ln(-h_i(z_k)) \leq f(\bar{z}) < f(\bar{z}^*). \quad (4.30)$$

Hence $\lim_{k \rightarrow \infty} \frac{1}{t^{(k)}} \sum_{i=1}^c \ln(-h_i(z_k)) > 0$. Because $1/t^{(k)}$ decreases to zero as $k \rightarrow \infty$, a contradiction occurs. Therefore, it is proved that \bar{p}^* is a global minimum of the original optimisation problem. \square

4.3.2.5 Complexity Analysis

The primal-dual interior point method requires a total of $O(\sqrt{n})$ iterations [100], where n is the size of the problem. In the relaxed MTS optimisation problem, n is equal to $(M \times P \times L \times N)$. While considering the number of computations in

4.3 Interior Point MTS Optimization Algorithm

Algorithm 3 Round Relaxed MTS Algorithm: Algorithm for Integer Rounding of Output of Algorithm 2

1. UE Association: For all $u \in \mathcal{U}$, perform the following steps:
 - a) Compute the throughput it get From MBS and PBS according to solution obtained from the step 1 as follows:

$$R_u^{macro} = \sum_{l=1}^{l_{max}} r_u^{ml} \hat{x}_u^l$$

$$R_u^{pico} = \sum_{l=1}^{l_{max}} r_u^{pl} \hat{y}_u^l$$

where \hat{x}_u^l and \hat{y}_u^l are the output of Algorithm 2

- b) If $R_u^{macro} > R_u^{pico}$, UE u associate with the MBS, else it with PBS.

Define \mathcal{U}_m^* and \mathcal{U}_p^* are the set of UEs which associate MBS m and PBS p after the procedure, respectively.

2. MTS Rounding: Compute integral N_m^{*l} as follows:

$$N_m^{*l} = \begin{cases} \lfloor N_m^l \rfloor & , \forall m \in \mathcal{M}, \forall l \in \mathcal{L}, l \neq 1 \\ N_m^l = N^D - \sum_{l=2}^{l_{max}} N_m^l & , \forall m \in \mathcal{M}, l = 1 \end{cases}$$

where \hat{N}_m^l is the output of Algorithm 2.

3. Airtime Computation: For each MBS m , for all $u \in \mathcal{U}_m^*$, the final value of x_u^* is

$$x_u^{*l} = \frac{\hat{x}_u^{*l} N_m^{*l}}{X_m^l}$$

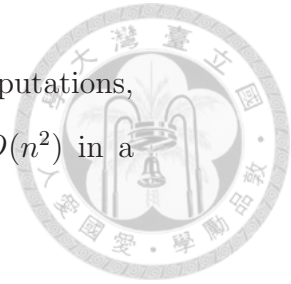
where $X_m^l = \sum_{u \in \mathcal{U}_m^*} \hat{x}_u^l$. Similarly, for each PBS p , for all $u \in \mathcal{U}_p^*$, the final value of y_u^{*l} is

$$y_u^{*l} = \frac{\hat{y}_u^{*l} A_p^{*l}}{Y_p^l}$$

where $Y_p^l = \sum_{u \in \mathcal{U}_p^*} y_u^l$

4. MULTI-TONE SUBFRAMES FOR ENHANCED INTER-CELL INTERFERENCE COORDINATION IN LTE HETNETS

exact arithmetic, solving the Newton step requires at most $O(n^3)$ computations, although typically the number of computations would be $O(n)$ or $O(n^2)$ in a problem in which the Hessian matrix is sparse [101].



4.3.2.6 Summary

In this chapter, we describe the algorithm to solve the MTS assignment problem, and the algorithm is divided into two steps: Relaxed MTS assignment algorithm and integer rounding for relaxed MTS algorithm. The first step is based on interior point method, and we introduce the basic idea of the interior point method. We provide the detailed description of the relaxed MTS assignment algorithm. The algorithm solves the problem iteratively toward to the desired approximation accuracy. Each subproblem is solved by Newton's method which is known to be efficient. In the second step, we round the solution obtained from the step one to integers, because the solution of MTS assignment problem is discrete. Besides, we provide the proof of optimality and convexity of the first step algorithm. The optimality proof shows that the algorithm would converge to the optimal solution and we show that the algorithm has linear convergence. Therefore, the algorithm is shown to be effective and efficient in the desired problem.

4.4 Numeric Example

In this section, we give a simple example to show the relationship among ABS, RPS, and MTS. The purpose is to present the effectiveness of the proposed MTS approach.

4.4.1 Correlation Among The Approaches

In the first of this chapter, we give a simple illustration of the relation among some related approaches. Suppose that the power levels used in 2-MTS is P_1 and P_2 , where P_1 is equal to the transmission power of reduce transmission power in RPS and P_2 is less than the maximum transmission power. The maximum transmission power is added in 3-MTS. Then, zero transmission power, namely mutes subframes, is added in 4-MTS. Another arbitrary transmission power is added in 5-MTS. Therefore, Fig. 4.5 is the sketch map of the performance among ABS, RPS and MTS with different levels. As shown in the figure, MTS can provide better performance than ABS in most conditions even there are only two power levels. With the number of power levels of MTS increased, the performance of MTS is better than ABS and RPS. In the following section, we give a detailed numeric example to explain this result.

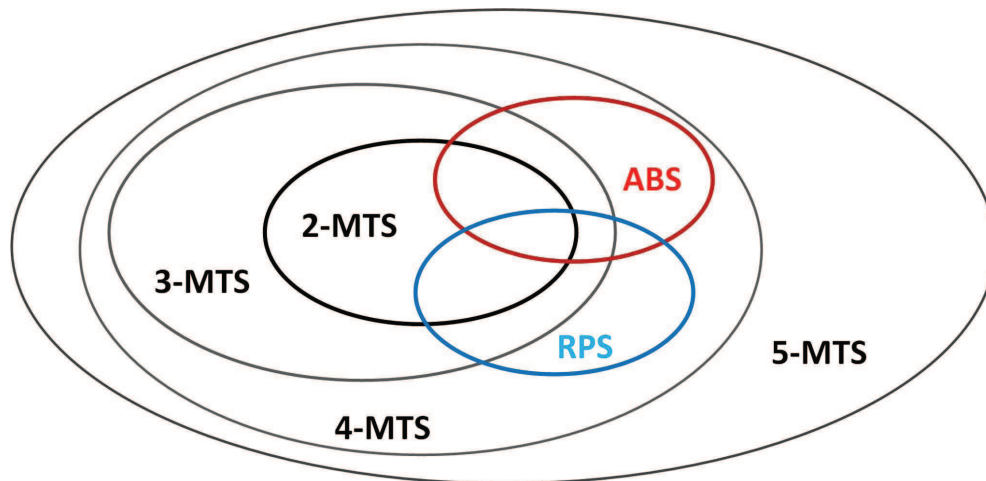
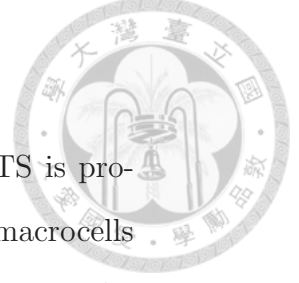


Figure 4.5: The sketch map of the performance relation among ABS, RPS and MTS with different levels.



4.4.2 Example

Through a simple analysis, an intuitive explanation of the idea of MTS is provided. In this example, our goal is to increase the performance of macrocells without harming that of picocells. We know that RPS and ABS involves a trade-off between the performance of macrocells and picocells. We only compare the performance of MTS and ABS, because RPSs always produce more interference to picocells than ABS does. We consider a HetNet with an MBS, a PBS and a pico UE; an illustration of the network topology is shown in Fig. 4.6. The MBS has two power levels, which are denoted by P_1^m and P_2^m ($P_1^m < P_2^m$), respectively. The path loss model is according to [102].

For the viewpoint of the MBS, more transmission power leads to better performance. Therefore, the MBS tends to use as great a proportion of P_2^m as possible in this example. Therefore, we first determine a combination of P_1^m and P_2^m that produces equal or less interference to pico UEs given a number of ABS frames, which is denoted by N^A . When subframes are not muted in ABS scenarios, the maximum transmission power is used, which is denoted by P_3^m . G_{mu} , G_{pu} and G_{mp} are the channel gains amongst the MBS, the PBS and the pico UE, and the transmission power of the PBS is P^p . The SINR of the pico UE is shown as follows:

$$SINR_i = \frac{P^p \times G_{pu}}{P_i^m \times G_{mu} + N_0}, \quad i = 0, 1, 2, 3 \quad (4.31)$$

where $P_0 = 0$, and we have four different SINR values in this example. $SINR_0$ and $SINR_3$ are used in ABS scenario, and $SINR_1$ and $SINR_2$ are used in MTS with two power levels. We use LTE table lookup for calculating capacities, which

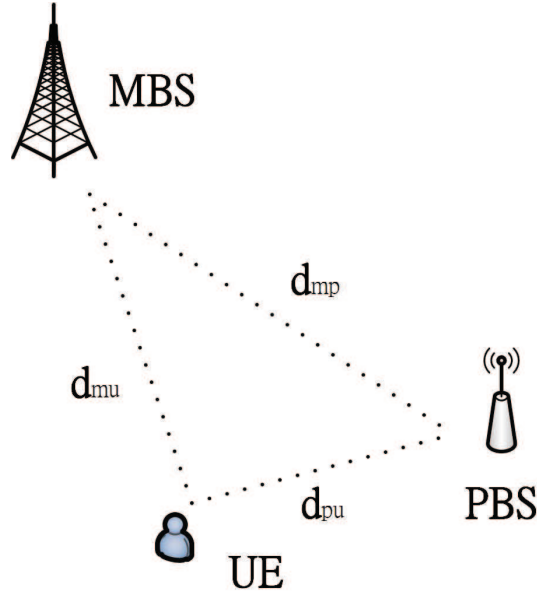


Figure 4.6: The topology used in the simple numeric analysis.

is the function of $SINR_i$ and denote it as $U(SINR_i)$. Denote N^D and N^1 as the ABS period and the number of subframes with power level P_1 , respectively. We need to find a combination of P_1 and P_2 to produce less or equal interference to the pico UE. So, we have the following equation:

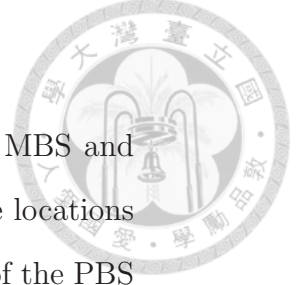
$$\sum_{i=1}^{N^1} U(SINR_1) + \sum_{i=1}^{N^D-N^1} U(SINR_2) \geq \sum_{i=1}^{N^A} U(SINR_0) + \sum_{i=1}^{N^D-N^A} U(SINR_3) \quad (4.32)$$

where the left-hand-side (LHS) is the capacity of MTS and right-hand-side (RHS) is the capacity of ABS scenario. To produce less or equal interference is equal to have higher or equal capacity. So, the greater or equal operation is held in (4.32). After some derivations, we have:

$$N^1 \geq \frac{N^A \times [U(SINR_0) - U(SINR_3)] + N^D \times [U(SINR_3) - U(SINR_2)]}{U(SINR_1) - U(SINR_2)} \quad (4.33)$$

Besides, N^1 is the number of subframes with power level P^1 , therefore, $0 \leq N^1 \leq$

4. MULTI-TONE SUBFRAMES FOR ENHANCED INTER-CELL INTERFERENCE COORDINATION IN LTE HETNETS

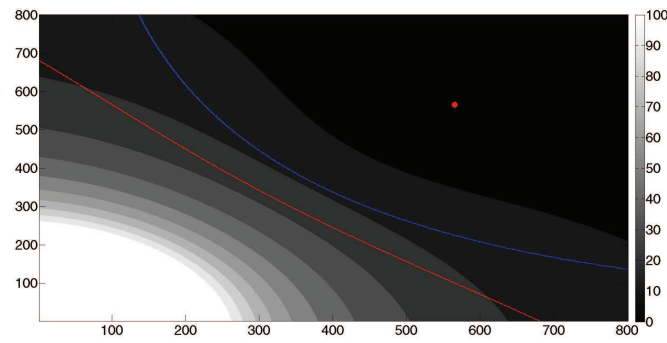


N^D .

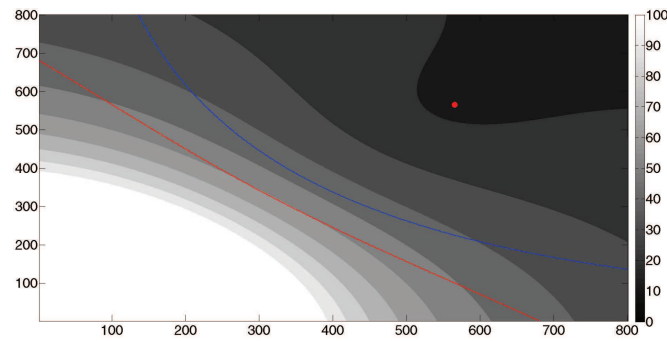
Fig. ?? shows some examples in which the distances between the MBS and the PBS are 800, 500 and 300 m. The red points in the figures are the locations of the PBS, and the MBSs are on the origin. The transmission power of the PBS is set to 30 dBm, and maximum power of the MBS is 46 dBm, namely, $P_3^m = 46$ dBm. We set P_1^m and P_2^m to 26 dBm and 43 dBm, respectively. The red and blue lines indicate the boundaries of the CRE bias (15 and 10 dB). The boundary of the CRE bias is an ellipse according to [?]. In eICIC, the CRE bias is usually set to around 10 dB; thus, the UEs outside the blue ellipse do not associate with the PBS in most conditions.

Each point in the figures represents the position of the pico UE. The grayscale stands for the minimum proportion of P_1^m needed to produce less or equal interference to the pico UE. A darker gray means that the MBS can use a lower proportion of P_1^m , and thus a higher proportion of P_2^m , to produce equal interference to the pico UE. We provide examples with different ABS proportion α , where $N^A = \alpha N^D$. In our intuition, the larger α leads to less interference experienced by the pico UE. A larger proportion of P_1^m is therefore needed. Accordingly, the figures with larger α values may seem brighter. Positions with white colour mean that we cannot use P_1^m and P_2^m to produce less or equal interference to the pico UE.

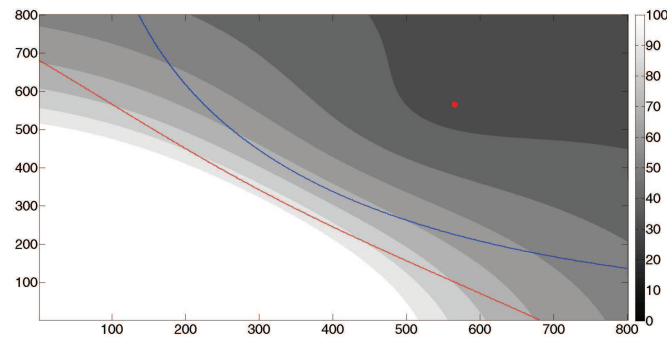
From Fig. ??, the MBS can use a larger proportion of P_2^m when the distance between the MBS and the PBS is 800 m. Even if the ABS proportion is increased to 40%, the MBS can still use P_2^m in some subframes no matter where the pico UE is located with 10-dB bias. When the distance between them is decreased to 300 m, some locations of the pico UE with 10-dB bias make it impossible for



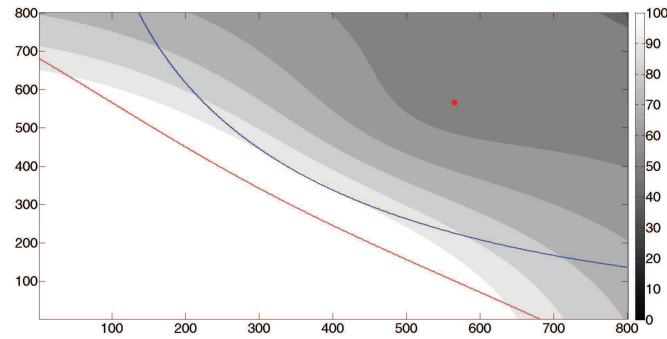
(a) 800m,10%



(b) 800m,20%



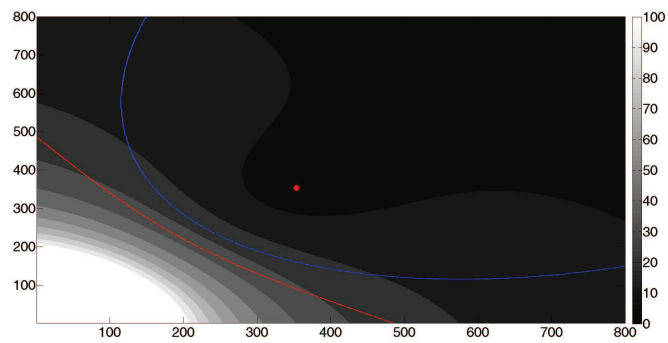
(c) 800m,30%



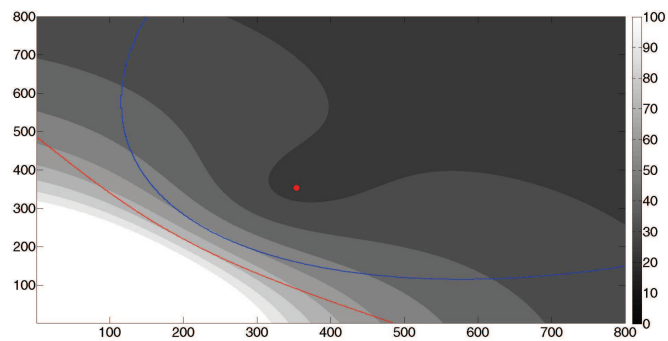
(d) 800m,40%

Figure 4.7: The distance between the MBS and the PBS is 800 meters, and different ABS proportions are evaluated.

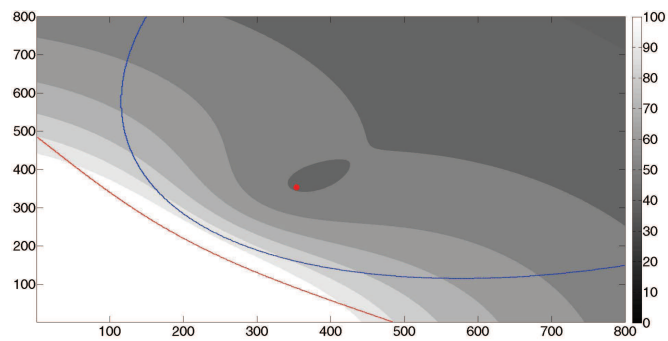
4. MULTI-TONE SUBFRAMES FOR ENHANCED INTER-CELL INTERFERENCE COORDINATION IN LTE HETNETS



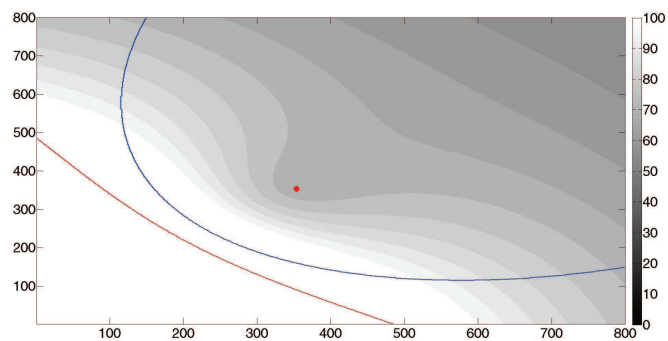
(a) 500m,10%



(b) 500m,20%

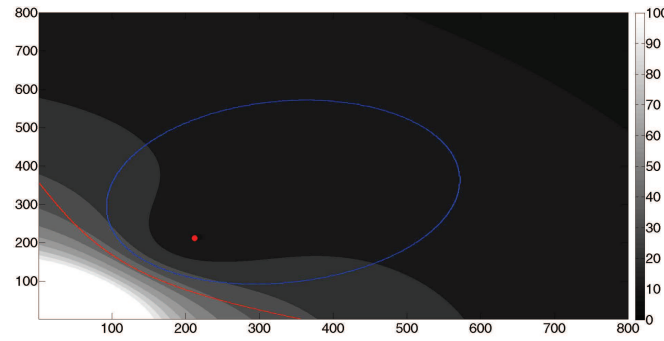


(c) 500m,30%

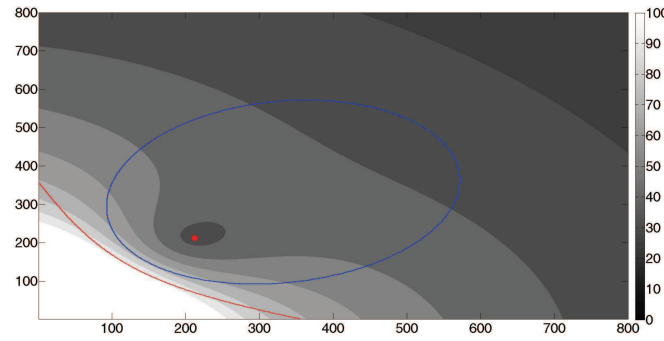


(d) 500m,40%

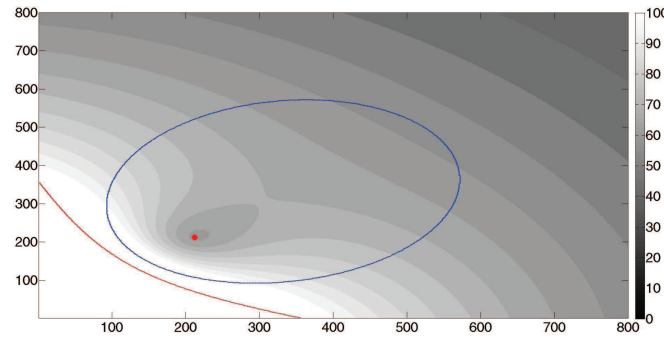
Figure 4.8: The distance between the MBS and the PBS is 500 meters, and different ABS proportions are evaluated.



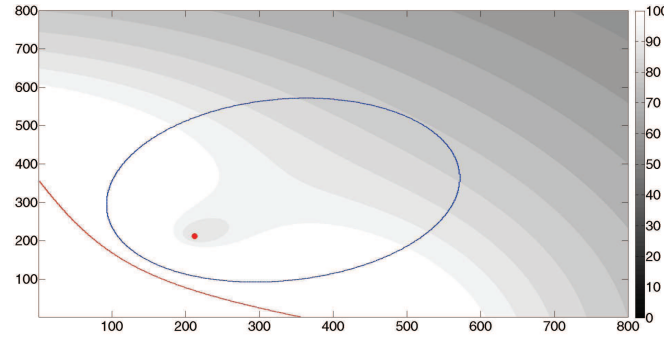
(a) 300m,10%



(b) 300m,20%



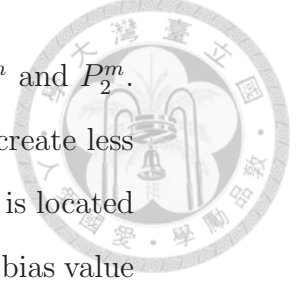
(c) 300m,30%



(d) 300m,40%

Figure 4.9: The distance between the MBS and the PBS is 500 meters, and different ABS proportions are evaluated.

4. MULTI-TONE SUBFRAMES FOR ENHANCED INTER-CELL INTERFERENCE COORDINATION IN LTE HETNETS



the MPS to produce less or equal interference to the pico UE with P_1^m and P_2^m . However, if we decrease the value of the CRE bias, the MBS can still create less or equal interference to the pico UE regardless of whether the pico UE is located with the decreased bias. For example, in Fig. 4.9(d), if we decrease the bias value to 3 dB, we find that the locations of the pico UE can make the MBS produce less or equal interference to the pico UE. According to this finding, we have the following proposition:

From this simple analysis, MTS has better performance than ABS even though there are only two power levels.

Theorem 5. *Through the proposed approach, the user further from the MBS would be assigned no less power than the users close to the MBS.*

Proof. According to Theorem 1, we know that a user further from the MBS would be assigned more transmission power. In the proposed approach, the transmission power is quantified into L levels instead of continuous assignment. Therefore, users with power level L_n would be further from the MBS than those with power level L_{n-1} . In a similar way, users with power level L_n would be nearer the MBS than those with power level L_{n+1} . The group of users with power level L_n is between the group of users with power level L_{n-1} and those with L_{n+1} . Therefore, the group of users with power level L_n is an annulus. We conclude that the users would be clustered into L groups, and these groups form annuluses.

$$\begin{aligned} U_1(P + \Delta P) - U_1(P) &< U_2(P + \Delta P) - U_2(P) \\ \Rightarrow U_1(P + \Delta P) + U_2(P) &< U_1(P) + U_2(P + \Delta P) \end{aligned} \tag{4.34}$$

According to (4.34), we conclude that assigning more power to the user who is further from the MBS creates more utility in the system. \square

Proposition 3. *The macro users scheduled by the proposed algorithm would be clustered into L groups, and these groups form annuluses.*

Proof. According to Theorem 1, we know that a user further to the macro BS would be assigned more transmission power. In the proposed approach, the transmission power is quantified into L levels instead of continuous assignment. Therefore, users with power level L_n would be further to the macro BS than those with power level L_{n-1} . In the similar way, users with power level L_n would be nearer to the macro BS than those with power level L_{n+1} . The group of users with power level L_n is between the group of users with power level L_{n-1} and L_{n+1} . So, the group of users with power level L_n is an annulus. We conclude that the users would be clustered into L groups, and these groups from annuluses. \square

4.4.3 Summary

In this section, we introduce the correlation among all approaches in the first. Then, we give a detailed numeric results to show the performance of the UE served the PBS in different locations. We give some propositions and theorems in the end of this chapter.

4.5 Simulation Results

4.5.1 Simulation Settings

In line with the system mode outlined in Chapter II, the network topology consists of a standard hexagonal grid of MBS complemented with a set of outdoor PBSs. Macrocells and picocells share the same 5 MHz of bandwidth at a carrier frequency of 2 GHz. The distance between the macrocells is 500 m, and the minimum distance amongst the small cells is 40 m. The propagation model consists of a deterministic distance-dependent component and an independent stochastic component for shadow fading, which we adopt as two-way ground fading. The simulation parameters are set according to HetNet simulations suggested by

4. MULTI-TONE SUBFRAMES FOR ENHANCED INTER-CELL INTERFERENCE COORDINATION IN LTE HETNETS



Table 4.2: Simulation Settings

Parameter	Value
Cellular layout	7 Hexagonal Grid
Carrier frequency	2 GHz
System bandwidth	5 MHz
Subframe duration	1 ms
Number of macrocells	1
Number of PBSs per macrocell	4
Max. macro BS transmit power	46 dBm
Max. pico BS transmit power	30 dBm
Number of UEs per Macrocell N_{UE}	120
Number of hotspot UEs $N_{hotspot}$	$\lceil 2/3 \cdot N_{UE} \rceil$
Thermal noise density	-174 dBm
Macro path loss model	$128.1 + 37.6 \log_{10}(km) dB$
Pico path loss model	$140.7 + 36.7 \log_{10}(km) dB$
Traffic model	Full buffer
Shadowing Model	Two-way Ground Fading
Fading Model	Raleigh Fading

3GPP [94, 102]. The summary of the simulation settings are shown in Table 4.2.

We apply a full buffer traffic model with infinite data packets in the queue for each BSs while evaluating the system capacity. The assignment of power levels are: $P_1 = 0$, $P_2 = P_s$, $P_L = P_m$, and $P_i = P_m + (P_m - P_s)/(L - 2)$. The power levels used in the simulation are shown in Table 4.3.

4.5.2 Compare with Optimal Solution

The proposed algorithm consists of two algorithms: the interior point relaxed MTS optimization algorithm and the round relaxed MTS algorithm. As mentioned before, the solutions for the MTS optimization problem are discrete and

**Table 4.3:** Transmission Power Level

4 Levels	0,30,38,46 (dBm)
5 Levels	0,30,35,41,46 (dBm)
6 Levels	0,30,34,38,42,46 (dBm)
7 Levels	0,30,33,36,39,42,46 (dBm)

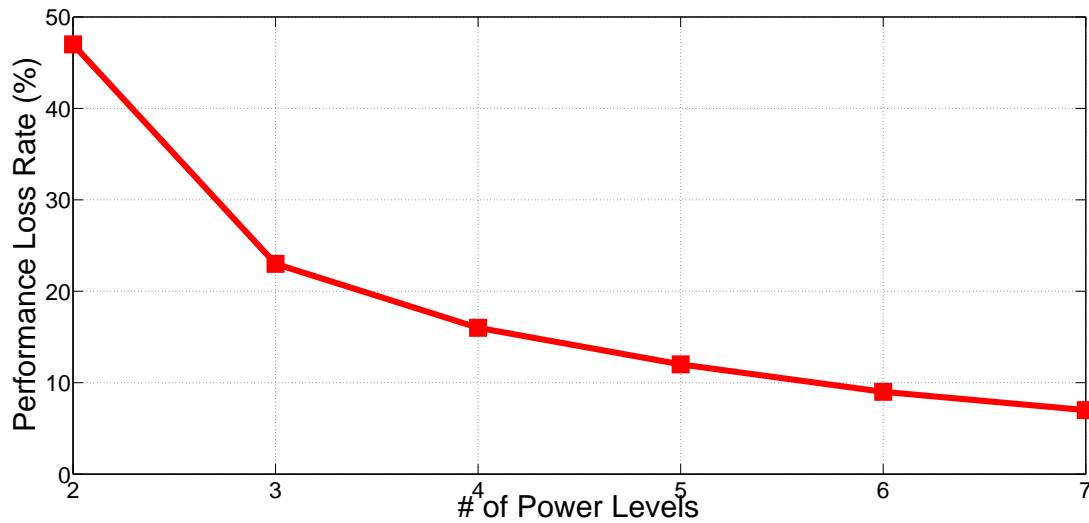


Figure 4.10: The performance loss rate with different power levels compared to the optimal solution obtained from the interior point relaxed MTS optimization algorithm.

4. MULTI-TONE SUBFRAMES FOR ENHANCED INTER-CELL INTERFERENCE COORDINATION IN LTE HETNETS

the purpose of the second algorithm is to transform the solution obtained from the first algorithm, which is continuous, into a discrete solution. Because we prove that the solution obtained from the first algorithm is optimal, the round procedure in the second algorithm would produce some loss of performance. Therefore, we compare the number of power levels with the performance loss rate in this section.

Fig. 4.10 shows the result. The rate of performance loss is more than 40% with two power levels, and the rate of loss is lower than 20% if the number of power levels is increased to 4. When the number of power levels is increased to 7, the rate of performance loss is lower than 10%. The rate of performance loss will achieve 0 if we increase the number of power levels to infinity. We consider a loss of lower than 10% to be acceptable, so we use seven power levels in our algorithm in the following simulations.

4.5.3 User Clustering

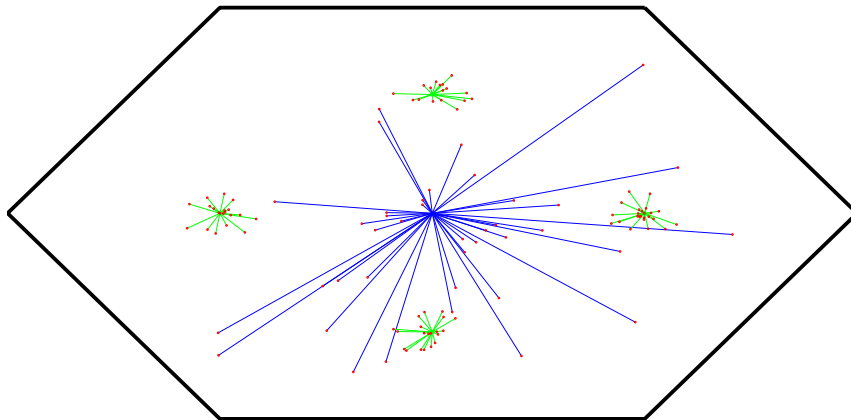


Figure 4.11: The user association in the center cell.

As mentioned in Proposition 2, macro-UEs may be clustered into several

**Table 4.4:** Number of UEs in the Groups

Power Level	Number of UEs
Power Level 2	4
Power Level 3	4
Power Level 4	8
Power Level 5	9
Power Level 6	9
Power Level 7	6

groups, depending on the number of power levels. In this section, we show the user-clustering phenomenon of the proposed algorithm. Because the simulation is conducted in seven macrocells, we choose the one in the centre for observation. Fig. 4.11 shows the corresponding macrocell, which includes the UEs, the MBS and the PBSs. The user association is also shown in the figure, where the blue and green lines represent associations with the MBS and the PBSs, respectively.

The number of power levels used in the simulation is 7, therefore, the number of groups the macro UEs be clustered would be 6. Because the power level P_0 stands for muting subframes, no UEs can be served in these subframes. Fig. 4.12, Fig. 4.13, Fig. 4.14, Fig. 4.15, Fig. 4.16 and Fig. 4.17 show groups of UEs served by different power levels. We find that only 6 UEs needs to be served by the maximum transmission power. More than half of UEs can be served by the power levels P_3 , P_4 and P_5 . The number of UEs in the groups is shown in Table 4.4. We will show that this behavior would save much power in the following section.

4. MULTI-TONE SUBFRAMES FOR ENHANCED INTER-CELL INTERFERENCE COORDINATION IN LTE HETNETS

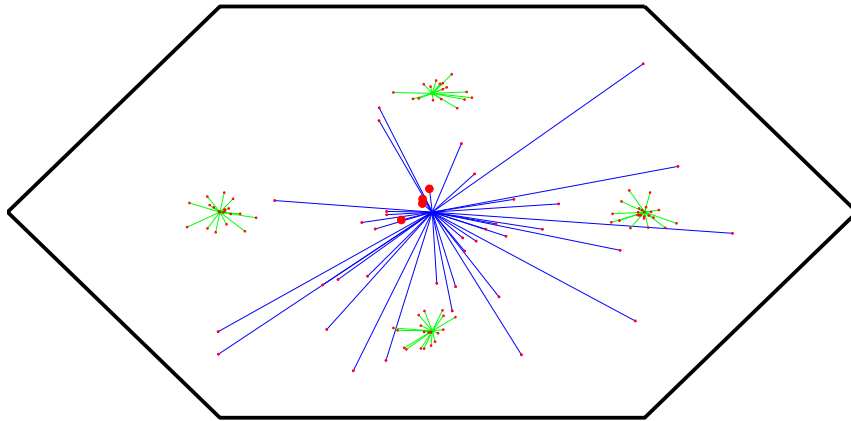


Figure 4.12: The group of UEs served by the power level P_2 .

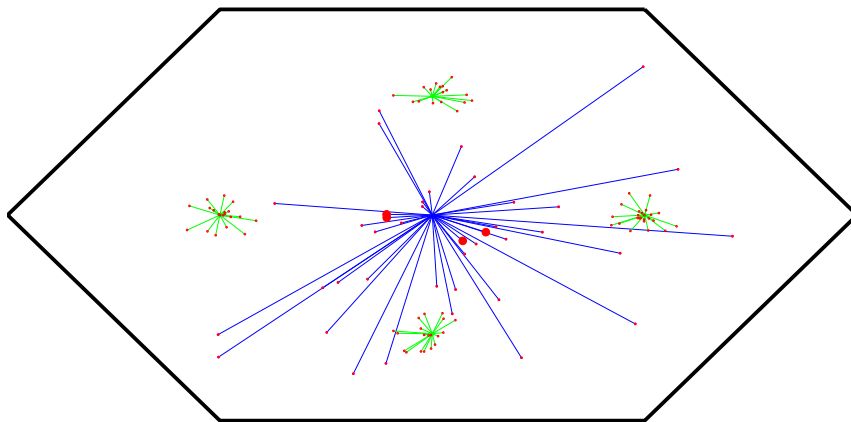


Figure 4.13: The group of UEs served by the power level P_3 .

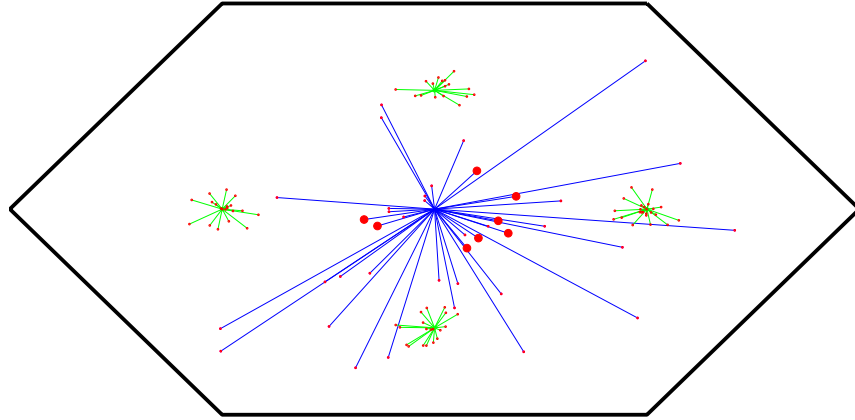


Figure 4.14: The group of UEs served by the power level P_4 .

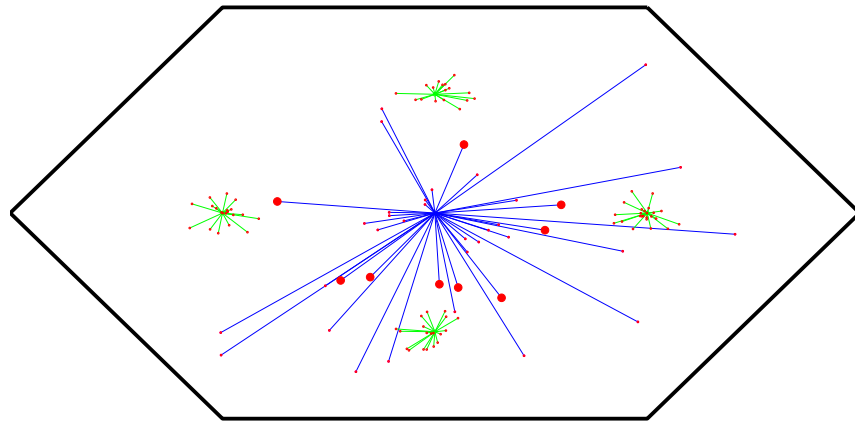


Figure 4.15: The group of UEs served by the power level P_5 .

4. MULTI-TONE SUBFRAMES FOR ENHANCED INTER-CELL INTERFERENCE COORDINATION IN LTE HETNETS

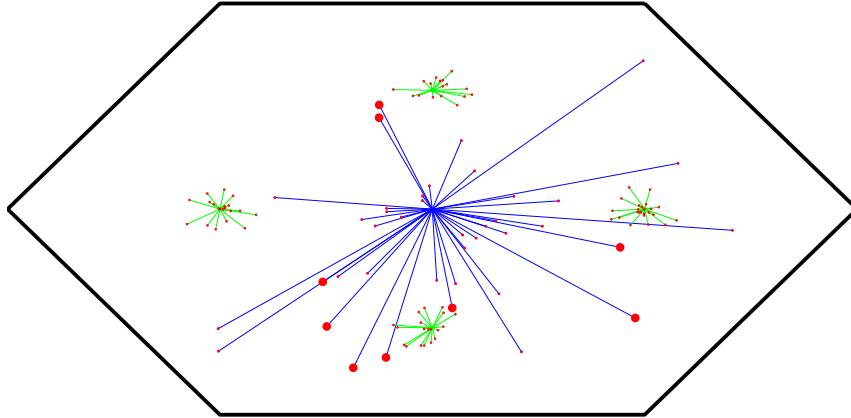


Figure 4.16: The group of UEs served by the power level P_6 .

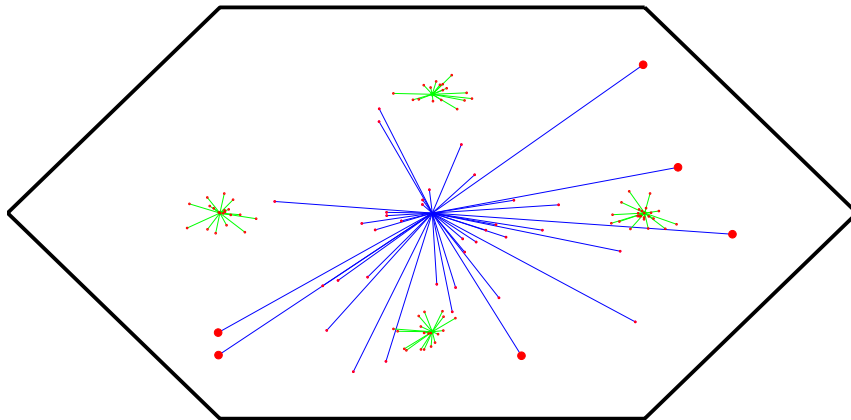


Figure 4.17: The group of UEs served by the power level P_7 .

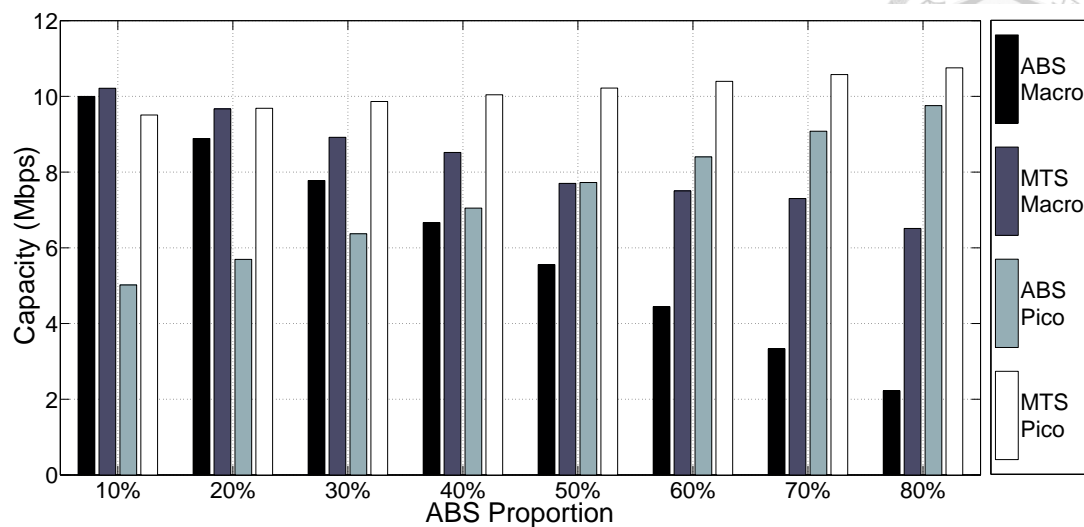


Figure 4.18: Comparison of the capacity of the MBS and the PBS in the original ABS scheme and the proposed MTS approach.

4.5.4 System Capacity

To evaluate the system capacity, a simple environment with one MBS and one PBS separated by 300 m is conducted first. It is straightforward that the capacity of the MBS is reduced when ABS proportion increases because the MBS sacrifices more subframes to protect the performance of the PBS. Therefore, the performance of the PBS gets better and better. In contrast, in the proposed scheme, the MBS does not use the maximum transmission power. Instead, P_6 and P_5 may be suitable for most conditions; therefore, the interference that the PBS surfs is lightened. In this way, the MBS can retain its performance and the PBS can have better performance in the original non-ABS frames.

In contrast, the MBS transmits with little power instead of blanking the subframes in the original ABS. In this way, the MBS is degenerated into a PBS; therefore, the cell centre UEs can still be served. The increased interference to the PBS can almost be ignored. Therefore, as seen in Fig. 4.18, the capacities

4. MULTI-TONE SUBFRAMES FOR ENHANCED INTER-CELL INTERFERENCE COORDINATION IN LTE HETNETS



of the MBS and the PBS are greater than those of the ABS scheme regardless of the ABS proportion. We increase the performance of the MBS without harming that of the PBS.

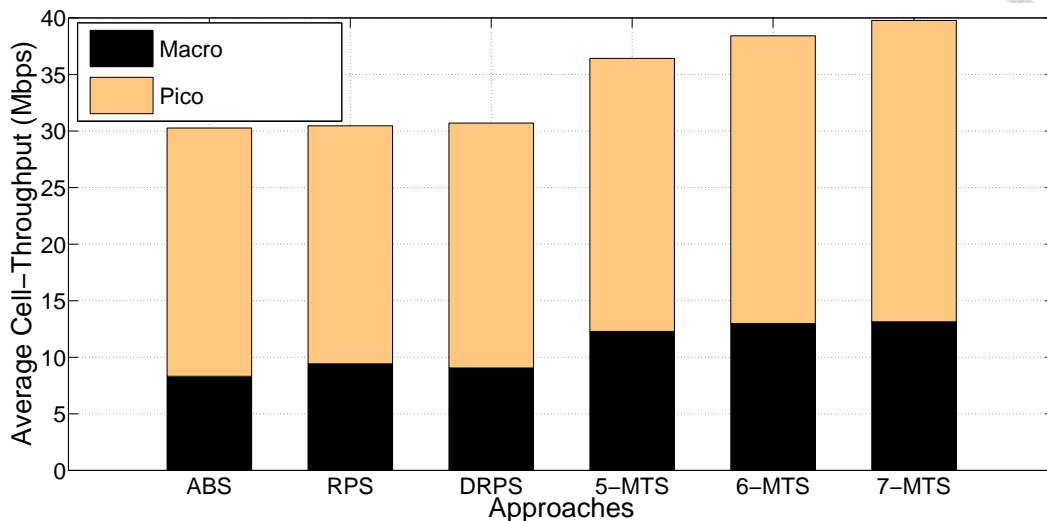


Figure 4.19: The average throughput of cells in different approaches.

Next, we compare the average cell throughput amongst all of the approaches. As mentioned before, RPS involves a trade-off between the performance of macro-cells and picocells. Therefore, from Fig. 4.19, we see that the performance of RPS and ABS are almost the same; the performance of the macrocells is greater than that of the PBS in RPS; however, on the contrary, it is worse in ABS. DRPS improves the shortcut of RPS, and the performance of DRPS is shown in the Figure. However, it is still lower than the proposed MTS scheme because both RPS and DRPS use the maximum transmission power during non-ABS subframes. MTS can adjust the most suitable power level on each subframe; therefore, the performance of the macrocells and that of the picocells both increase. We also find that better performance would be obtained with more power levels.

In the last part of this section, we show the cumulative density function (CDF)

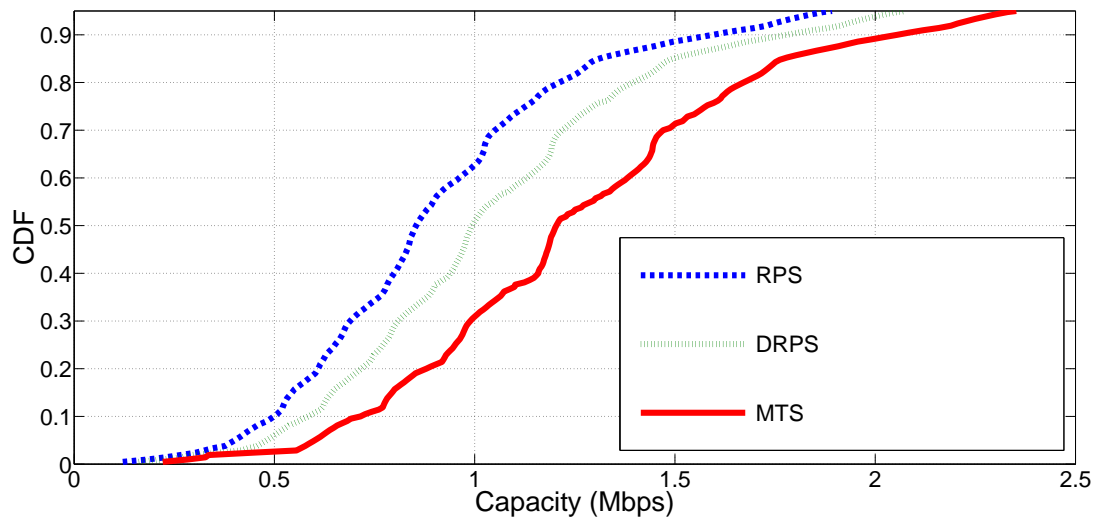


Figure 4.20: The CDF of UEs' capacity in three approaches: RPS, DRPS and MTS.

of the UEs' capacity amongst RPS, DRPS and MTS in Fig. 4.20. RPS and ABS involve a trade-off between the performance of the macrocells and picocells; therefore, the CDF of ABS is not plotted in the Figure. From Fig. 4.20, it is obvious that the performance of MTS is better than that of the others regardless of the cell edge UEs, the median UE and the average performance amongst the cells.

4.5.5 Power Consumption

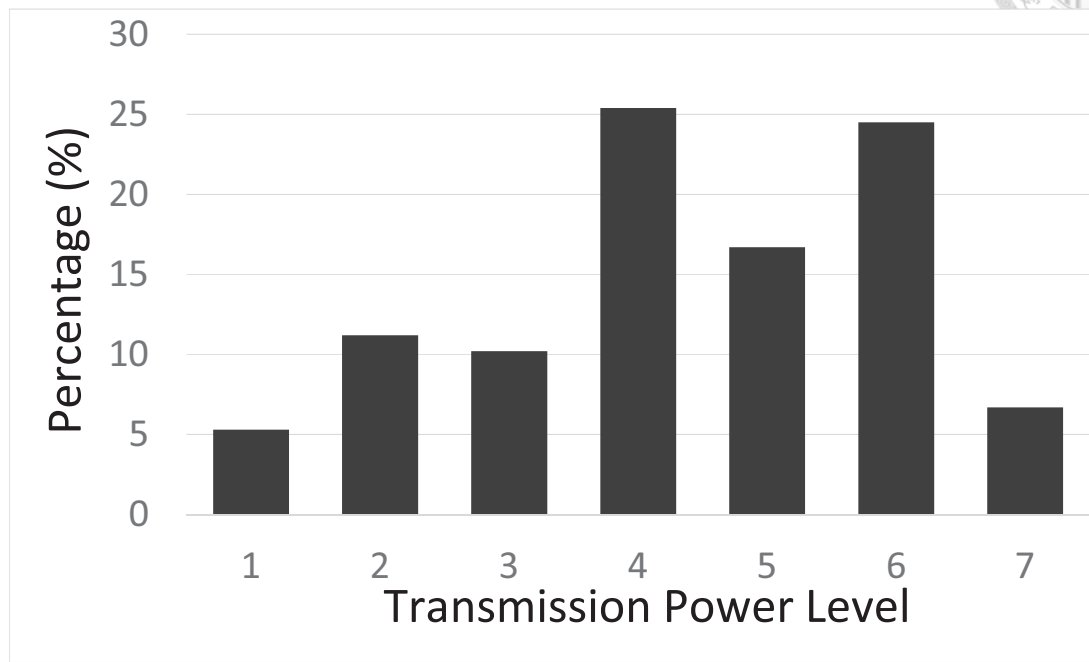


Figure 4.21: The distribution of transmission power levels in the system.

In this section, we compare power consumption amongst all of the approaches. First, we show the power level distribution in the proposed algorithm amongst all cells; as shown in Fig. 4.21, the maximum power, that is, power level 7, is only about 7%. This behaviour tells us that maximum power is not used for transmission in most conditions because it would be wasted; it is enough to use P_3 , P_4 and P_5 . In addition, the proportion of blank subframes is very low, about 5%, because using P_1 or P_2 instead of blanking subframes can increase the spectrum utilisation of MBSs without harming the performance of the picocells. Therefore, the performance of the whole system is increased.

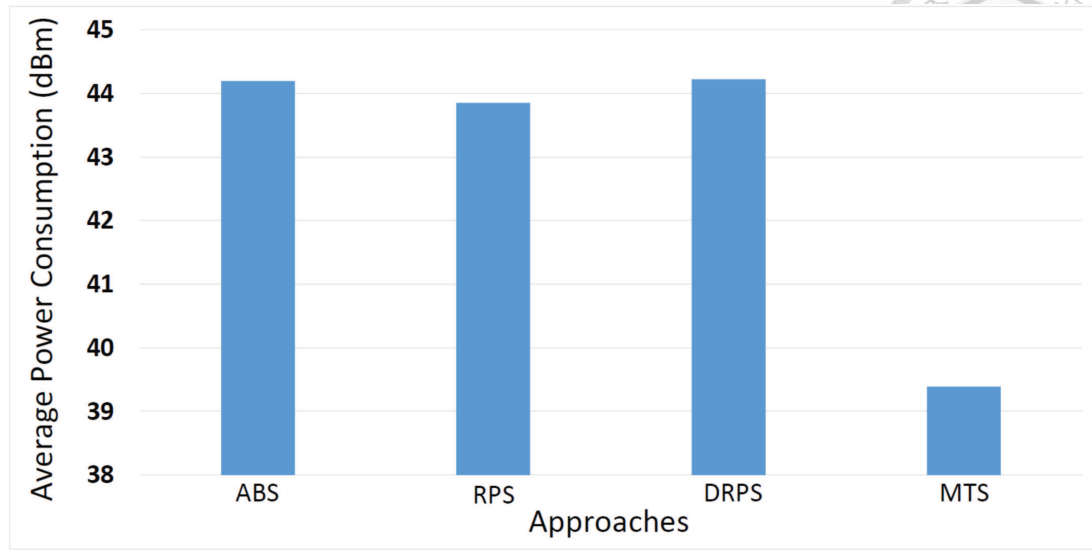
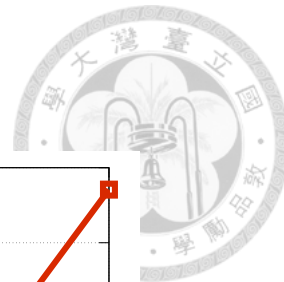


Figure 4.22: The power consumption of all approaches.

Fig. 4.22 shows the average power consumption amongst all of the approaches. It is obvious that the proposed approach has the lowest power consumption, only about 30% of that of the other approaches, due to the very low proportion of maximum power transmission of MTS. From the aspect of green communication, the proposed approach saves a great deal of power.



4.5.6 VoLTE Latency

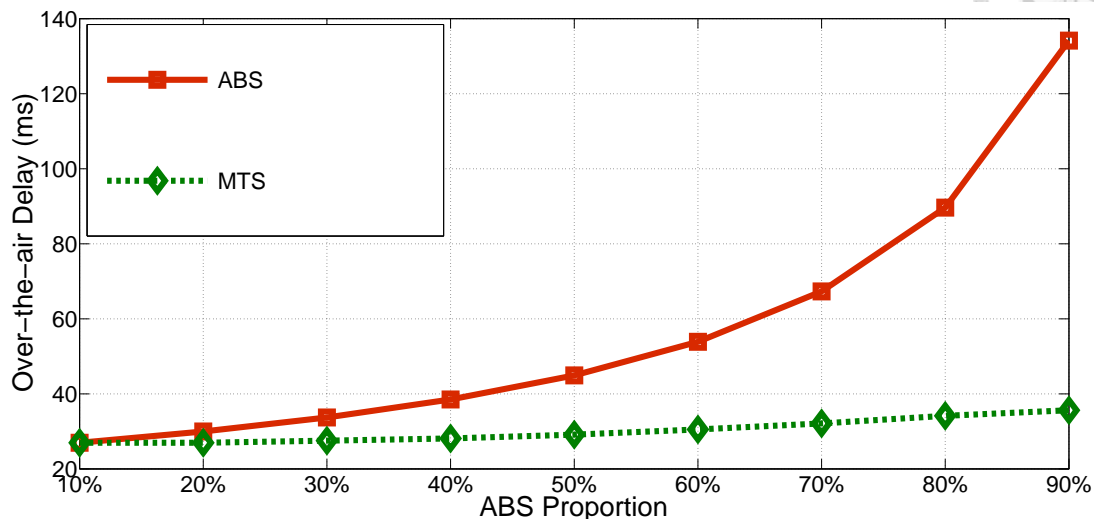
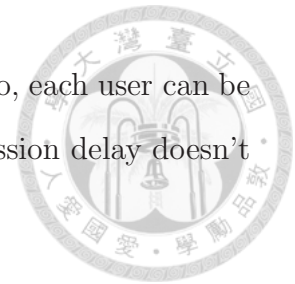


Figure 4.23: The over-the-air delay of the ABS scheme and the proposed approaches.

In this section, we study VoLTE traffic latency of ABS and MTS. The simulation settings are according to the work in [103], and the load of macrocells is about 275 VoLTE users based on the same work. We set the number of VoLTE users to 250 in a macrocell, and assume that there is no limit on the number of physical downlink control channel (PDCCH) available. We study the over-the-air transmission delay, and it is unacceptable while the delay is more than 50 ms.

Fig. 4.23 shows the delay time versus proportion of ABSs. We find that delay time increased dramatically while ABS proportion gets higher. This is because that the higher ABS proportion, the less subframes MBSs can use. It leads to that UEs need to wait a lot of subframes to transmit a packet, therefore, the delay for UEs is increased. By contrast, Multi-tone ABS increases the spectrum utilization of MBSs, therefore, MBSs do their best to use each subframe. Under this condition, subframes with lower power can be used by cell-center users, and



subframes with higher power can be used by cell-edge users. So, each user can be scheduled in appropriate subframes. The over-the-air transmission delay doesn't get higher in Multi-tone ABS.

4.5.7 Summary

In this section, we provide various simulation results to show the performance of the proposed approach. First, we show the performance loss compared to the optimal solution obtained from the first algorithm, namely interior point relaxed MTS optimization algorithm. We show that using seven power levels has lower than 10% performance loss. Second, an example of UE clustering is provided. Third, we compare the proposed algorithm with other approaches from the view point of system capacity to show the outstanding of the proposed algorithm. Fourth, the power consumption of all algorithms is also conducted, and the result shows that the proposed algorithm saves much. In the last, we show the over-the-air delay of the proposed algorithm and ABS scheme. The result shows the proposed algorithm also has outstanding in this aspect.

4.6 Concluding Remarks

Ultra-dense small cell deployment is the most appealing approach with which to meet the requirements of the dramatically increasing demand for data traffic. Therefore, heterogeneous networks (HetNets) that contain macrocells and small cells have recently become a popular research topic. The most important issue regarding HetNets is intercell interference; therefore, an almost-blank subframe is proposed to deal with the interference between macrocells and small cells. However, the macrocells will waste spectrum resources while using an almost-blank

4. MULTI-TONE SUBFRAMES FOR ENHANCED INTER-CELL INTERFERENCE COORDINATION IN LTE HETNETS

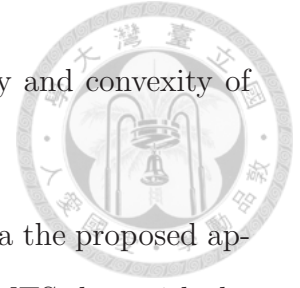


subframe. Reduced-power subframes have been proposed as a key technique for further enhancement of intercell interference coordination in the Third Generation Partnership Project to compensate for the insufficiencies of the almost-blank subframe. However, according to the literature, these two approaches involve a trade-off between the performance of the system as a whole and the performance of the outage users. In this work, we propose a scheme called multitone subframes to handle this situation by increasing the system capacity without harming the performance of the outage users. We formulate the multitoned subframe assignment problem as an optimisation problem and solve it with the interior method. We provide mathematical analysis of the optimality and complexity of the proposed algorithm and evaluate its performance via computer simulation. According to the simulation results, the proposed scheme has (1) improved system capacity without a reduction in the performance of outage users and (2) lower power consumption and better performance than other approaches. The contributions are summarized as follows:

1. We address the insufficiencies of RPS and propose an algorithm to improve the system performance. RPS and ABS involve a trade-off between the average capacity and the capacity of the edge UEs. The proposed algorithm improves both capacities at the same time. The goal of the proposed algorithm is to increase the capacity of macrocells without harming that of picocells.
2. The proposed algorithm is based on the interior point method. It is difficult to provide reliable design guidelines to make the method suitable for all types of problems. In this study, we customise the interior point method to

provide a powerful algorithm and provide the optimality and convexity of the proposed algorithm.

3. From the simulation results, we find many advantages via the proposed approaches. First, the spectrum utilisation is greater with MTS than with the ABS scheme. Second, we increase the capacity of MBSs without harming the performance of PBSs. Third, from the viewpoint of green communication, we save a great deal of power compared to other approaches. Finally, we reduce the latency of real-time traffic in MBSs compared to ABS scheme.



4. MULTI-TONE SUBFRAMES FOR ENHANCED INTER-CELL INTERFERENCE COORDINATION IN LTE HETNETS





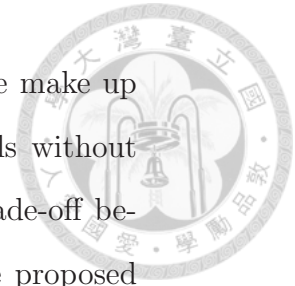
Chapter 5

Conclusion

It is forecasted that at least a $100\times$ network capacity increase will be required to meet the traffic demands in 2020. As a result, vendors and operators are now looking at using every tool at hand to improve network capacity. Increasing the network densification is considered at the most workable solution to meet the requirements. Therefore, the so called heterogeneous networks which contain traditional macrocells and small cells is used to increase the network densification efficiently. Small cells, such as femtocell, picocell and relay nodes, are used to increase the network capacity and make up the insufficiency of macrocells. This dissertation focuses on the issue on relay node and picocells. For the relay node, we propose a relay node assignment algorithm called "Decentralized Learning based Relay Assignment" (DLRA) to performance relay node selection in cooperative communication. There are several advantages in DLRA: (1) DLRA is a fully decentralized approach; (2) the selection procedure in only based on existing environmental feedback; (3) Comprehensive mathematical analysis and performance manipulation are provided. On the other hand, we mitigate the interference between macrocells and picocells, and propose an approach called "Multi-Tone

5. CONCLUSION

Subframes” (MTS) scheme to achieve this goal. The proposed scheme make up insufficiency of ABS and RPS: it increases the capacity of macrocells without harming the performance of the picocells since ABS and RPS are trade-off between them. We give an simple example to show the efficient of the proposed approach. Besides, the optimality and the complexity of the proposed approach are also provide in the dissertation. For both relay assignment and interference mitigation problem, we give simulation results to show the both approaches outperform other approaches.





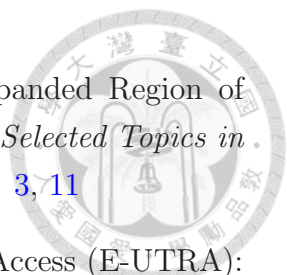
Bibliography

- [1] Qualcomm, “the 1000x mmobile data challenge: More sspectrum, more small ccell, more indoor ccell and higher efficiency”,
<http://www.qualcomm.com/>. 1
- [2] X. Chu, D. L. L.-P. Yang, and F. Gunnarsson, “Heterogeneous Cellular Networks: heory, Simulation and Deployment,” *University Cambridge Press*, 2013. 1
- [3] H. Claussen, L. T. W. Ho, and L. G. Samuel, “An Overview of the Femtocell Concept,” *Bell Labs Technical Journal*, vol. 13, no. 1, pp. 221–245, 2008. 1, 3
- [4] V. Chandrasekhar, J. G. Andrews, and A. Ga, “Femtocell Networks: A Survey,” *IEEE Communications Maga*, vol. 46, no. 9, pp. 59–67, 2008. 1, 3
- [5] J. Andrews, H. Claussen, M. Dohler, S. Rangan, and M. Reed, “Femtocells: Past, present, and future,” *IEEE Journal on Selected Areas in Communications*, vol. 30, no. 3, pp. 497–508, April. 1
- [6] 3GPP TR 36.808, “Evolved Universal Terrestrial Radio Access (E-UTRA); Carrier Aggregation; Base Station (BS) radio transmission and reception,” 2013. 1
- [7] 3GPP TR 36.889, “Feasibility Study on Licensed-Assisted Access to Unlicensed Spectrum,” 2014. 1
- [8] T. S. Rappaport, R. W. H. Jr., R. C. Daniels, and J. N. Murdock, “Millimeter Wave Wireless Communications,” *Prentice Hall*, 2014. 1

BIBLIOGRAPHY

- [9] L. L. Hanzo, Y. Akhtman, L. Wang, and M. Jiang, “MIMO-OFDM for LTE, WiFi and WiMAX: Coherent versus Non-coherent and Cooperative Turbo Transceivers,” *John Wiley & Sons Ltd*, 2011. 2
- [10] M. D. Hanwen, “Muulti-point Cooperative Communication Systems: Theory and Applications,” *Springer*, 2013. 2
- [11] Z. S. Khoyaev and E. E. E. Pan, “Dynamic uplink-downlink configuration and interference managemnt in TD-LTE,” *IEEE Communications Magazine*, vol. 50, pp. 51–59, 2012. 2
- [12] M. Ding, D. Lopez-Perez, and W. C. C. Vasilakos, “Dynamic TDD TTransmission in Homogeneous Small Cell Networks,” *IEEE International Conference on Communications (ICC)*, 2014. 2, 13
- [13] Webb, “Wireless Communications: Is the Future Playing Out as Predicted?” *International Journal of Interdisciplinary Telecommunications and Networking*, vol. 1, 2009. 2
- [14] Cisco, “Cisco visula networking index: Global mobile data traffic forecast update, 2014 – Global Mobile Data TTraffic Forecast Update, 2014–2019,” *White Paper*, 2015. 3
- [15] A. Damnjanovic, J. Montojo, Y. Wei, T. Ji, T. Luo, M. Vajapeyam, T. Yoo, O. Song, and D. Malladi, “A survey on 3GPP heterogeneous networks,” *IEEE Wireless Communications*, vol. 18, no. 3, pp. 10 –21, June 2011. 3, 58
- [16] D. Lopez-Perez, I. Guvenc, G. de la Roche, M. Kountouris, T. Q. S. Quek, and Z. Jie, “Enhanced Inter-Cellell Interference Coordination Challenges in Heterogeneous Networks,” *IEEE Wireless Communications*, vol. 18, no. 3, pp. 22–30, 2011. 3, 58
- [17] S. C. Forum, “Small Cell Market Status Dec 2012,” *White paper*, 2012. 3
- [18] D. Lopez-Perez, A. Valcarce, G. de la Roche, and J. Zhang, “OFDMA femtocells: A roadmap on interference avoidance,” *IEEE Communications Magazine*, vol. 47, no. 9, pp. 41–48, September 2009. 3



- 
- [19] D. Lopez-Perez, X. Chu, and I. Guvenc, “On the Expanded Region of Picocells in Heterogeneous Networks,” *IEEE Journal of Selected Topics in Signal Processing*, vol. 6, no. 3, pp. 281–294, June 2012. [3](#), [11](#)
- [20] 3GPP TS 36.300, “Evolved Universal Terrestrial Radio Access (E-UTRA): Further Advancements for E-UTRA Physical Layer Aspects,” *Technical Specification Group Radio Access Network*, April 2010. [5](#), [60](#)
- [21] E. C. V. D. Meulen, “Three terminal communication channels,” *Advanced in Applied Probability*, vol. 3, pp. 120–154, 1971. [7](#)
- [22] T. Cover and A. Gamal, “Capacity theorems for the relay channel,” *IEEE Transactions on Information Theory*, vol. 25, no. 5, pp. 572–584, 1979. [7](#)
- [23] Y. Zhao, R. Adve, and T. J. Lim, “Improving amplify-and-forward relay networks: optimal power allocation versus selection,” *IEEE Transactions on Wireless Communications*, vol. 6, no. 8, pp. 3114–3123, 2007. [7](#), [15](#)
- [24] Y. Yang, H. Hu, J. Xu, and G. Mao, “Relay technologies for WiMax and LTE-advanced mobile systems,” *IEEE Communications Magazine*, vol. 47, no. 10, pp. 100–105, 2009. [7](#)
- [25] Y. Jing and H. Jafarkhani, “Single and multiple relay selection schemes and their achievable diversity orders,” *IEEE Transactions on Wireless Communications*, vol. 8, no. 3, pp. 1414–1423, 2009. [7](#)
- [26] D. Yang, X. Fang, and G. Xue, “HERA: An Optimal Relay Assignment Scheme for Cooperative Networks,” *IEEE Journal on Selected Areas in Communications*, vol. 30, no. 2, pp. 245–253, 2012. [8](#)
- [27] X. Zhang, A. Ghrayeb, and M. Hasna, “On relay assignment in network-coded cooperative systems,” *IEEE Transactions on Wireless Communications*, vol. 10, no. 3, pp. 868–876, 2011. [8](#)
- [28] P. Li, S. Guo, W. Zhuang, and B. Ye, “Capacity Maximization in Cooperative CRNs: Joint Relay Assignment and Channel Allocation,” in *IEEE ICC*, June 2012, pp. 6619–6623. [8](#)

BIBLIOGRAPHY

- [29] M. Peng, C. Yang, Z. Zhao, W. Wang, and H.-H. Chen, “Cooperative network coding in relay-based int-advanced systems,” *IEEE Communications Magazine*, vol. 50, no. 4, pp. 76–84, 2012. [8](#)
- [30] C. Fragouli, D. Katabi, A. Markopoulou, M. Medard, and H. Rahul, “Wireless Network Coding: Opportunities & Challenges,” in *IEEE Military Communications Conference, 2007.*, 2007, pp. 1–8. [8](#)
- [31] N. Linh-Trung, V. N. Q. Bao, P. Duhamel, and M. Debbah, “Challenging issues in multimedia transmission over wireless networks based on network coding,” in *2012 IEEE International Symposium on Signal Processing and Information Technology (ISSPIT)*, 2012, pp. 000 124–000 128. [8](#)
- [32] J. Cai, X. Shen, J. W. Mark, and A. Alfa, “Semi-distributed user relaying algorithm for amplify-and-forward wireless relay networks,” *IEEE Transactions on Wireless Communications*, vol. 7, no. 4, pp. 1348–1357, 2008. [8](#), [9](#), [16](#)
- [33] Y. Shi, S. Sharma, Y. T. Hou, and S. Kompella, “Optimal Relay Assignment for Cooperative Communications,” in *Proceedings of the 9th ACM international symposium on Mobile ad hoc networking and computing*. Hong Kong, Hong Kong, China: ACM, 2008, pp. 3–12. [8](#)
- [34] Y. Li, B. Vucetic, Z. Zhou, and M. Dohler, “Distributed adaptive power allocation for wireless relay networks,” *IEEE Transactions on Wireless Communications*, vol. 6, no. 3, pp. 948–958, 2007. [8](#)
- [35] M. Chen, S. Serbetli, and A. Yener, “Distributed power allocation strategies for parallel relay networks,” *IEEE Transactions on Wireless Communications*, vol. 7, no. 2, pp. 552–561, 2008. [8](#)
- [36] S. Kadloor and R. Adve, “Relay selection and power allocation in cooperative cellular networks,” *IEEE Transactions on Wireless Communications*, vol. 9, no. 5, pp. 1676–1685, 2010. [8](#)




- [37] R. Madan, N. Mehta, A. Molisch, and J. Zhang, “Energy-efficient cooperative relaying over fading channels with simple relay selection,” *IEEE Transactions on Wireless Communications*, vol. 7, no. 8, pp. 3013–3025, 2008. [8](#)
- [38] C. Y. Lee and G. Hwang, “Fair and minimal power allocation in a two-hop relay network for qos support,” *IEEE Transactions on Wireless Communications*, vol. 10, no. 11, pp. 3864–3873, 2011. [8](#)
- [39] S. Mallick, M. Rashid, and V. Bhargava, “Joint relay selection and power allocation for decode-and-forward cellular relay network with channel uncertainty,” *IEEE Transactions on Wireless Communications*, vol. 11, no. 10, pp. 3496–3508, 2012. [8](#)
- [40] T. Guo and R. Carrasco, “Crbar: Cooperative relay-based auto rate mac for multirate wireless networks,” *IEEE Transactions on Wireless Communications*, vol. 8, no. 12, pp. 5938–5947, 2009. [8](#)
- [41] N. Yi, Y. Ma, and R. Tafazolli, “Joint rate adaptation and best-relay selection using limited feedback,” *IEEE Transactions on Wireless Communications*, vol. 12, no. 6, pp. 2797–2805, 2013. [8](#)
- [42] M. Abouelseoud and A. Nosratinia, “Heterogeneous relay selection,” *IEEE Transactions on Wireless Communications*, vol. 12, no. 4, pp. 1735–1743, 2013. [8](#)
- [43] S. Sharma, Y. Shi, Y. Hou, and S. Kompella, “An optimal algorithm for relay node assignment in cooperative ad hoc networks,” *IEEE/ACM Transactions on Networking*, vol. 19, no. 3, pp. 879–892, 2011. [8](#), [15](#), [17](#), [40](#), [41](#), [42](#)
- [44] D. Yang, X. Fang, and G. Xue, “OPRA: Optimal Relay Assignment for Capacity Maximization in Cooperative Networks,” in *2011 IEEE International Conference on Communications (ICC)*, 2011, pp. 1–6. [8](#), [15](#)
- [45] 3GPP TR 36.839, “Evolved Universal Terrestrial Radio Access (E-UTRA); Mobility Enhancements in Heterogeneous Networks.” *V 11.1.0*, 2012.

BIBLIOGRAPHY

- [46] 3GPP R1-113806, “Performance Study on ABS with Reduced Macro Power,” *Pana*, 2011. [9](#), [10](#)
- [47] 3GPP R1-113118, “Performance Evaluation of Cell Range Expansion in Combination with ABS Ratio Optimization,” *Panaso*, 2011. [9](#)
- [48] M. Simsek, M. Bennis, and I. Guvenc, “Learning Based Frequency- and Time-Domain Inter-Cell Interference Coordination in HetNets,” *IEEE Transactions on Vehicular Technology*, vol. PP, no. 99, pp. 1–1, 2014. [9](#)
- [49] 3GPP R1-104968, “New work item proposal: EEnhanced ICIC for non-CA Based Deployments of Heterogeneous Networks for LTE,” *CMCC*, 2010. [10](#)
- [50] 3GPP TS 36.133, “Evolved Universal Terrestrial Radio Access (E-UTRA); Requirements for support of radio resource management.” *V 11.4.0*, 2013. [11](#)
- [51] A. Morimoto, N. Miki, and Y. Okumura, “Investigation of Inter-Cell Interference Coordination Applying Transmission Power Reduction in Heterogeneous Networks for LTE-Advanced Downlink,” *IEICE Transactions on Communications*, vol. E96-B, no. 6, pp. 1327–1337, 2013. [11](#)
- [52] I. Guvenc, M.-R. Jeong, I. Demirdogen, B. Kecicioglu, and F. Watanabe, “Range Expansion and Inter-Cell Interference Coordination (ICIC) for Picocell Networks,” in *2011 IEEE Vehicular Technology Conference (VTC Fall)*, Sept 2011, pp. 1–6. [11](#)
- [53] S. Brueck, “Heterogeneous networks in LTE-Advanced,” in *2011 8th International Symposium on Wireless Communication Systems (ISWCS)*, Nov 2011, pp. 171–175. [11](#)
- [54] R. Madan, J. Borran, A. Sampath, N. Bhushan, A. Khandekar, and T. Ji, “Cell Association and Interference Coordination in Heterogeneous LTE-A Cellular Networks,” *IEEE Journal on Selected Areas in Communications*, vol. 28, no. 9, pp. 1479–1489, December 2010. [11](#)




- 
- [55] A. Damnjanovic, J. Montojo, J. Cho, H. Ji, J. Yang, and P. Zong, “UE’s role in LTE advanced heterogeneous networks,” *IEEE Communications Magazine*, vol. 50, no. 2, pp. 164–176, February 2012. [11](#)
- [56] S. Mukherjee and I. Guvenc, “Effects of Range Expansion and Interference Coordination on Capacity and Fairness in Heterogeneous Networks,” in *2011 Conference Record of the Forty Fifth Asilomar Conference on Signals, Systems and Computers (ASILOMAR)*, Nov 2011, pp. 1855–1859. [11](#)
- [57] M. Shirakabe, A. Morimoto, and N. Miki, “Performance Evaluation of Inter-Cell Interference Coordination and Cell Range Expansion in Heterogeneous Networks for LTE-Advanced Downlink,” in *2011 8th International Symposium on Wireless Communication Systems (ISWCS)*, Nov 2011, pp. 844–848. [11](#)
- [58] A. Merwaday, S. Mukherjee, and I. Guvenc, “On the capacity analysis of HetNets with range expansion and eICIC,” in *2013 IEEE Global Communications Conference (GLOBECOM)*, Dec 2013, pp. 4257–4262. [11](#)
- [59] —, “HetNet capacity with reduced power subframes,” in *2014 IEEE Wireless Communications and Networking Conference (WCNC)*, April 2014, pp. 1380–1385. [11](#), [13](#), [61](#)
- [60] —, “Capacity analysis of LTE-Advanced HetNets with reduced power subframes and range expansion,” *EURASIP Journal on Wireless Communications and Networking*, vol. 189, 2014. [11](#), [13](#)
- [61] A. Simonsson, “Frequency Reuse and Inter-cell Interference Co-Ordination In E-UTRA,” in *IEEE 65th Vehicular Technology Conference (VTC Spring)*, April 2007, pp. 3091–3095. [13](#)
- [62] J. Ellenbeck, C. Hartmann, and L. Berlemann, “Decentralized inter-cell interference coordination by autonomous spectral reuse decisions,” in *The 14th European Wireless Conference*, June 2008, pp. 1–7. [13](#)

BIBLIOGRAPHY

- [63] L. G. U. Garcia, K. I. Pedersen, and P. E. Mogensen, “Autonomous Component Carrier Selection: Interference Management in Local Area Environments for LTE-Advanced,” *IEEE Communications Magazine*, vol. 47, pp. 110 – 116, September 2009. [13](#)
- [64] L. G. U. Garcia, I. Z. Kovacs, K. I. Pedersen, G. W. O. da Costa, and P. E. Mogensen, “Autonomous Component Carrier Selection for 4G Femtocells - A fresh look at an old problem,” *IEEE Journal on Selected Areas in Communications*, vol. 30, pp. 525 – 537, 2012. [13](#)
- [65] G. Costa, A. Cattoni, I. Kovacs, and P. Mogensen, “A fully distributed method for dynamic spectrum sharing in femtocells,” in *IEEE Wireless Communications and Networking Conference Workshops (WCNCW)*, April 2012, pp. 87 –92. [13](#)
- [66] Z. Chen and T. Lin, “Stochastic Learning Automata Based Resource Allocation for LTE-Advanced Heterogeneous Networks,” in *IEEE 24th International Symposium on Personal Indoor and Mobile Radio Communications (PIMRC)*, 2013, pp. 1952–1956. [13](#), [22](#)
- [67] I.-H. Wang and D. Tse, “Interference mitigation through limited receiver cooperation,” *IEEE Transactions on Information Theory*, vol. 57, no. 5, pp. 2913–2940, 2011. [13](#)
- [68] M. Cierny, W. Haining, R. Wichman, D. Zhi, and C. Wijting, “On Number of Almost Blank Subframes in Heterogeneous Cellular Networks,” *IEEE Transactions on Wireless Communications*, vol. 12, no. 10, pp. 5061–5073, 2013. [13](#)
- [69] S. Deb, P. Monogioudis, J. Miernik, and J. Seymour, “Algorithms for Enhanced Inter-Cell Interference Coordination (eICIC) in LTE HetNets,” *IEEE/ACM Transactions on Networking*, vol. 22, no. 1, pp. 137–150, Feb 2014. [13](#)



- 
- [70] M. Vajapeyam, A. Damnjanovic, J. Montojo, T. Ji, Y. Wei, and D. Mal-ladi, “Downlink FTP Performance of Heterogeneous Networks for LTE-Advanced,” in *2011 IEEE International Conference on Communications Workshops (ICC)*, June 2011, pp. 1–5. [13](#)
- [71] D. Lopez-Perez and H. Claussen, “Duty cycles and load balancing in Het-Nets with eICIC almost blank subframes,” in *2013 IEEE 24th International Symposium on Personal, Indoor and Mobile Radio Communications (PIMRC Workshops)*, Conference Proceedings, pp. 173–178. [13](#)
- [72] B. Soret and K. Pedersen, “Macro transmission power reduction for HetNet co-channel deployments,” in *2012 IEEE Global Communications Conference (GLOBECOM)*, Dec 2012, pp. 4126–4130. [13](#)
- [73] B. Soret and K. I. Pedersen, “Centralized and Distributed Solutions for Fast Muting Adaptation in LTE-Advanced HetNets,” *IEEE Transactions on Vehicular Technology*, vol. 64, no. 1, pp. 147–158, Jan 2015. [13](#)
- [74] A. Nosratinia, T. Hunter, and A. Hedayat, “Cooperative communication in wireless networks,” *IEEE Communications Magazine*, vol. 42, no. 10, pp. 74–80, 2004. [15](#)
- [75] J. Laneman, D. Tse, and G. W. Wornell, “Cooperative diversity in wireless networks: Efficient protocols and outage behavior,” *IEEE Transactions on Information Theory*, vol. 50, no. 12, pp. 3062–3080, 2004. [15](#), [18](#)
- [76] G. Li and H. Liu, “Resource allocation for ofdma relay networks,” in *Conference Record of the Thirty-Eighth Asilomar Conference on Signals, Systems and Computers, 2004.*, vol. 1, 2004, pp. 1203–1207 Vol.1. [15](#)
- [77] I. Maric and R. Yates, “Bandwidth and power allocation for cooperative strategies in gaussian relay networks,” in *Conference Record of the Thirty-Eighth Asilomar Conference on Signals, Systems and Computers, 2004.*, vol. 2, 2004, pp. 1907–1911 Vol.2. [15](#)

BIBLIOGRAPHY

- [78] Z. Kenan and T. M. Lok, “A relay selection scheme under optimal power allocation,” in *11th IEEE Singapore International Conference on Communication Systems*, 2008, pp. 1609–1613. [15](#)
- [79] H. Wu, Y. Wang, C. Xiong, and D. Yang, “A novel relay selection scheme with simplified power allocation for wireless relay networks,” in *IEEE Global Telecommunications Conference, 2009.*, 2009, pp. 1–5. [15](#)
- [80] F. Ke, S. Feng, and H. Zhuang, “Relay selection and power allocation for cooperative network based on energy pricing,” *IEEE Communications Letters*, vol. 14, no. 5, pp. 396–398, 2010. [15](#)
- [81] L. Song, “Relay selection for two-way relaying with amplify-and-forward protocols,” *IEEE Transactions on Vehicular Technology*, vol. 60, no. 4, pp. 1954–1959, 2011. [15](#)
- [82] F. He, Y. Sun, L. Xiao, X. Chen, C.-Y. Chi, and S. Zhou, “Capacity region bounds and resource allocation for two-way ofdm relay channels,” *IEEE Transactions on Wireless Communications*, vol. 12, no. 6, pp. 2904–2917, 2013. [15](#)
- [83] A. Bletsas, A. Khisti, D. Reed, and A. Lippman, “A simple cooperative diversity method based on network path selection,” *IEEE Journal on Selected Areas in Communications*, vol. 24, no. 3, pp. 659–672, 2006. [16](#)
- [84] D. Gunduz and E. Erkip, “Outage minimization by opportunistic cooperation,” in *2005 International Conference on Wireless Networks, Communications and Mobile Computing*, vol. 2, 2005, pp. 1436–1442 vol.2. [16](#)
- [85] A. Barto and P. Anandan, “Pattern-recognizing stochastic learning automata,” *IEEE Transactions on Systems, Man and Cybernetics*, vol. SMC-15, no. 3, pp. 360–375, 1985. [16](#)
- [86] J. de Lope, D. Maravall, and Y. Quinonez, “Response threshold models and stochastic learning automata for self-coordination of heterogeneous multi-task distribution in multi-robot systems ,” *Robotics and Autonomous Systems*, vol. 61, no. 7, pp. 714 – 720,



- 2013, collective and Social Autonomous Robots. [Online]. Available: <http://www.sciencedirect.com/science/article/pii/S092188901200111X> 16
- [87] R. S. Sutton and A. G. Barto, *Reinforcement Learning : An Introduction*. MIT Press, Cambridge, MA , 1998. 21
- [88] L. P. Kaelbling, M. L. Littman, and A. W. Moore, “Reinforcement Learning : A survey,” *Journal on Artificial Intelligence Research*, 1996. 22
- [89] T. Joshi, D. Ahuja, D. Singh, and D. Agrawal, “Sara: Stochastic automata rate adaptation for ieee 802.11 networks,” *IEEE Transactions on Parallel and Distributed Systems*, vol. 19, no. 11, pp. 1579–1590, 2008. 22
- [90] Y. Xu, J. Wang, Q. Wu, A. Anpalagan, and Y.-D. Yao, “Opportunistic Spectrum Access in Unknown Dynamic Environment: A Game-Theoretic Stochastic Learning Solution,” *IEEE Transactions on Acoustics Speech and Signal Processing Wireless Communications*, vol. 11, no. 4, pp. 1380–1391, 2012. 22
- [91] G. I. Papadimitriou, “A new approach to the design of reinforcement schemes for learning automata: stochastic estimator learning algorithms,” *IEEE Transactions on Knowledge and Data Engineering*, vol. 6, no. 4, pp. 649–654, August 1994. 24
- [92] J. Jacod and A. N. Shiryaev, *Limit theorems for stochastic processes*. Springer, 1987. 29
- [93] B. Oommen and J. Lanctot, “Discretized pursuit learning automata,” *IEEE Transactions on Systems, Man and Cybernetics*, vol. 20, no. 4, pp. 931–938, 1990. 29
- [94] 3GPP TR 36.814, “Further Advancements for E-UTRA: Physical Layer Aspects,” *Technical Specification Group Radio Access Network*, June 2009. 44, 92
- [95] R. Jain, D. Chiu, and W. Hawe, “A Quantitative Measure Of Fairness And Discrimination For Resource Allocation In Shared Computer Systems,” DEC Research Report TR-301, Tech. Rep., 1984. 51

BIBLIOGRAPHY

- [96] Cisco, “Cisco VNI Global Mobile Data Traffic Forecast, 2012-2017,” available at www.cisco.com, 2013. [Online]. Available: www.cisco.com 57
- [97] L. Lindbom, R. Love, S. Krishnamurthy, C. Yao, N. Miki, and V. Chandrasekhar, “Enhanced Inter-cell Interference Coordination for Heterogeneous Networks in LTE-Advanced: A Survey,” *CoRR abs/1112.1344*, 2011. 58
- [98] S. Boyd and L. Vandenberghe, *Convex Optimization*. Cambridge University Press, 2004. 73, 77
- [99] A. Ruszczyński, *Nonlinear Optimization*. Princeton, NJ, USA: Princeton University Press, 2006. 77
- [100] Y. Xing, C. N. Mathur, M. Haleem, R. Chandramouli, and K. Subbalakshmi, “Dynamic Spectrum Access with QoS and Interference Temperature Constraints,” *IEEE Transaction on Mobile Computing*, vol. 6, no. 4, pp. 423–433, April 2007. 80
- [101] S. G. Nash and A. Sofer, “On the complexity of a practical interior-point method,” *SIAM Journal on Optimization*, vol. 8, no. 3, pp. 833–849, 1998. 82
- [102] 3GPP TR 36.931, “Evolved Universal Terrestrial Radio Access (E-UTRA); Radio Frequency (RF) requirements for LTE Pico Node B (Release 11),” April 2010. 84, 92
- [103] O. Ozturk and M. Vajapeyam, “Performance of VoLTE and data traffic in LTE heterogeneous networks,” in *2013 IEEE Global Communications Conference (GLOBECOM)*, Dec 2013, pp. 1595–1601. 104